Title

The Molecular and Epigenetic Regulation of Osteoblast and Osteoclast Differentiation and the Implications in Osteoporosis

Author

Yu, Bo

Publication Date

2014

Peer reviewed|Thesis/dissertation

UNIVERSITY OF CALIFORNIA

Los Angeles

The Molecular and Epigenetic Regulation of Osteoblast and Osteoclast Differentiation and the Implications in Osteoporosis

A dissertation submitted in partial satisfaction of the requirements for the degree Doctor of Philosophy in Oral Biology

by

Bo Yu

2015

ABSTRACT OF THE DISSERTATION

The Molecular and Epigenetic Regulation

of Osteoblast and Osteoclast Differentiation

and the Implications in Osteoporosis

by

Bo Yu

Doctor of Philosophy in Oral Biology

University of California, Los Angeles, 2015

Professor No-Hee Park, Co-Chair

Professor Cun-Yu Wang, Co-Chair

The human skeleton undergoes continuous bone remodeling, a process relying on orchestrated balance between the actions of osteoblasts and osteoclasts. Complex molecular signaling networks govern the differentiation and functions of mesenchymal stem cell (MSC)-derived osteoblasts and monocyte macrophage-derived osteoclasts, as local factors, immune cytokines and systemic hormones exert their regulatory effects. Moreover, the lineage decisions of MSCs to choose

osteogenesis over adipogenesis is critical for maintenance of bone mass. MSC cell fate is determined by epigenetic regulations of various lineage-specific genes and genes promoting 'stemness'. In most bone pathologies especially osteoporosis, the balance in bone remodeling and in MSC lineage decisions become disrupted. To explore the molecular regulation of bone cells, we evaluated the effect of Wnt4 on bone loss associated with osteoporosis and skeletal aging. We generated transgenic mice overexpressing Wnt4 in osteoblasts, and discovered that Wnt4 signaling could attenuate bone loss and suppress inflammation in models of osteoporosis, inflammatory and age-related bone loss. Mechanistically, non-canonical Wnt4 signaling could attenuate Nf-κb signaling by competitive sequestering of transforming growth factor associated kinase 1 (Tak1) in bone marrow macrophages. Furthermore, Wnt4 recombinant protein injection effectively prevented and reversed bone loss induced by estrogen-deficiency. Hence, non-canonical Wnt4 signaling could not only promote bone formation, but also inhibit bone resorption and inflammation in marrow microenvironment by a novel crosstalk with NF-κB signaling. To explore the epigenetic regulation of MSC differentiation towards osteoblasts, we discovered two novel histone demethylases KDM4B and KDM6B, which promoted osteogenesis and inhibited adipogenesis of human MSCs. Mechanistically, KDM4B and KDM6B epigenetically activated different osteogenic transcription factors by removing gene silencing marks H3K9me3 and H3K27me3 respectively. Furthermore, H3K27me3- and H3K9me3- positive MSCs in osteoporotic and aged mouse bone marrow become elevated, along with a reduction in KDM4B and KDM6B. These findings supported that these histone demethylases play a critical role in MSC cell fate decisions, and may become potential therapeutic targets for treatment of osteoporosis.

The dissertation of Bo Yu is approved.

Guoping Fan

Mo Kang

No-Hee Park, Committee Co-chair

Cun-Yu Wang, Committee Co-chair

University of California, Los Angeles

2015

TABLE OF CONTENTS

LIST OF FIGURES AND TABLES

ACKNOWLEDGEMENTS

I would like to thank Dr Cun-Yu Wang and Dr No-Hee Park, my co-mentors for their invaluable support and guidance during my DDS/PhD program. I am grateful for the opportunity to work on two interesting projects. Their passion and enthusiasm in research, unrelenting work ethic, patience and continued guidance are the cornerstones of this thesis work. I would also like to thank them for providing me with generous support regarding my tuition and with my application for R90 training grant.

I am deeply appreciative of Dr David Wong and the R90 administrative team at UCLA for their financial support over the past two years.

I am thankful for Dr Guo-Ping Fan and Dr Flavia Pirih for their kind accommodations and invaluable help during the committee meetings and for their suggestions and guidance in completion of this work.

Many thanks to Ms Megan Scott at the Oral Biology department for her patience in helping me circumventing countless difficult administrative situations.

I want to thank all the current and past members of Wang Lab for the stimulating work discussions and support. I especially would like to thank my co-first authors Dr Jia Chang, Dr Ling Ye and Dr Zhipeng Fan for their significant contributions towards the work described here.

Lastly, I would like to acknowledge my wife and my family for their accommodation and support during my studies. I could not have made it to here without you.

BIOGRAPHICAL SKETCH

NAME	POSITION TITLE
Yu, Bo	PhD Candidate in Oral Biology

EDUCATION/TRAINING

INSTITUTION AND LOCATION	DEGREE	MM/YY	FIELD OF STUDY
University of California, Berkeley	B.S	05/07	Electrical Engineering & Computer Science
University of California, Los Angeles, School of Dentistry	D.D.S.	06/11	Dentistry
University of California, Los Angeles, School of Dentistry			Oral Biology

PUBLICATIONS

1. Yu B, Chang J, Liu YS, Li J, Kevork K, Al Hezaimi K, Graves D, Park NH, Wang CY. (2014). Wnt4 signaling prevents skeletal aging and inflammation by inhibiting nuclear factor –κB. Nature Medicine, 20 (9): 1009-17.
2. Xu J, Yu B, Hong C, Wang CY. (2013). KDM6B epigenetically regulates odontogenic differentiation of dental mesenchymal stem cells. International Journal of Oral Sciences, 5(4): 200-5.
3. Ye L, Fan Z, Yu B, Chang J, Al Hezaimi K, Zhou X, Park NH, Wang CY. (2012). Histone demethylases KDM4B and KDM6B promotes osteogenic differentiation of human MSCs. Cell Stem Cell, 11(1):50-61. [Co-first author, designed the featured journal cover figure]
4. Shin KH, Kim RH, Yu B, Kang MK, Elashoff D, Christensen R, Pucar A, Park NH. (2011). Expression and mutation analysis of heterogeneous nuclear ribonucleoprotein G in human oral cancer. Oral Oncology, 47(11):1011-6.
5. Ho S, Yu B, Yun W, Marshall GW, Marshall SJ. (2009). Structure, chemical composition and mechanical properties of human and rat cementum and its interface with root dentin. Acta Biomaterialia, 5:707-18.

1 INTRODUCTION

1.1 Bone remodeling

The human skeleton undergoes continuous bone remodeling, a process of alternating synthesis and destruction to allow maturation and reshaping of the bone[1,2]. This process involves mainly two types of bone cells. Osteoclasts, which are fused macrophages derived from hematopoetic stem cell/monocyte lineage, start the remodeling cycle by degrading the existing bone collagenous matrix, thereby releasing calcium into the bloodstream[3]. Following resorption, osteoblasts, which are terminally differentiated mesenchymal stem cells (MSCs), secrete collagenous extracellular matrix (ECM) that become mineralized to form new bone. Bone remodeling is critical not only for adapting bone strength to growth and mechanical loading, but also for maintenance of blood calcium level[4]. To this end, the formation and resorption of bone are coupled to achieve an orchestrated balance in healthy adults. However, in certain physiological conditions and various diseases, these two arms of bone remodeling become uncoupled, leading to a net bone loss also known as osteopenia, which eventually results in osteoporosis, a condition with decreased bone strength and increased fragility. Unsurprisingly, to maintain homeostasis of bone mass, the differentiation and functions of osteoblasts and osteoclasts are tightly controlled. On a molecular level, the differentiation and activation of bone cells are regulated by a complex signaling network involving both locally secreted factors and systemic hormones[5-8]. Furthermore, environmental and stochastic stressors often, through epigenetic mechanisms, effect profound changes in gene expression and lineage decisions associated with progenitor cell differentiation[9-11]. Thus, the pathogenesis of multi-factorial metabolic bone disorders such as osteoporosis could have an important epigenetic component. Hence, development of an effective treatment for various

metabolic bone diseases hinges upon a deeper understanding of the molecular and epigenetic regulation of bone cell differentiation and functions.

Throughout the adult life, bone formation and resorption continuously vary their rates to adapt bone strength to mechanical load patterns, as well as to serve as a depot for calcium. During lactation, bone resorption could prevail over formation, leading to a net bone loss also known as osteopenia[12]. On the contrary, with intensive exercise, bone formation could exceed resorption to result in a bone mass gain[13]. More importantly, the uncoupling between bone formation and resorption is linked to a multitude of metabolic bone diseases. The imbalance could be of metabolic origin (such as osteomalacia) or endocrine origin (such as hyperparathyroidism and postmenopausal osteoporosis)[14]. In particular, osteoporosis is the most common metabolic bone disease afflicting over 9 million people worldwide and 40% of women over 50[15]. It has become a growing public health concern with the aging population. The pathogenesis of osteoporosis was first believed to be either a result of estrogen deficiency at menopause or that of calcium deficiency with skeletal aging. This understanding has been replaced with the current concept that osteoporosis is a multifactorial deterioration of the skeletal microarchitecture, hallmarked by excessive osteoclastic activation and inadequate bone formation to compensate for the accelerated resorption[5]. In addition to osteoporosis, uncoupled bone remodeling cycle is manifested in other scenarios of bone pathologies including inflammatory and aging-related bone loss. In inflammatory bone loss such as rheumatoid arthritis, inflammatory cytokines could trigger signaling events that activate osteoclasts while inhibiting osteoblast differentiation. With advanced age, the bone turnover slows down especially bone formation in light of the altered marrow microenvironment and diminished capacity of osteoblastic progenitor population[16]. As such, an imbalance in the bone remodeling cycle is a focal point of most skeletal pathologies.

1.2 Osteoblastic Differentiation of Mesenchymal Stem Cells

1.2.1 Definition of Mesenchymal Stem Cells

MSCs were initially identified by Friedenstein in 1970s as colony-forming unit fibroblasts (CFU-Fs) that can are multipotent progenitor populations with the capabilities to self-renew and differentiate into several mesenchymal lineages including adipocytes, osteoblasts and chondroblasts[17]. Stromal cells that fulfill the above definition have been isolated from almost every type of connective tissue[18], including the bone marrow. While the stromal cells in the bone marrow are a heterogenous population containing a mixture of progenitors at different stages of commitment to various mesodermal lineages, only a small percentage of this population possess self-renewal capacity to be considered as MSCs[19]. Classically isolated from the bone marrow, MSCs only account for up to 0.01% of all mononuclear cells in the healthy adults[20].

Since their discovery, MSCs have generated substantial excitement in the biomedical community as a source for stem-cell regenerative therapies. This is due to their convenient isolation, ease of *ex vivo* expansion, lack of immunogenicity, as well as their ability to transdifferentiate and to create a tissue microenvironment favorable for tissue repair[21-23]. In various clinical trials, allogenic bone marrow-derived MSCs have been introduced to patients of osteogenesis imperfecta, delayed fracture healing or avascular necrosis of femoral head, and improved patient recovery has been reported[24,25]. The clinical application of MSCs in regenerative medicine hinges on the understanding of the molecular mechanisms governing their differentiation. Growing evidence suggests that the lineage decisions of MSCs rely on an orchestrated activation of lineage-specific genes while inhibiting transcription of genes promoting stemness or commitment to other lineages[23,26,27]. In both healthy and diseased conditions, inhibition of

adipogenesis could enhance the differentiation of MSCs towards osteoblast lineage, thereby promoting bone growth[28-30]. Until the recent emergence of epigenetics, most studies have focused on the molecular regulation of MSC differentiation in response to external stimuli, involving the activation or repression of certain lineage-specific transcriptional factors. For the purpose of this dissertation, we will briefly review the well-known osteogenic master regulatory genes and the major signaling pathways influencing their transcriptional activation. On the other hand, stem cell populations also undergo dynamic reprogramming of gene expression profiles during lineage commitment and maturation. These epigenetic regulatory mechanisms allow MSCs to favor differentiation down a specific lineage in response to the stimuli provided by the microenvironment.

1.2.2 Molecular Regulations of Osteoblastic Differentiation

MSCs proliferate and differentiate into preosteoblasts and subsequently into mature osteoblasts[31]. Early studies in the late 1990s suggest that MSC differentiation is triggered by cell-specific transcription factors acting as switches[32,33]. However, most of the other proteins expressed by osteoblasts are also expressed in other cells such as fibroblasts and chondroblasts. The truly osteoblast-specific gene, osteocalcin, is only expressed in mature, fully differentiated osteoblasts[32]. In a quest to identify a triggering factor for osteoblast differentiation, studies have focused on the cis-acting elements at the promoter of osteocalcin. The first master regulatory gene for osteogenesis, runt-related transcriptional factor 2 (RUNX2) was discovered as a DNA binding protein at the osteocalcin promoter[34]. RUNX2 was later found to be required for MSC differentiation towards osteoblasts, based on both its expression pattern throughout the

differentiation process and the phenotypes of two separate *Runx2* knockout mice strains (lack of rigid rib cage and cartilaginous skeleton)[35,36]. These evidence established *RUNX2* as a requisite gene for osteoblast development. Osterix (OSX/SP7) is another essential osteogenic master regulator. Osterix-deficient mice do not form bone despite having normal levels of Runx2, indicating that OSX is activated downstream of RUNX2[37].

Several major signaling pathways are involved in the activation of these master regulators of osteoblastogenesis. Bone morphogenic proteins (BMPs), specifically BMP-2, -4, -6, -7 and BMP-9, are potent osteogenic inducers[30]. Multiple murine studies involving genetically modified BMP ligands, BMP receptors and inhibitors demonstrate its critical role in bone formation[38-40]. BMPs signal through intracellular SMAD proteins SMAD1/5/8 as well as downstream mitogen-activated protein kinase (MAPK) activation, to activate the transcription of RUNX2, as well as OSX in both RUNX2-dependent and -independent manners[41]. The conditional knockout mice involving deletion of Bmp-2, Bmp-4, Smad1/5 have shown various degrees of skeletal deficiencies[42], further affirming the osteogenic roles of BMP signaling *in vivo*. Mechanistically, SMADs can interact with RUNX2 to synergistically regulate its transcription and function[43-46]. The SMAD-interaction domain identified in RUNX2 is continuous with a nuclear matrix targeting sequence, which is necessary for RUNX2 function[47]. Of note, BMP signaling is also a central pathway in stimulation of MSC adipogenesis. There exist significant overlapping influences of various BMP ligands in promoting osteogenesis and adipogenesis of MSCs. Both osteogenic and adipogenic effects are mediated by concomitant activation of Smad/MAPK pathways. The exact determinants governing how BMP signaling favor osteogenesis over adipogenesis are poorly understood. BMP receptor types have been suggested as one of the factors although conflicting evidence does exist. In general, binding of BMP ligands with Type IB BMP receptors promotes

osteoblastogenesis through turning on the expression of OSX[48]. On the other hand, binding with Type IA BMP receptors leads to expression of transcription factor peroxisome proliferator-activated receptor γ (PPAR-γ) which induces adipogenesis and blocks osteoblastogenesis[49]. The complex effects of BMP signaling on MSC lineage commitment also expose one of the motivations for investigating the regulatory mechanisms of osteogenic programs on an epigenetic level.

Another pivotal signaling pathway involved in the differentiation and activation of osteoblasts is the WNT signaling pathway. WNT proteins comprise a family of 19 highly conserved glycoproteins secreted by various cells especially in a heterogenous cell population such as the bone marrow. Bone marrow stromal cells and osteoblasts have been reported to express and secrete many WNT ligands and several parts involved in WNT signaling pathways. The WNT family proteins are divided into two categories based on their dependence on transduction through β-catenin: canonical and non-canonical. In canonical WNT signaling, binding of WNT ligands to FRIZZLED (FZD) receptors and the low-density lipoprotein receptor-related protein 5 or 6 (LRP5 or 6) co-receptor leads to transduction through Disheveled (DVL) to prevent the proteolytic degradation of cytosolic β-catenin. As a result, β-catenin accumulating in the cytoplasm can then enter the nucleus to interact with TCF/LEF family proteins to enable transcriptional activation of target genes[50,51]. On the other hand, non-canonical Wnt signaling can function via a diverse number of ways including the planar cell polarity (PCP) pathway, intracellular Ca^{2+}, and/or activating proteins such as the GTPase Rac, calcium/calmodulin-depenent kinase II (CAMKII) or c-Jun N-terminal kinase (JNK). The PCP pathway is activated through binding of WNT ligands to FZD receptors alone without LRP co-receptor involvement. These signals activate DVL which in turn induces GTPase Rho and Rac, as well as JNK. The WNT/Ca^{2+} signaling is characterized by

WNT-Fz-induced phospholipase C activation and results in a spike in cytoplasmic Ca^{2+} levels. Several Ca^{2+}-responsive proteins such as CAMKII become activated to induce transforming growth factor-beta activated kinase (TAK1) and Nemo-like kinase (NLK) to effect downstream signaling cascade. Functionally, the Wnt/Ca^{2+} signaling is mianly associated with cellular adhesion, cytoskeletal rearrangement, dorsoventral patterning in embryonic morphogenesis.

Canonical WNT signaling has important modulatory roles in osteoblastogenesis and bone formation. The initial evidence of the involvement of canonical Wnt signaling arose from the osteoporosis-pseudoglioma syndrome in lack-of-function mutations in the Lrp5 receptors[52]. However, it was later shown that while Lrp5 deletion reduced osteoblast numbers in the long bone, osteoblast differentiation was not affected[53]. Conditional deletion of β-catenin showed deficient skeletal phenotypes in the embryos and osteoblast differentiation was arrested in the early progenitor populations, suggesting a critical role of β-catenin in osteoblastogenesis[54]. Inactivation of β-catenin in the early mesenchyme and late mesenchymal progenitors both resulted in commitment to chondroblasts, indicating β-catenin is necessary to inhibit MSC commitment to chondroblast lineage[55]. In postnatal bone growth, conditional deletion of β-catenin using either osteocalcin-cre or osterix-cre mice showed decreased bone mass and reduced osteoblast differentiation[56,57]. Further *in vitro* evidence supported the essential role of canonical Wnt signaling in osteoblastogenesis. Canonical Wnt3a, Wnt1, Wnt10b and constituitively-active β-catenin stimulate osteoblastogenesis while Dickkopf-related protein (Dkk1), an inhibitor of canonical Wnt signaling reduced osteoblast differentiation[58]. In murine osteoprogenitor cells, canonical Wnt signaling upregulates Runx2 whereby β-catenin occupies a cognate binding site in the Runx2 promoter[31]. Interestingly, considerable evidence suggests canonical Wnt/β-catenin signaling inhibits adipogenesis while stimulating osteoblastogenesis in MSC differentiation[27,59,60].

Taken together, activation of canonical WNT signaling generally promotes MSC differentiation towards osteoblasts while suppressing commitment to other lineages.

The roles of non-canonical WNT signaling on osteoblast differentiation are less elucidated. Wnt5a and Wnt11 are classically non-canonical Wnt ligands, but they have been shown to induce canonical Wnt signaling and osteoblast differentiation in murine mesenchymal progenitor cell lines[61,62]. Furthermore, Wnt5a may favor osteoblast lineage by repressing adipogenesis through chromatin inactivation of master adipogenic regulator PPAR-ϒ[27]. Non-canonical Wnt7b could induce osteoblast differentiation through G protein-linked protein kinase δ signaling[63]. Wnt4 has been reported to enhance osteoblastic differentiation in human MSCs and promote bone regeneration via activation of p38/MAPK pathways[64]. Given the mouse genetic data currently available, one may speculate that under physiological conditions, co-stimulation of both canonical and non-canonical WNT signaling occurs. Whether these pathways act in synergy or antagonism, and the effect of exclusive activation of non-canonical WNT signaling on bone metabolism remains to be elucidated[65].

Other pathways involved in the regulation of osteoblastogenesis in MSCs including the sonic hedgehog (SHH), insulin-growth factor-1 (IGF-1), fibroblast-growth factor (FGF), activator-protein-1 (AP-1) pathways have been elegantly reviewed elsewhere[42,65,66]. Of note, extensive crosstalk takes place between these signaling pathways in bone. For instance, Dkk1 and other WNT antagonists are targets of type-IA BMP receptor-mediated BMP signaling in osteoblasts to negatively impact bone formation[67]. Parathyroid hormone (PTH) is the principle regulator of calcium homeostasis. While sustained elevation of PTH induces long-term bone loss due to accelerated osteoclastic resorption (as in the case of hyperparathyroidism), intermittent administration of PTH results in enhanced bone formation[68]. PTH crosstalks with WNT/β-catenin

signaling by several mechanisms. PTH can associate *in vitro* with the extracellular domains of Lrp6, triggering signaling in the absence of Wnt ligands[69]. In addition, PTH could phosphorylate β-catenin and thereby stabilizing it[70]. These signaling crosstalk highlight the complexity of molecular regulatory mechanisms for osteoblast differentiation.

1.2.3 Epigenetic Regulations of Osteoblastic Differentiation

Epigenetic mechanisms are defined as heritable modifications to DNA and chromatin without altering the genomic sequence. As the MSCs enter into a specific lineage differentiation program, the cells must modify their gene expression profiles to activate lineage-specific genes, while repressing genes promoting stemness and commitment to other lineages. The epigenetic regulatory mechanisms can be roughly categorized into three classes: microRNAs (miRNAs), histone modification and DNA methylation.

MiRNAs are short non-coding RNAs ranging from 18 to 25 nucleotides, that regulate gene expression by binding to the 3'-UTRs of target gene mRNA. Binding of miRNAs often promote degradation of the target mRNA or inhibit their translation[71]. Gene profiling analysis has allowed the identification of several miRNAs that play a role in the lineage specification between osteogenesis and adipogenesis of MSCs. For instance, miR-22 targets histone deacetylase 6 (HDAC6), a repressor of Runx2 transcription, thereby promotes osteogenesis[72]. miR-637 and certain miR-17 family directly targets osterix and BMP2 respectively to repress osteoblastogenesis and promote adipogenesis[73,74].

Epigenetic processes can also confer a specific chromatin configuration on gene regulatory and coding regions to control expression of key transcription factors for MSC differentiation. In

particular, modifications at the N-terminal tails of histones such as acetylation, methylation, phophorylation, ubiquitination, and ADP-ribosylation can control access to regulatory regions on the DNA by altering chromatin compaction[75]. Modified histone domains have thus become epigenetic signatures that either mark for gene activation, such as acetylated Histone 3 Lysine 9 (H3K9) and trimethylated Histone 3 Lysine 4 (H3K4), or mark for gene repression, such as dimethylated H3K9 and trimethylated H3K27. H3K27 trimethylation (H3K27me3) is an established hallmark for gene silencing in many developmental events such as mammalian X chromosome inactivation, stem cell identity and cell cycle regulation[76]. The chromatin regions of embryonic stem cells are enriched with bivalent histone domains. In the self-renewing state, genes promoting cell stemness become activated while master genes driving lineage-specific differentiation remain repressed. Upon differentiation, the gene silencing signatures on the master differention genes must be removed in concert with the emergence of activation signatures. Existence of demethylases is therefore essential to facilitate rapid removal of methyl group from trimethylated H3K27 during activation of gene transcription. The methylation status of H3K27 is dynamically controlled via the synergistic actions of methyltransferases and histone demethylases.

In the context of osteogenesis of MSCs, several methyltransferases and histone methylation have been associated with the epigenetic regulation of lineage decisions. HOXA10, a gene necessary for embryonic patterning of skeletal elements, could contribute to activation of osteogenic genes via H3K4 hypermethylatin of Runx2, alkaline phosphatase (Alp), osteocalcin (Bglap) and bone sialoprotein (Ibsp)[77,78]. Another study found that a BCL-6 corepressor (BCOR) mutation increases the H3K4 and H3K36 methylation of osteogenic genes in MSCs[79]. The enhancer of zeste homology 2 (EZH2) scatalytic subunit of polycomb repressive complex 2 (PRC2) is responsible for methylation of various histone sites including H3K27 trimethylation. Studies

have shown that cyclin-dependent kinase 1 (CDK1) promotes osteogenic differentiation through suppression of EZH2 activity[26], and that enforced activity of EZH2 in MSCs inhibited osteogenic differentiation *in vitro* and *in vivo*[80].

In addition to methyltransferases, histone demethylases also play a key role in the regulation of MSC lineage determination. Two H3K27me3 demethylases, KDM6A (UTX) and KDM6B were recently discovered. These demethylases specifically target and convert tri-methylated H3K27 and di-methylated H3K27 to mono-methylated H3K27[81]. More histone demethylases have been discovered to possess the ability of removing methyl groups from various methylated histone lysine residues such as K4, K9, K27, K36 and K79, thereby enabling the dynamic and reversible regulation of transcription[82,83]. Growing evidence suggests that histone demethylases may be associated with lineage decisions of MSCs. The demethylase activity of KDM6B is involved in macrophage transdifferentiation during inflammation[84], activation of neural differentiation genes[85], and in epigenetic control of mammalian epidermal differentiation[86]. KDM6A homozygous mutations in mouse cause severe heart defects and KDM6A-deficient embryonic stem cells displayed a failure in cardiac differentiation program[87]. In addition, KDM6A reportedly activates muscle-specific genes during myogenesis via demethylation of H3K27me3[88]. However, the roles of histone demethylases in osteogenic differentiation of MSCs remain poorly understood. Intriguingly, a recent study suggested that KDM6A, in contrary to EZH2, could promote osteogenesis and inhibit adipogenesis of MSCs both *in vitro* and *in vivo*[80].

In addition to methylation, acetylation and deacetylation have been the most studied histone modifications in the regulation of osteogenic genes. Histone acetyltransferases, such as p300, CBP, PCAF are coactivators of Runx2[89]. Histone acetylation is often associated with a more open euchromatin configuration and active transcription states, while histone deacetylation,

catalyzed by histone deacetylases (HDACs) is associated with chromatin condensation and gene silencing. For instance, Runx2 binds and is functionally inhibited by several HDACs (HDAC-3, -4, -5, -6, and -7)[90]. Moreover, acetylation via BMP signaling can protect Runx2 protein from proteolytic degradation[91]. Transcriptional induction of osteocalin gene during osteogenesis is also associated with enhanced histone acetylation[92].

DNA methylation is another epigenetic mechanism by which gene expression could be dynamically modulated during MSC differentiation. For instance, significant hypermethylation, often associated with chromatin condensation, at the osteocalcin gene locus was observed in undifferentiated cells, and the methylation at CpG islands decreased during the course of osteogenic differentiation *in vitro*[93]. Also, differentiation of MSCs was accompanied by reduced expression of stemness genes such as Brachyury and Lin28, via hypermethylation of their promoter regions[94].

Taken together, extensive and coordinated epigenetic regulations of various lineage-specific genes take place during cell fate decisions of MSC differentiation. While there have been certain studies on DNA methylation, miRNA and histone acetylation, the recent discoveries of histone demethylases makes the dynamic and orchestrated regulation of histone methylation marks an intriguing topic of investigation.

1.3 Osteoclastic Differentiation and Activation

Osteoclast differentiation and activation are regulated by both systemic hormones and cytokines secreted locally into the bone microenvironment. As the bone formation and resorption are coupled, osteoclasts can be regulated by osteoblasts, marrow stromal cells, osteocytes as well as

lymphocytes in the bone marrow. Two key transcription factors required for osteoclasts are c-Fos and nuclear factor of associated T-cells c1 (NFATc1). Mice lacking *c-fos* can develop monocyte macrophages but cannot form osteoclasts[95]. The activation of NFATc1 is also essential for the transcription of various genes essential for osteoclast differentiation and function, including genes encoding the tartrate-resistant acid phosphatase (TRAP), matrix metalloproteinase-9 (MMP-9) and cathepsin K, which allows the acidification and degradation of bone matrix[96,97].

The initial step of osteoclast differentiation from hematopoietic stem cells, a step towards monocytes and macrophages, requires macrophage colony-stimulating factor (M-CSF). Through the activation of extracellular signal-regulated kinases and anti-apoptotic serine/threonine kinase (AKT), M-CSF subsequently induces, via cyclin D1, the profileration and survival of osteoclast progenitor cells[98]. The next step of osteoclast differentiation requires signaling of receptor activator of nuclear factor-kappa B ligand (RANKL). RANKL is a member of the tumor-necrosis factor-α (TNF α) superfamily, and is expressed by osteoblasts, marrow stromal cells and lymphocytes. Binding of RANKL to the surface receptor RANK activates signaling transduction involving the adaptor TNF receptor-associated factor 2/5/6 (TRAF2/5/6). Various TRAF proteins can then activate canonical and non-canonical nuclear factor-κB (NF-κB), ERK, p38/MAPK, Src/Akt and JNK pathways, which in turn activate genes that are required for differentiation, survival and resorptive function of osteoclasts (Figure 1)[99,100]. Particularly for NF-κB activation, TRAF6 forms a complex with TGFβ activated kinase 1 (Tak1) and Tak-binding protein 2 (Tab2), leading to phosphorylation and activation of Tak1[101]. In canonical NF-κB signaling, Tak1 then phosphorylates IκB kinase (IKK) complex and thereby initiates degradation of IκBα, followed by phosphorylation and nuclear translocation of p65 to activate downstream target genes including NFATc1. RANKL signaling can be modulated by systemic hormones including PTH, Interkeulin-

11, prostaglandins, and 1,25-$(OH)_2D_3$[102,103]. Interestingly, osteoclasts can regulate its own formation via autocrine secretion of cytokines. For instance, IL-6 is secreted by osteoclasts and could induce human osteoclast formation by acting directly on osteoclast progenitors independent of RANKL signaling[104].

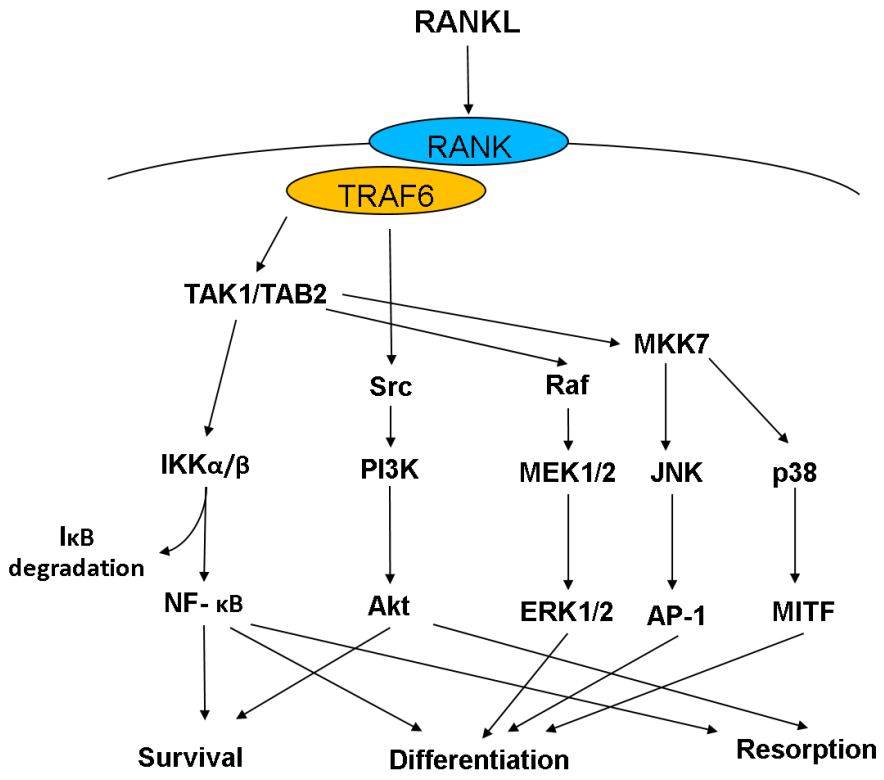

Figure 1-1. RANKL signaling pathways in osteoclasts.

Binding of RANKL triggers the activation of multiple signaling pathways including NF-κB, Akt, ERK, AP-1, p38/MAPK pathways. These pathways in turn activate transcriptions of genes required for the differentiation, survival and resorptive functions of osteoclasts.

WNT signaling not only influences MSC differentiation and osteoblast formation, but also has profound effect on osteoclasts. Since in healthy conditions, osteoblasts and osteoclasts function as a coupled unit, osteoclasts constantly interact with osteoblasts and other cells in the bone marrow microenvironment to modulate bone resorption. One principle osteoblast-produced

modulator of osteoclast formation is osteopontegrin (OPG), a RANKL decoy receptor that can repress RANKL signaling and thereby inhibit osteoclast formation. As canonical WNT signaling promotes osteoblastogenesis, it also inhibits osteoclasts through increased secretion of OPG[56,105]. Furthermore, WNT signaling can also directly affect osteoclast proliferation and differentiation. Wnt3a induced β-catenin promotes proliferation of osteoclast progenitors but suppresses osteoclast differentiation[106]. On the other hand, non-canonical Wnt5a, secreted by osteoblasts, stimulates RANK expression on osteoclasts and thereby promote bone resorption[107]. Another osteoblast-derived ligand Wnt16 can both directly inhibits osteoclast progenitors via a non-canonical pathway, and indirectly increase expression of Opg in osteoblasts via both canonical and non-canonical Wnt signaling[108]. As such, non-canonical WNT ligands, which are highly expressed in osteoblasts, osteoclasts and other marrow stromal cells, serve a critical, albeit poorly understood, role in the interactions between osteoblasts and osteoclasts, as well as in regulating their differentiation and functions.

Furthermore, there is also close link between the adaptive immune system with osteoclast activation, representing a major mechanisms of inflammatory bone loss[109]. Although osteoblasts are the major source of RANKL expression, other mesenchymal cells such as fibroblasts and non-mesenchymal cells like T-lymphocytes also express this osteoclastogenic cytokine. In addition, TNF expressing T-lymphocytes can induce bone loss, and may play a significant role in estrogen-deficiency induced osteoporosis[110]. We will discuss the osteoimmune interactions that regulate bone metabolism under inflammatory conditions in more details later.

The epigenetic regulation of osteoclast differentiation remains poorly understood. Several studies suggested that osteoclastogenesis can be regulated by miRNAs. Osteoclast-derived miR-223 was shown to directly inhibit osteoclast differentiation *in vitro*[111]. Conversely, miR-29

promotes osteoclast-commitment of progenitor populations[112]. Interestingly, KDM6B, a H3K27 demethylase, is reportedly induced by RANKL stimulation in osteoclast progenitors. Correspondingly, gene silencing marks H3K27me3 are reduced at the promoter of key osteoclastic transcription factor *Nfatc1*, suggesting a potential role of KDM6B in promoting osteoclast lineage commitment[113].

1.4 Inflammation and Osteoimmunological Regulation of Bone Remodeling

1.4.1 Chronic Inflammation and Bone loss

Chronic inflammation is a cardinal yet often neglected risk factor for metabolic bone diseases involving both local and systemic bone loss[96,114]. Systemic osteoporosis and increased fracture rates are found in correlation with various rheumatological diseases, including rheumatoid arthritis, systemic lupus erythematousus, psoriatic arthritis, as well as inflammatory bowel disease, celiac disease, cystic fibrosis and periodontitis[114]. In addition to the clinical observation of coincidence, there is a temporal link between inflammation and osteoporosis in aging, menopause, pregnancy and steroid administration[115]. Supporting evidence is also observed in animal models of arthritis and colitis[116,117].

Chronic periodontitis is the most common inflammatory diseases resulting in destruction of alveolar bone and periodontal tissues[118]. Although elicited by bacterial infection, periodontitis has been associated with increased risk of other bone disorders including rheumatoid arthritis[119] and systemic osteoporosis[120]. The local alveolar bone loss appears to be at least partly mediated by bacteria-activated T cells stimulating RANKL signaling to promote osteoclastogenesis[121,122].

Furthermore, the negative bone mass balance that occurs in the course of chronic inflammatory diseases is mostly mediated by cytokines that activate osteoclasts while simultaneously impeding osteoblast function. Inhibition of inflammatory cytokines such as TNF blockers have been an effective approach to dramatically slow down the progression of local and systemic bone loss in rheumatoid arthritis and respective experimental models of arthritis[116,123]. The genetic or chemical inhibition of NF-κB signaling, a main pathway involved in inflammatory responses, has been shown to attenuate bone loss in osteoporosis and arthritis[124]. Growing evidence suggests that osteoblasts and osteoclasts are under tight regulation by the immune system and inflammatory responses have profound influence on the balance in bone remodeling.

1.4.2 NF-κB Signaling and Its Effects on Bone Cells

Inflammation is characterized by the activation of various cell types in the innate and adaptive immunity, resulting in an elevation of immune cytokine production in the cellular environment. The cytokines activated during the course of inflammatory responses have profound effects on the differentiation and activity of osteoblasts and osteoclasts, and are therefore considered to be the mediators of inflammation-associated osteoporosis.

NF-κB signaling is a major signaling pathway activated during most inflammatory responses[125-127]. NF-κB represents a family of five proteins (c-Rel, RelA/p65, RelB, NF-κB1/p50 and NF-κB2/p52), all of which play critical roles in inflammation, osteoimmunology and aging[125]. In their active forms, NF-κB proteins exist as homo- or heterodimers and form a complex with inhibitors of κB (IκBs) in the cytoplasm. Upon stimulation by various inflammatory cytokines, activation and phosphorylation of IκB kinases (IKKs) lead to the degradation of IκBs, and the subsequent nuclear translocation of NF-κB activates transcription of various target genes.

Given the genetic animal models of various NF-κB pathway components, NF-κB signaling has profound effect on bone formation and resorption. Double knockout mice of *Nfkb1* and *Nfkb2* do not form osteoclasts *in vivo* or *in vitro*[128]. Conditional *Ikkb* knockout mice using a Mx1 promoter showed osteopetrotic phenotype and decreased osteoblast numbers compared to wildtype controls[129]. In addition, an osteocalcin promoter driven *IkkϒF* dominant-negative mice showed enhanced osteoblast formation following suppression of NF-κB signaling[130].

In primarily inflammation-induced bone loss such as rheumatoid arthritis, the number and activity of osteoblasts are too low to compensate for the accelerated osteoclast action. Inflammatory responses could severely impair osteoblast differentiation via several pathways. For instance, TNF inhibits RUNX2 expression in osteoblasts[131] and promotes RUNX2 degradation by upregulating its E3 ubiquitin ligases Smurf1/2[132]. NF-κB signaling could presumably inhibit JNK pathways via an unknown mechanism, as inhibition of IKKϒ led to increased AP-1 activation and enhanced osteoblastogenesis[130]. Furthermore, a recent study suggested that NF-κB mediated induction of Smurf1/2 also promotes β-catenin degradation in MSCs, thereby abrogating the osteoblastogenic effects of canonical WNT signaling[133]. In addition, antagonists DKK1[134] and sclerostin[135] are also induced by TNF to interfere with WNT signaling pathway and mediate the inhibitory effects of NF-κB activation on osteoblast differentiation.

Proinflammatory cytokines such as TNF, interleukin-1 (IL-1) and IL-6 all affect osteoclastogenesis. All three cytokines are produced by an array of cells, and can function via partly redundant signaling pathways, which in turn amplify the immunological responses as well as osteoclast function. As TNF and IL-1 activate NF-κB signaling pathway, which is also downstream of RANKL stimulation, increased cytokine production effectively induces RANKL signaling, thus promoting osteoclastogenesis[136]. Of note, proinflammatory cytokines can induce

osteoclast formation independent of RANKL/RANK/TRAF6 pathway[137]. For instance, osteoclast activation may be mediated by spleen tyrosine kinase (SYK) downstream of the Fc receptor ϒ chain (FcϒRs) expressed by monocytes and macrophages. FcϒRs can be activated via immune complexes that are present in patients with rheumatoid arthritis and systemic lupus erythematosus[138,139].

In summary, under inflammatory conditions, activation of NF-κB signaling could enhance osteoclasts while inhibiting osteoblast differentiation and function, resulting in a net bone loss.

1.4.3 Osteoporosis from an Osteoimmunological Perspective

While the pathogenesis of osteoporosis was originally perceived in an estrogen-centric paradigm, emerging evidence suggests an indispensable osteoimmune component to the uncoupling mechanisms of bone remodeling. Estrogen withdrawal is known to induce TNFα production by T-cells through a complex pathway involving both the thymus and bone marrow. In the bone marrow, ovariectomy, the removal of ovaries to simulate estrogen withdrawal, promotes T-cell activation by increasing antigen presentation of macrophages and dendritic cells[140,141]. Estrogen-deficiency promotes the expression of the gene encoding class II transactivator (CIITA). CIITA expression is required and sufficient for the stimulation of antigen presentation in bone marrow monocytes with the final effect of up-regulation of expression of major histocompatibility complex class II on macrophages[142,143]. Activation of T cells in turn increases production of TNFα, as observed in both ovariectomized mice and patients with postmenopausal osteoporosis[110,144]. T-cell deficient and TNFα-deficient mice do not suffer from bone loss following ovariectomy, suggesting an indispensable role of immune cytokines in the pathogenesis of osteoporosis. In addition to TNF, other inflammatory cytokines, such as IL-1, IL-6, IL-7 and IL-17 are also

respsonsible for estrogen-deficiency induced osteoporosis[145,146]. Moreover, RANKL-expression on lymphocytes and marrow stromal cells is also significantly upregulated by estrogen-deficiency in patients, and positively correlates with heightened markers for bone resorption[147].

Conversely, interferon-ϒ (IFN-ϒ) is a critical effector cytokine secreted by T-helper cells and known for its inhibitory effects on osteoclast formation by directly degrading RANKL adaptor protein TRAF6[148]. This posts an interesting question, as to which T-cell lineage is responsible for the induction of osteoclasts, since the conventional Th1/Th2 lineages mainly secrete IFN-ϒ, IL-4 and IL-13, all of which inhibit osteoclastogenesis. Intriguingly, another subset of $CD4^+$ T-helper lineage, Th17 cells, have been recently identified as responsible for the pathogenesis of osteoporosis and rheumatoid diseases[146]. Upon stimulation in inflammatory conditions or during estrogen withdrawal, Th17 cells are able to directly produce RANKL, increase the expression of RANKL in osteoblasts and marrow fibroblasts, as well as upregulate production of TNF and IL-1 in macrophages, all of which drive forth osteoclastic bone formation.

Aside from inflammation, another important risk factor of osteoporosis and inflammatory bone loss is advanced age. With age, the bone marrow microenvironment becomes increasingly proinflammatory[16,149]. The increased production of immune cytokines and accumulating reactive oxidative stress entail that bone metabolism is more susceptible to osteoimmunological influences.

Taken together, the osteoimmune interactions that govern osteoblast/osteoclast differentiation have profound effects on the pathogenesis of metabolic and inflammatory bone loss, as well as skeletal aging.

1.5 Specific Aims

In health and diseases, bone remodeling is under tight regulation through extensive signaling crosstalk and complex interactions between the bone cells, immune cells as well as other marrow stromal cells. Chronic inflammation is closely associated with osteoporosis and various age-related bone diseases. Activated inflammatory responses exert profound influences on the differentiation and functions of osteoblasts and osteoclasts on a molecular level, and shape an important aspect of the pathogenesis of metabolic bone diseases. The study of these osteoimmune interactions has only recently become an emerging topic of interest[150,151]. Molecular signaling events in inflammatory conditions also interfere with key pathways regulating bone metabolism such as WNT pathways. Previously, our group found that Wnt4 is able to promote osteoblast differentiation of MSCs via non-canonical Wnt signaling[64]. To further explore the therapeutic potential of Wnt4, we generated transgenic mice expressing Wnt4 in osteoblasts. Using this animal model, we could examine the in vivo effect of Wnt4 on osteoblasts and bone formation. Since Wnt4 is a secreted growth factor, and osteoclasts are constantly subjected to modulations by osteoblasts, we could also investigate potential influences of Wnt4 on osteoclast formation, in various scenarios of bone loss simulating osteoporosis, arthritis as well as physiological aging.

On the other hand, in both skeletal aging and osteoporosis, a shift in MSC lineage commitment results in reduced trabecular bone mass along with increased adiposity in the bone marrow. The osteogenesis of MSCs relies on orchestrated regulatory mechanisms that promote osteogenic genes while inhibiting lineage commitment to other lineages. Investigating the epigenetic regulation of MSC cell fate decisions may shed light on potential therapeutic targets to improve MSC-based bone regeneration, and could provide implications for treatment of metabolic bone diseases. We have recently identified a demethylase complex regulating the osteogenic

differentiation of MSCs[79]. To evaluate the roles of histone demethylases in MSC cell fate determination, we systemically profiled the expression of histone demthylases in BMP4/7-stimulated MSCs, and identified two potential histone demethylases KDM4B and KDM6B that are induced by BMPs, thereby may play a role in regulating MSC lineage commitment.

Hence, in this thesis dissertation, I will focus primarily on addressing two topics: 1) the molecular regulation of osteoblast and osteoclast differentiation via non-canonical Wnt4 signaling; 2) the epigenetic regulation of MSC commitment to osteoblast lineage via histone demethylases KDM4B and KDM6B.

2 MATERIALS AND METHODS

2.1 Generation of transgenic mice and experimental animals.

We used the plasmid pGL647, which contained the Col2.3 promoter to specifically drive osteoblast-specific gene expression in vivo. We subcloned the mouse Wnt4 gene into pGL647, flanked by the Col2.3 promoter. The fragments of the Wnt4 transgene were purified and microinjected into C57BL/6 x SJL mouse oocytes (Charles River Laboratory) and the oocytes were surgically transferred to pseudopregnant C57BL/6 dams by the University of Michigan Transgenic Animal Model Core. We screened the founders by PCR using mouse tail genomic DNA and confirmed them by Southern blot analysis. We bred two transgenic founder mice with C57BL/6 mice for six generations to obtain a defined genetic background. TNFtg mice expressing hemizygous human TNF were purchased from Taconic Farms (#1006; B6.Cg(SJL)-Tg(TNF) N21+; Oxnard, California). Wild-type (WT) C57BL/6 mice for rWnt4 injection were purchased from Jackson Laboratory (Bar Harbor, Maine). In all experiments, female transgenic mice and female WT littermates as controls were used. We established a sample size of at least 8 mice per group in OVX and aging experiments based on our previous experience[130]. We used a sample size of at least 6 mice per group in TNFtg/Wnt4 experiments. The animals were randomly assigned to procedure groups including sham, OVX and rWnt4 injection. However, not all animal experiments were conducted in a completely blinded fashion. We ovariectomized 3-month-old transgenic and WT mice to induce osteoporosis. Two months after operation, we euthanized the mice and gathered their femurs for histological and μCT analysis. We collected blood samples and isolated serums for serology. Serum ELISA were performed with a mouse Trap5b assay kit (SBA Sciences), an Ocn ELISA kit (Biomedical Technologies), Il-6 and Tnf Quantikine ELISA kits (R&D Systems). All mouse protocols were approved by The University Committee on Use and Care of

Animals at the University of Michigan, the Animal Research Committee at the University of California-Los Angeles or both.

2.2 Cell Culture and Viral Infection.

Primary human and mouse MSCs were purchased from Texas A&M Health Science Center College of Medicine Institute for Regenerative Medicine at Scott & White Hospital. Cells were grown in a humidified 5% CO2 incubator at 37^0C in Dulbecco's modified Eagle's medium supplemented with 15% fetal bovine serum (FBS; Invitrogen, California, USA). These cells highly expressed CD73, CD90, CD105 and CD146 and were negative for CD34, CD45 and HLA. Lentiviral and retroviral packaging was prepared as described previously[79]. For viral infection, MSCs were plated overnight and then infected with viruses in the presence of polybrene (6 μg/ml, Sigma-Aldrich, USA) for 6 hr. The cells were then selected with puromycin for 3 days. Resistant clones were pooled and knock-down or over-expression was confirmed via Real-time RT-PCR or Western blot analysis. The target sequences for shRNA were: *KDM6B*sh1, 5'-GCAGTCGGAAACCGTTCTT-3'; *KDM6B*sh2, 5'-GTGGGAACTGAAATGGTAT-3'; *KDM4B*sh1, CCTGCCTCTAGGTTCATAA; and *KDM4B*sh3, GCTACGAAGTGAACTTCGA. For culturing of RAW264.7 cells, we used Dulbecco's modified Eagle's medium supplemented with 10% FBS. For primary bone marrow macrophages, we extracted bone marrow cells from mouse femurs, and treated them with 100 ng ml^{-1} mouse macrophage colony-stimulating factor (M-Csf; R&D systems) for 2 days. This allowed the induction to form osteoclast precursors used in the experiments. For induction of osteoclastogenesis, we treated the osteoclast precursors with 100 ng ml^{-1} mouse Rankl (R&D systems) for up to 3 days. In all *in vitro* experiments involving Wnt3a and Wnt4 recombinant proteins (R&D systems) and Rankl, we used 100 ng ml^{-1}.

2.3 Western Blot Analysis.

Cells were lysed in RIPA buffer (10 mM Tris-HCL, 1 mM EDTA, 1% sodium dodecyl sulfate (SDS), 1% Nonidet P-40, 1: 100 proteinase inhibitor cocktail, 50 mM β-glycerophosphate, 50 mM sodium fluoride). The samples were separated on a 10% SDS polyacrylamide gel and transferred to PVDF membrane by a semi-dry transfer apparatus (Bio-Rad). The membranes were blocked with 5% milk for 1 hr and then incubated with primary antibodies overnight. The immunocomplexes were incubated with horseradish peroxidase-conjugated anti-rabbit or anti-mouse IgG (Promega, Madison, WI) and visualized with SuperSignal Chemiluminiscent substrate (Pierce, Rockford, IL). Primary antibodies were purchased from the following commercial sources: anti-phospho-Tak1 (1:1000; 4531S; Cell Signaling, Danvers, Massachusetts), anti-Tak1 (1:1000; MAB5307; R&D systems), anti-phospho-p65 (1:2000; 3033S; Cell Signaling), anti-p65 (1:2000; 06-418; Millipore, Billerica, Massachusetts), anti-phospho-Iκbα (1:1000; 9246; Cell Signaling), anti-Iκbα (1:1000; sc-371; Santa Cruz, Santa Cruz, California), anti-phospho-JNK (1:500; 9251; Cell Signaling), anti-JNK (1:1,000; 9258; Cell Signaling), anti-phospho-p38 (1:1000; 9215; Cell Signaling), anti-p38 (1:1000; 8680; Cell Signaling), anti-phospho-Erk (1:1000; 4284; Cell Signaling), anti-Erk (1:1000; 4696; Cell Signaling), anti-Traf6 (2μg for immunoprecipitation; 1:1000 for Western blot; sc-8409; Santa Cruz), anti-Nlk (2μg for immunoprecipitation; AB10206, Millipore), anti-Tab2 (1:1000; 3744; Cell Signaling), anti-Nfatc1 (1:1000; sc-7294; Santa Cruz), anti-HA (1:2000; H9658; Sigma-Aldrich), anti-Smad4 (1:1000; Cell Signaling), anti-Tbp (1:2000; T1827; Sigma-Aldrich) anti-Flag (1:2000; Sigma-Aldrich) and anti-α-tubulin (1:10000; 75168; Sigma-Aldrich).

2.4 ALP, Alizarin Red Staining and Oil-Red-O Staining.

To induce MSC differentiation, MSCs were grown in mineralization-inducing media containing 100 μM/ml ascorbic acid, 2 mM β-glycerophosphate and 10 nM dexamethasone. For ALP staining, after induction, cells were fixed with 4% paraformaldehyde and incubated with a solution of 0.25% naphthol AS-BI phosphate and 0.75% Fast Blue BB dissolved in 0.1 M Tris buffer (pH 9.3). ALP activity assay was performed with an ALP kit according to the manufacturer's protocol (Sigma-Aldrich) and normalized based on protein concentrations. For detecting mineralization, cells were induced for 2-3 weeks, fixed with 4% paraformaldehyde and stained with 2% Alizarin red (Sigma-Aldrich). To quantitatively determine calcium mineral levels, Alizarin Red was destained with 10% cetylpyridinium chloride in 10 mM sodium phosphate for 30 minutes at room temperature. Concentration was determined by absorbance measurements at 562nm on a multiplate reader using a standard calcium curve in the same solution. The final calcium level in each group was normalized with the total protein concentrations.

To induce adipogenic differentiation, MSCs were grown in adipogenic-inducing media containing 0.5 mM isobutylmethylxanthine, 0.5 μM hydrocortisone, and 60 μM indomethacin (Sigma-Aldrich). Media were changed every 3 days. After 3 weeks of culture in vitro; Oil-Red-O staining was performed to detect the lipid droplets using an OIL-RED-O STAIN KIT according to the manufacturer's instruction (DBS, Pleasanton, CA, USA).

2.5 Real-time Reverse Transcriptase-Polymerase Chain Reaction (Real-time RT-PCR).

Total RNA was isolated from MSCs using Trizol reagents (Invitrogen). 2-μg aliquots of RNAs were synthesized using random hexamers and reverse transcriptase according to the manufacturer's protocol (Invitrogen). The real-time PCR reactions were performed using the QuantiTect SYBR Green PCR kit (Qiagen) and the Icycler iQ Multi-color Real-time PCR

Detection System. The human gene primer sequences used in real-time qPCR (mainly in Chapter 4) are provided in Table 2-1. The primers for histone demethylase profiling are provided in Table 2-2. The mouse gene primer sequences used in qPCR (mainly in Chapter 3) are provided in Table 2-3.

For extraction of tissue RNA, we dissected mouse femurs and pulverized them in liquid nitrogen. After extracting total RNA as described above, we removed residual genomic DNA using Turbo DNA-free DNase removal kit (Ambion).

2.6 Chromatin Immunoprecipitation (ChIP) assay

The assay was performed using a ChIP assay kit (Upstate, USA) according to the manufacturer's protocol. Cells were incubated with a dimethyl 3,3' dithiobispropionimidate-HCl (DTBP) (Pierce) solution (5 mmol) for 10 min at room temperature, followed by formaldehyde treatment for 15 min in a 37^0C water-bath. For each ChIP reaction, 2x 10^6 cells were used. All resulting precipitated DNA samples were quantified with Real-time PCR. Data are expressed as the percentage of input DNA. Antibodies for CHIP assays were purchased from the following commercial sources: polyclonal anti-KDM6B (Abgent, San Diego, CA); polyclonal anti-KDM4B (Millipore); polyclonal anti-H3K27me3 (Millipore); polyclonal anti-H3K9me3 (Abcam); polyclonal anti-p65 (Millipore); polyclonal anti-NFATc1 (Santa Cruz). The primer sequences used in ChIP assays are provided in Table 4.

2.7 Transplantation in nude mice

2 x 10^6 of cells were mixed with 40 mg of hydroxyapatite/tricalcium phosphate (HA/TCP) carrier (Zimmer) and then transplanted subcutaneously into the dorsal side of 10-week-old nude mice. 8 weeks after transplantation, the transplants were collected. The sample preparation and histology analysis were performed as previously described[130].

Table 2-1. Human Gene Primer sequences for real-time qPCR.

GENES	FORWARD (5'- 3')	REVERSE (5'-3')
RNA18S5	CGGCTACCAC ATCCAAGGAA	GCTGGAATTACCGCGGCT
SPP1	ATGATGGCCGAGGTGATAGT	ACCATTCAACTCCTCGCTTT
ALP	GACCTCCTCGGAAGACACTC	TGAAGGGCTTCTTGTCTGTG
BGLAP	AGCAAAGGTGCAGCCTTTGT	GCGCCTGGGTCTCTTCACT
IBSP	CAGGCCACGATATTATCTTTACA	CTCCTCTTCTTCCTCCTCCTC
HOXC6-1	CGGATAAGGGAGTCGAGTAGATCCG	TGAGGCATTTCTCGACCTATGG
DLX2	CCTGAGAAGGAGGACCTTGA	TTCCGGACTTTCTTTGGCT
DLX5	CGCTAGCTCCTACCACCAGT	GGCTCGGTCACTTCTTTCTC
PPARG	CGAGACCAACAGCTTCTCCTTCTCG	TTTCAGAAATGCCTTGCAGTGGT
CD36	CGATTAACATAAGTAAAGTTGCCATA	CGCAGTGACTTTCCCAATAGGAC

Table 2-2. Primer sequences used in profiling of histone demethylases.

GENES	FORWARD (5'-3')	REVERSE (5' – 3')
KDM4A	CCTCACTGCGCTGTCTGTAT	CCAGTCGAAGTGAAGCACAT
KDM4B	CGGGTTCTATCTTTGTTTCTCTCACCCG	AAGGAAGCCTCTGGAACACCTG
KDM4C	GGCATAGGTGACAGGGTGTGTC	CGGGGACCAAACTCTGGAAACCCG
KDM4D	CGGGATCTGCACAGATTATCCACCCG	AGTTTCTGAGGAGGGCGACCA
KDM5A	GTTTCTTAAGGTGGCAAGTC	TCTTTTGTACTGTTCCCTAC
KDM5B	AGCTTTCTCAGAATGTTGGC	GCAGAGTCTGGGAATTCACA
KDM5C	GGGTTTCTAAAGTGTAGATCT	CCACACATCTGAGCTTTAGT
KDM5D	ATCTCCTCACCTCTCCAAAG	TTGTCTCTAGGCGTGGCCGT
KDM3A	ACCTGCAGTTATTCTTCAGC	TAATGCCAGTCCTATGCCAT
KDM3B	TGTTCCCTGGGGACTCCTCT	GGGCACTACAGTACAGCTGG
JMJD1C	TTTGTTGAAGCTATTGACTG	CACTTTAACAAAAGCAAGCC
KDM2B	GTTAGTGGTAGTGGTGTTTTGG	AGCAGATGTGGTGTGTGGTC
KDM2A	CGGATAGTTGAGAAAGCCAAGATCCG	CTCTTTGGTGGGCCTCTGTAGC
KDM6A	CGTCCGAGTGTCAACCAACTGGACG	TGAGAGTCCTGGAGTAGGAGCAG
KDM6B	CTCAACTTGGGCCTCTTCTC	GCCTGTCAGATCCCAGTTCT
UTY	ATTCTGAAGCAATATCAGAC	TACAGTAATGAGCTGGTTCA
PHF2	TCGGCACTTCTCTGTTCTCCC	AAATCCAGCCCCTCCGTGTC
PTH8	CTTTCTCTACCTTGGGGACC	TAGGGACTCACGTGCTAGGG
KIAA1718	ATCTGTGAACTTTGGAGAGG	TAGGGACTCACGTGCTAGGG
LOC339123	AGCAAGCGACACACACTCAC	GCACTCAACTCTTCACAGGA
JMJD4	GGCCCTTCCAGAAATAAAGACC	CAGGCAGTGGCCATGAACAG
JMJD5	GTGGGGAGAGCCCAGAAGGACATT	GACCCACCCGTTTCCCAAAA
HAIRLESS	AGACCTCTGCCCTCTCTGCT	GCTTGGAACACAGCCCAGTC
FIH1	TTACTTAACCTCTCTGAGCC	CCAACAACCCTGAGGTAGAT
HSPBAP1	ACGTAGAAGCTACACTCGAAG	TAAGCCCAGAACTTGGAATG
JARID2	AAGTGCTGCTTACATCACTG	AGTGGATCATAGGACGTTCC
PTDSR	AGGTGGATCACTTGAGGTCA	CACCACACCTGGCTAATTTT
PLA2G4B	GCCCAGGCCACACATAATTT	AGTGGTAGCTTTCCATGTGG

Table 3. Mouse Gene Primer sequences used for real-time qPCR.

GENES	FORWARD (5'-3')	REVERSE (5'-3')
Runx2	AGGGACTATGGCGTCAAACA	GGCTCACGTCGCTCACTT
Sp7	CGCTTTGTGCCTTTGAAAT	CCGTCAACGACGTTATGC
Bglap	AGCAAAGGTGCAGCCTTTGT	GCGCCTGGGTCTCTTCACT
Alp	GGACAGGACACACACACACA	CAAACAGGAGAGCCACTTCA
Ibsp	ACAATCCGTGCCACTCACT	TTTCATCGAGAAAGCACAGG
Acp5	GTGCTGCTGGGCCTACAAAT	TTCTGGCGATCTCTTTGGCAT
Mmp9	TCCTTGCAATGTGGATGT	CTTCCAGTACCAACCGTCCT
Ctsk	GAAGAAGACTCACCAGAAGCAG	TCCAGGTTATGGGCAGAGATT
Birc3	ACGCAGCAATCGTGCATTTTG	CCTATAACGAGGTCACTGACGG
Cox2	AACCCAGGGGATCGAGTGT	CGCAGCTCAGTGTTTGGG
Tnf	CTGTAGCCCACGTCGTAGC	TTGAGATCCATGCCGTTG
Dkk1	CTCATCAATTCCAACGCGATCA	GCCCTCATAGAGAACTCCCG
Axin2	TGACTCTCCTTCCAGATCCCA	TGCCCACACTAGGCTGACA
Wnt4 (endogenous)	CTGGAGAAGTGTGGCTGTGA	CAGCCTCGTTGTTGTGAAGA
Wnt4 (transgene)	CTAAAGCCATTGACGGCTGC	GCGTAATCTGGAACATCATATGGG
Opg	ACCCAGAAACTGGTCATCAGC	CTGCAATACACACACTCATCACT
Tnfsf11	CAGCTATGATGGAAGGCTCA	GACTTTATGGAACCCGA
β-actin	CGTCTTCCCCTCCATCG	CTCGTTAATGTCACGCAC

Table 4. Primer sequences used for ChIP assays.

GENES	FORWARD (5'-3')	REVERSE (5'-3')
BMP2	TGGATCCCACGTCTATGCTA	TCAGGGTCTGGCCTCTTATT
BMP2 (3kb down)	CAATCATAAGAATTACCTGTTGGG	TGGTCGCATTATACTCATATTGG
BMP4	CAGTTTATGGAAGGCCACCT	GTAACTGCTGCCCAAACTGA
BMP4 (3kb down)	TCTCTCCGGAATCGTCTCTC	AGAAGGTGGTCTGGGAGCTA
HOXC6-1	CGTGATGGCATTTTCAGCCTATATC	GAAACAGCGGAAAGTGTGCAG
HOXC6-1 (3kb down)	CATTTATCAACCCTGGCCTT	GACCCTCCTCAACACCTCTC
DLX5	GGATTTCGGGAGTTTCCATT	CGGAGTCGCCAGAAATAAAG
DLX5 (3kb down)	CCAAGAGCTGCAGTCAGATT	CCGTCCTACTCCCTTCACTC
Nfatc1	CTGTGTTCCCACATGTCCTC	GCGACTGCAGTGTGTTCTTT
Nfatc1 (9kb down)	CTGGCACCAAAGTTGAGAGA	GATGGCTCTACCTGCACAGA

2.8 OVX, bone histomorphometry, and scoring of arthritic joint swelling.

We performed OVX or sham operation on 3-month-old female WT and Wnt4 mice under isofluorane anesthesia. For the preventive model, rWnt4 proteins (8 μg kg^{-1}) were intraperitoneally injected daily for three weeks immediately after the surgery. For dual-labeling, mice received intraperitoneal injection of calcein (0.5 mg per mouse, Sigma-Aldrich) ten and three days before euthanasia. Mice were euthanized one month after OVX. For the therapeutic model, we first performed OVX on 3 month-old mice and waited for one month to establish bone loss. Mice received intraperitoneal injection of rWnt4 (20 μg kg^{-1}) or vehicle control daily for one month before collection of bone samples. Eight to twelve mice were used in each group.

Following euthanasia, we fixed right femurs in 70% ethanol for 48 h and embedded in methyl methacrylate. 8 μm longitudinal sections were either stained with Toluidine blue for osteoblast count or examined under fluorescent microscope to evaluate BFR and MAR as described previously[22]. We fixed left femurs in 10% formaldehyde and embedded them in paraffin for preparation in 5 μm-thick sections. We analyzed osteoclast parameters after TRAP staining as described. For all bright-field and fluorescent microscopy analysis, we used Olympus-IX51 inverted microscope with SPOT advanced 4.0 and CellSens software. We also collected blood samples and isolated serums to perform ELISA with a mouse Trap5b assay kit (SBA Sciences), an Ocn ELISA kit (Biomedical Technologies), Il6 and Tnf Quantikine ELISA kits (R&D Systems).

We scored the swelling of hindpaws on 1-year-old TNFtg and TNFtg/Wnt4 mice on a scale of 0 to 3, as previously described: 1 = mild arthritis (mild swelling of joint and paw); 2 = moderate arthritis (severe swelling and joint deviation); 3 = severe arthritis (ankylosis detected upon flexion). We used histological sections of hindpaw and ankle joints to examine the tibiotalar and interdigital

joints, and performed μCT imaging to further evaluate bone erosion and destruction of joint space associated with arthritis.

2.9 Immunostaining and μCT analysis of mice.

We extracted femurs from euthanized mice and fixed them in 10% neutral buffered formalin for 24 hrs. For μCT scanning, the specimens were fitted in a cylindrical sample holder (20.5 mm in diameter) with the long axis of the femur perpendicular to the X-ray source. We used a Scanco μCT40 scanner (Scanco Medical) set to 55kVp and 70μA. The bone volume (mm^3) over tissue volume and bone mineral density in the region of interest were measured directly with μCT Evaluation Program V4.4A (Scanco Medical). We defined the regions of interest as the areas between 0.3 mm and 0.6 mm proximal to the growth plate in the distal femurs, in order to include the secondary trabecular spongiosa. We used a threshold of 250 was used for evaluation of all scans[22]. For visualization, we imported the segmented data and reconstructed them as a 3D-image displayed in μCT Ray V3.0 (Scanco Medical).

After scanning, we decalcified the specimens, sectioned them for staining as previously described[22]. Antibodies used include rabbit polyclonal anti-NLS-p65 (600-401-271; 1:200; Rockland), rabbit polyclonal anti-Mmp9 (38898; 1:500; Abcam), rabbit polyclonal anti-Tnf (34674, 1:200; Abcam), and rabbit polyclonal anti-Cox2 (15191, 1:400, Abcam). For quantification of p65 positive staining, we selected at least 10 images from each section per femur, measured the integral optical density (IOD) of nuclear-stained p65 using the Image Pro Plus 6.0 software (MediaCybernetics). We normalized the IOD by stained area, and presented the data as reported previously[62].

For immunofluorescence double staining, antigen retrieval was performed by pressure cooking in a Decloaking chamber (Biocare Medical) in citrate buffer (2.1 g/L citric acid, pH 6.0) at 120 ^{0}C for 20 min. The sections were incubated with monoclonal anti-nestin (Lifespan BioSciences, 1 in 500) and polyclonal anti-H3K9me3 (Abcam, 1 in 500) or polyclonal anti-H3K27me3 (Millipore, 1:500) at 4°C overnight. After washing with PBS solution for 3 times, the sections were incubated with appropriate Cy2 (red) and Cy3 (green) conjugated secondary antibodies (Jackson ImmunoResearch, 1:100) in darkness at room temperature for 1 hour. After applying the Slowfade® antifade reagent (Invitrogen), the sections were imaged with a confocal laser scanning microscope (Leica TCS-SP inverted), and the Leica Confocal Software (LCS version 2.61 Build 1537).

2.10 Microarray procedure and data analysis.

Scrsh, KDM4Bsh and KDM6Bsh MSCs were treated with 150ng/ml BMP4/7 for 0, 4 and 24hrs respectively. The extraction of total RNA was performed with miRNeasy kit (Qiagen) per manufacturers' instructions. 1μg of RNA from each sample was hybridized to Affymetrix U133 Plus 2.0 Arrays at the UCLA DNA Microarray Facility. Differential gene expression analysis was performed based on the generated metadata txt file. >1.6fold change (37% inhibition) in expression compared to Scrsh was considered significant down-regulation, and >1.4fold change at any time point was considered as BMP-induction. To investigate enriched biological functions associated with KDM4B/KDM6B-dependent genes, GO analysis was performed using the online Database for Annotation, Visualization and Integration Discovery (DAVID) Bioinformatics Resources v6.7. P values were calculated based on hypergeometric distribution. Only significantly overexpressed

($p<0.05$) GO terms were included. Heatmap was generated via PermutMatrix v1.9.3 (Caraux and Pinloche, 2005) to reflect fold change relative to median expression of each gene in Log_2 ratio.

2.11 Statistical Analysis

Numerical data and histograms were expressed as the mean ± standard deviation. In comparisons between two groups, two tailed Student's t-test was performed and a difference was considered statistically significant with $P < 0.05$. In multiple group comparisons, one-way ANOVA was employed with Tukey's methods as post-hoc adjustment for Type I errors. To compare the rate of decline in BMD and BV/TV in aged mice, we employed two-way ANOVA analysis to test for interaction between genotype and age. An interaction with $P < 0.05$ was considered significant.

3 MOLECULAR REGULATION OF OSTEOBLAST AND OSTEOCLAST DIFFERENTIATION BY NON-CANONICAL WNT4 SIGNALING

3.1 Wnt4 promotes bone formation *in vivo*

Previously we found that Wnt4 could promote osteoblastic differentiation of MSCs *in vitro* and enhance craniofacial bone regeneration[64]. To explore whether Wnt4 promoted bone formation *in vivo*, we generated transgenic mice in which Wnt4 was driven by the mouse 2.3 kb type 1 collagen promoter (Col2.3) promoter. The Col2.3 promoter contains a 2.3kb DNA fragment upstream of the transcription start site of the *Col1a1* gene[152], and has been shown to drive gene expression specifically in differentiated osteoblasts[153]. After zygote injection, seven of the 10 potential founders screened displayed strong expression of the transgene (**Fig. 3-1A**), thus allowing establishment of two separate transgenic mouse lines (TG1 and TG7). While transgenic Wnt4 proteins were undetectable in primary calvarial cells from WT mice, Wnt4 proteins in calvarial cells from TG1 and TG7 mouse lines were induced as the cells differentiated into osteoblasts in osteogenic media (**Fig. 3-1B**). Reverse transcriptase-polymerase chain reaction (RT-PCR) confirmed that Wnt4 transgene mRNA was expressed in bone tissue, but not in brain, heart, kidney, liver, spleen, or muscle using the TG7 line (**Fig. 3-1C**).

Next we investigated if Wnt4 would enhance bone formation *in vivo* using the TG7 line. Of note, Wnt4 mice had a phenotypically normal skeleton at birth (data not shown). μCT analysis of the secondary spongiosa of distal femur metaphyses revealed that the bone mineral density (BMD) of Wnt4 mice was significantly higher compared to wild type littermates (WT) at 1, 2 and 3 months (**Fig. 3-2A**). Similarly, bone volume/tissue volume (BV/TV) was significantly higher in Wnt4 mice compared to WT mice (**Fig. 3-2B**), in consistence with the greater amount of trabecular bones shown in HE staining (**Fig. 3-2C**). Similarly, characterization of the TG1 mouse line also

confirmed that Wnt4 enhanced bone formation *in vivo*, ruling out variations due to mouse strains (**Fig. 3-2D**). Histomorphometric analysis revealed mildly higher osteoblast counts in Wnt4 mice compared to WT mice (**Fig. 3-3A**). To further confirm that increased BMD was due to enhanced osteoblast function, we performed dynamic histomorphometric analysis over a 7-day period using calcein labeling[22], and found that bone formation rate (BFR) in 3-month-old Wnt4 mice was significantly higher compared to WT mice (**Fig. 3-3B**).

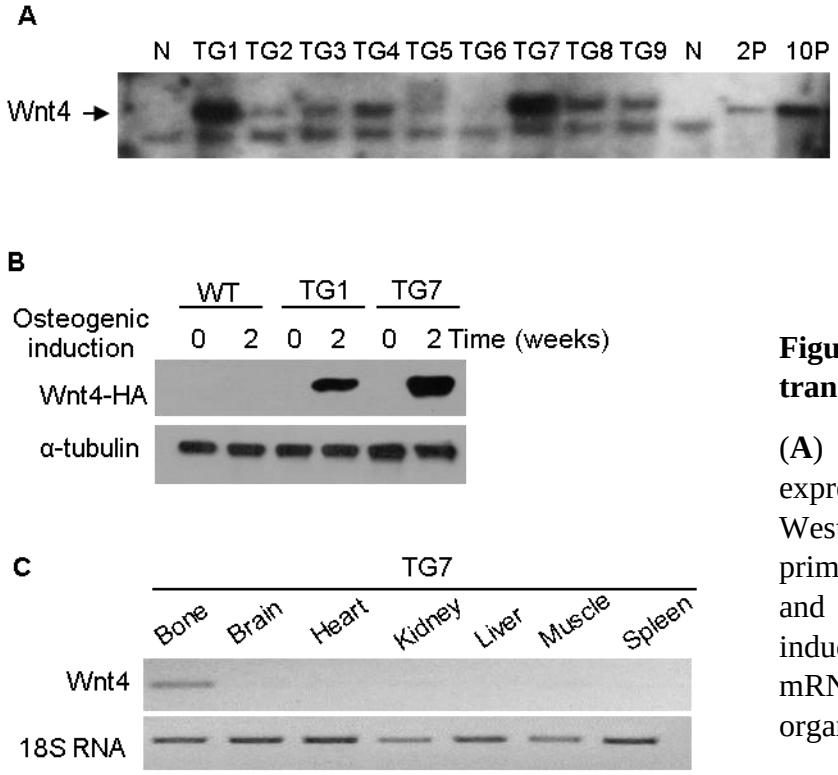

Figure 3-1. Generation of Wnt4 transgenic mice.

(**A**) Southern blot of Wnt4 transgene expression in 10 founder mouse lines. (**B**) Western blot showing Wnt4 expression in primary calvarial cells extracted from WT and Wnt4 mice following osteogenic induction. (**C**) RT-PCR analysis of *Wnt4* mRNA expression in various tissues and organs.

To examine if Wnt4 enhanced osteoblastic activity in a cell-autonomous manner, we isolated bone marrow MSCs from femurs of Wnt4 mice and WT mice. Primary MSCs from Wnt4 mice demonstrated enhanced osteogenic potential, as evidenced by alkaline phosphatase (ALP) staining and Alizarin Red staining (ARS), when cells were induced by osteogenic medium (**Fig. 3-4A, B**). Furthermore, Real-time RT-PCR showed greater mRNA expression of the master

osteogenic transcription factors *Runx2* and *Sp7* (**Fig. 3-4C**), as well as mineralization markers *Ibsp* and *Biglap* (**Fig. 3-4D**) in differentiated osteoblasts from Wnt4 mice compared with WT mice.

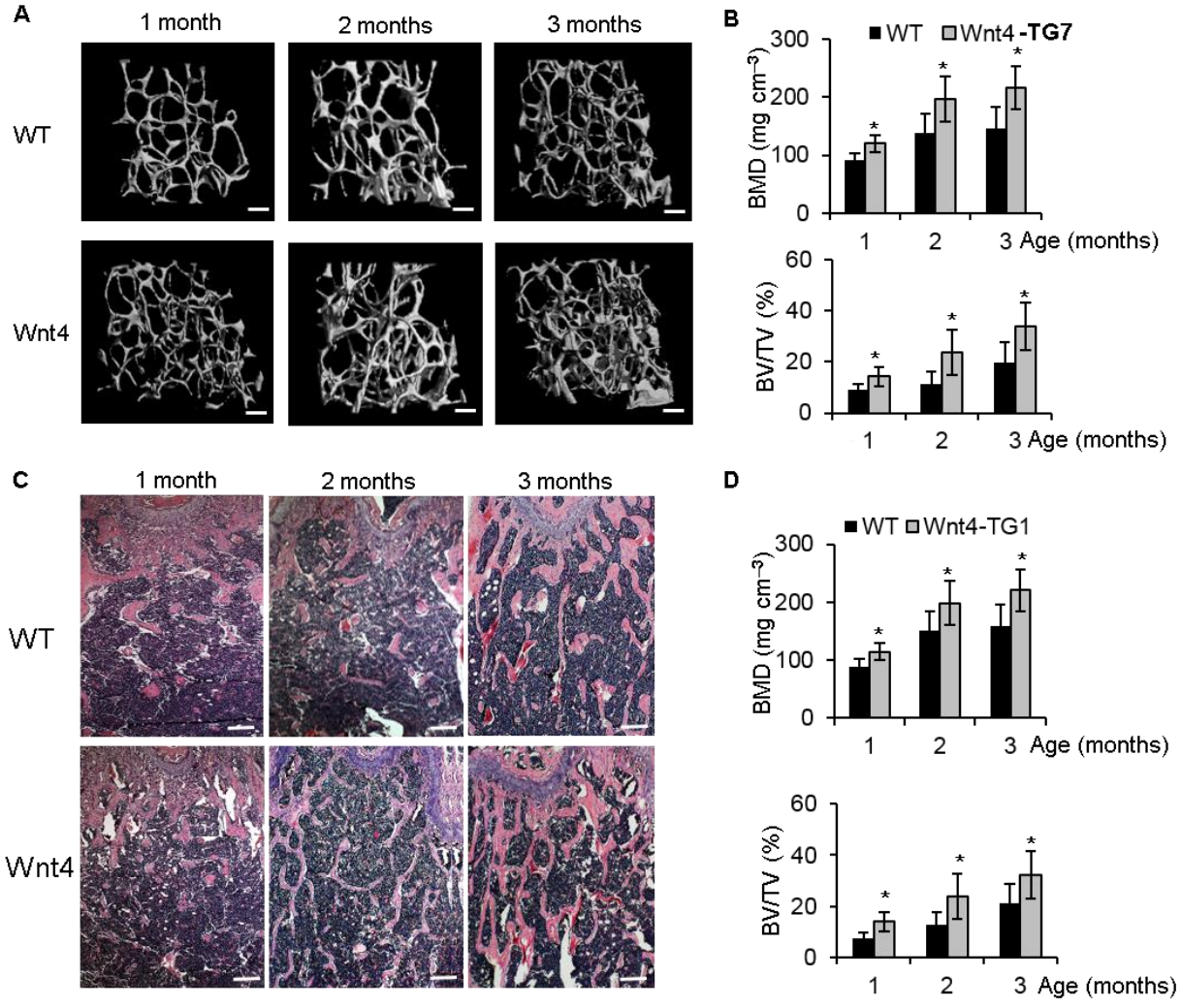

Figure 3-2. Wnt4 promoted postnatal bone formation *in vivo*.

(**A-B**) μCT reconstruction (**A**), BMD as well as BV/TV (**B**) of trabecular bone of distal femurs from 1, 2, and 3-month-old Wnt4 mice (TG7 strain) and WT littermates. Scale bars, 200 μm; $n = 12$ per group. (**C**) Representative H&E staining of femur sections from 1, 2, and 3-month-old WT and Wnt4 mice. Scale bars, 300 μm. (**D**) BMD as well as BV/TV of trabecular bone of distal femurs from 1, 2, and 3-month-old Wnt4 mice (TG1 strain) and WT littermates.

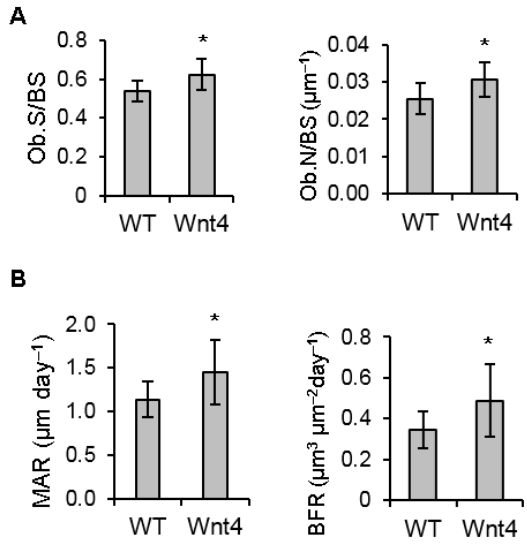

Figure 3-3. Wnt4 increased osteoblast differentiation and bone formation.

(**A**) Histomorphometric analysis of osteoblast counts in 3-month-old Wnt4 (*n* = 10) vs WT mice (*n* = 8). Ob.S, osteoblast surface. Ob.N, osteoblast number. BS, bone surface. (**B**) BFR and MAR measurements from dual-fluorescent calcein labeling of 3-month-old Wnt4 (*n* = 10) vs WT mice (*n* = 8). *: P < 0.05 by two-tail Student's t-test.

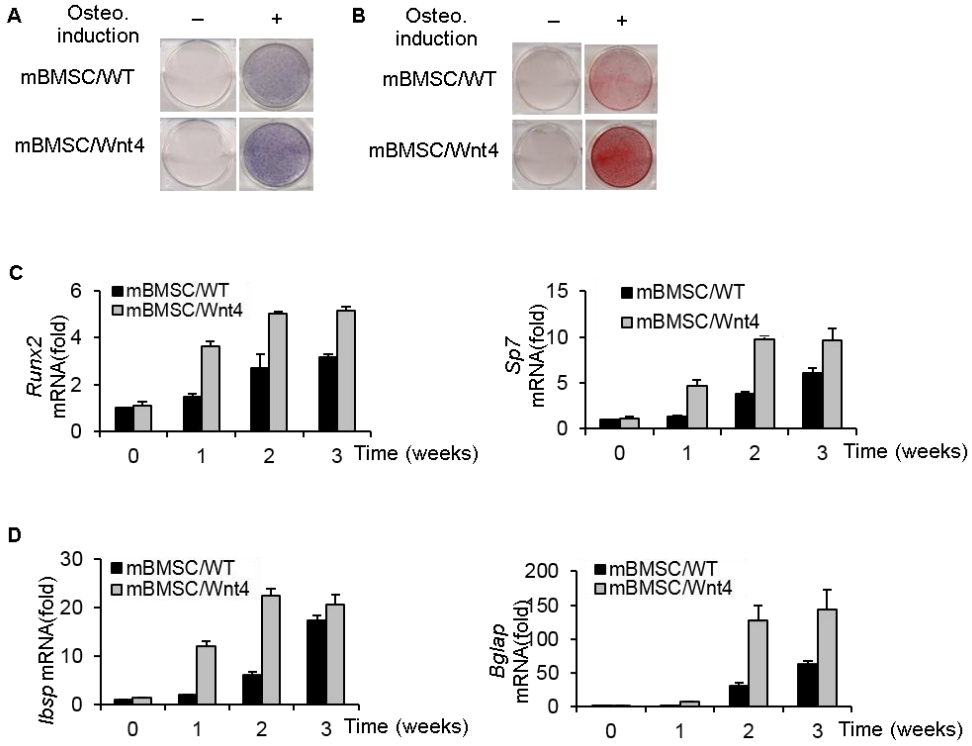

Figure 3-4. Wnt4 from osteoblasts promoted osteoblast differentiation of MSCs.

(**A**) ALP staining of femur bone marrow MSCs from Wnt4 vs WT mice, after osteogenic induction for 7 days. (**B**) ARS of MSCs from Wnt4 vs WT mice after osteogenic induction for 2 weeks. (**C**) mRNA expression of master regulators *Runx2* and *Sp7* in MSCs isolated from WT and Wnt4 mouse bone marrow. (**D**) mRNA expression of early and late stage osteogenic marker genes.

3.2 Wnt4 prevents estrogen deficiency-induced osteoporosis

To mimic the molecular pathogenesis of osteoporotic bone loss, mouse ovariectomy (OVX) has been widely used as a model to induce estrogen deficiency-mediated osteoporosis[130,154,155]. We performed OVX or sham operation on 3-month-old WT and Wnt4 mice. μCT analysis of femurs revealed significant trabecular bone loss in WT mice compared to sham control 2 months post OVX. In contrast, bone loss was markedly lower in Wnt4 mice after OVX (**Fig. 3-5A**). Quantitative measurements showed that, whereas 47% of BMD and 48% of BV/TV were lost in WT mice after OVX, only 27% of BMD and 24% of BV/TV were lost in Wnt4 mice (**Fig. 3-5B**). Following OVX, BFR increased in WT mice to compensate for the accelerated bone resorption, while in Wnt4 mice, osteoblastic activity was further enhanced (**Fig. 3-5C**). Similarly, osteoblast number and surface were significantly higher in Wnt4 versus WT mice in both OVX and sham groups (**Fig. 3-5D**). In contrast, we observed lower osteoclast number and surface in Wnt4 mice compared to WT mice in both OVX and sham groups (**Fig. 3-5E**), consistent with TRAP staining results (**Fig. 3-5F**). We also performed ELISA to assess the serum markers of bone turnover. The serum concentrations of osteocalcin (Ocn), a marker for bone formation, were significantly higher in Wnt4 mice compared to WT mice after OVX (**Fig. 3-6A**). In contrast, OVX induced higher serum concentrations of Trap5b, a marker for bone resorption, in WT but not in Wnt4 mice (**Fig. 3-6B**).

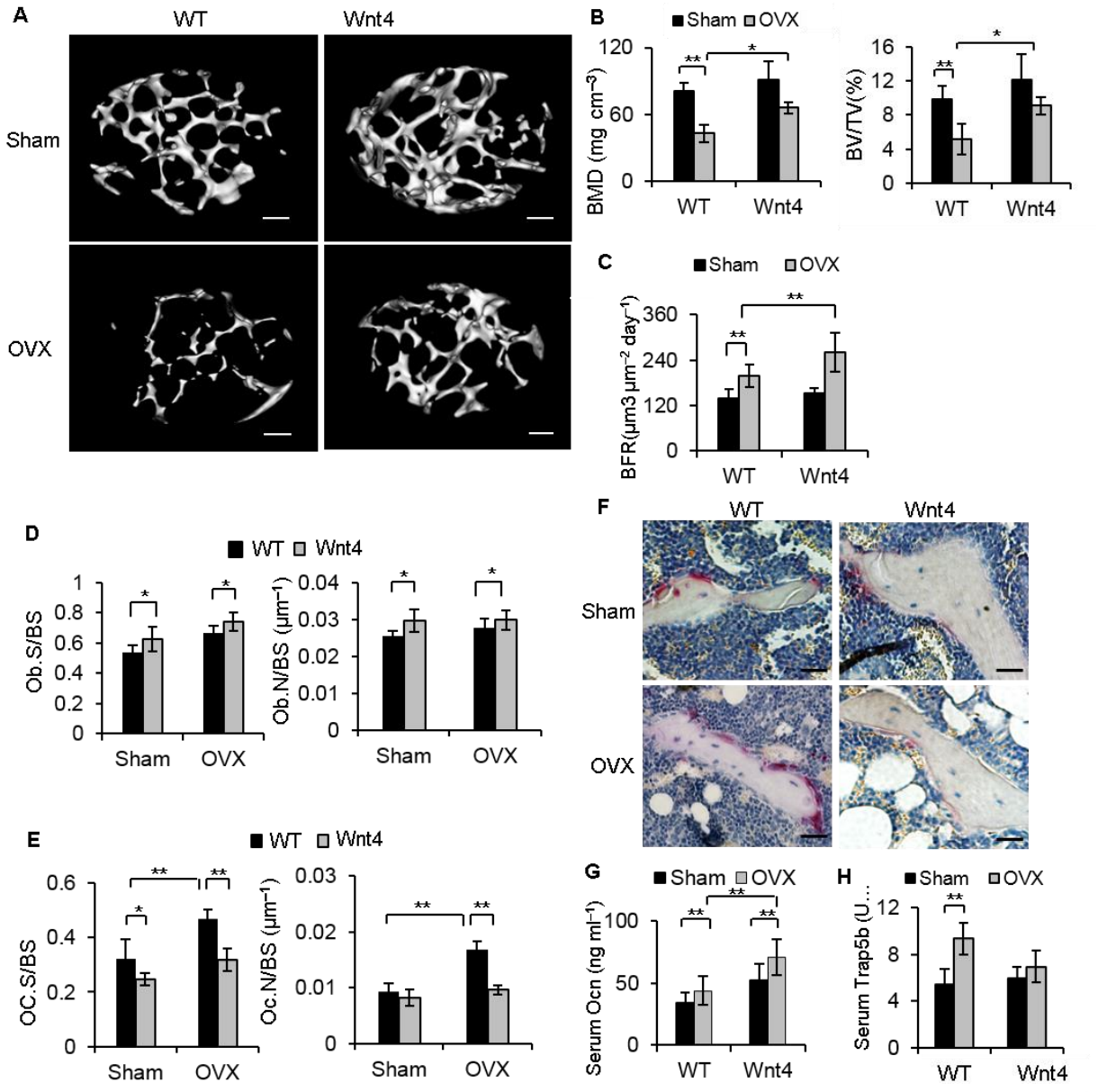

Figure 3-5. Wnt4 suppressed estrogen-deficiency induced bone loss.

(**A, B**) μCT reconstruction (**A**) of metaphysis of distal femurs, as well as trabecular BMD and BV/TV (**B**) in WT vs Wnt4 mice at two months post OVX. Scale bars, 200 μm. (**C**) BFR measurement of calcein dual labeling in WT vs Wnt4 mice two months after OVX or sham operation. (**D, E**) Morphometric analysis of osteoblast counts (**D**) and osteoclast counts (**E**) in WT vs Wnt4 mice after OVX or sham operation. **P* < 0.05, ** *P* < 0.01 by One-way ANOVA with Tukey's posthoc test. (**F**) TRAP staining of femur sections from WT and Wnt4 mice after OVX or sham operation. Scale bars, 30μm. (**G, H**) ELISA of serum concentrations of Ocn (**G**), Trap5b (**H**) in WT vs Wnt4 mice after OVX or sham operation. **P* < 0.05, ** *P* < 0.01, unpaired two-tailed t-test. For **B–E,** and **G–H**, *n* = 8 for sham groups; *n* = 12 for OVX groups.

Studies have implicated pro-inflammatory cytokines, including tumor necrosis factor (Tnf) and interleukin-6 (Il-6), as important mediators of accelerated bone loss in osteoporosis[144,156]. Consistently, OVX induced an elevation in serum concentrations of Tnf and Il-6 in WT mice, but such induction was suppressed in Wnt4 mice (**Fig. 3-6A**). Immunostaining of activated p65 in femur sections revealed enhanced NF-κB activity in osteoclasts and bone marrow cells surrounding trabecular bones following OVX. In contrast, the NF-κB activation by OVX was significantly less pronounced in Wnt4 mice (**Fig. 3-6B**). To further confirm the inhibition of NF-κB by Wnt4 *in vivo*, we immunostained NF-κB-dependent targets, including Tnf, Cycloxygenase-2 (Cox-2) and Matrix metallopeptidase 9 (Mmp9). Consistently, we found that Wnt4 also potently reduced the expression of Tnf (**Fig. 3-6C**), Mmp9 (**Fig. 3-6D**), and Cox2 (**Fig. 3-6E**) induced by OVX *in vivo*.

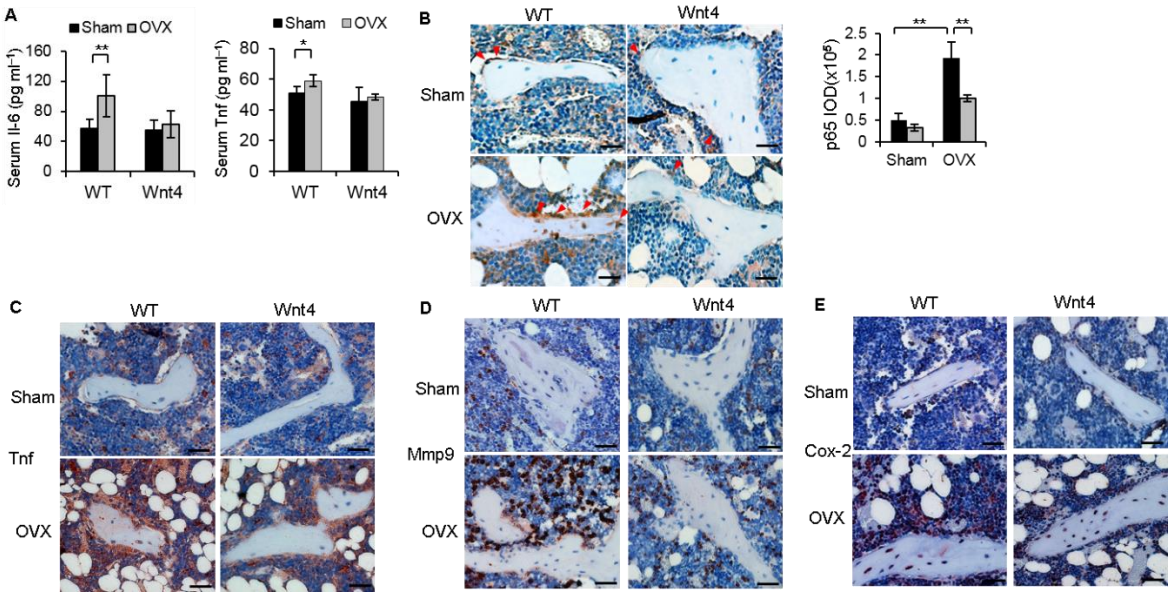

Figure 3-6. Wnt4 attenuated OVX-induced NF-κB signaling in bone marrow.

(**A**) ELISA of serum concentrations of Il-6 and Tnf after OVX or sham operation. (**B-E**) Immunostaining and quantification of active p65 (**B**), Tnf (**C**), Mmp9 (**D**) and Cox-2 (E) in trabecular bone cells and surrounding bone marrow cells in WT and Wnt4 mice after OVX or sham operation. Scale bars, 30μm. IOD, integral optical density. *: $P < 0.05$; **: $P < 0.01$ by one-way ANOVA.

3.3 Wnt4 inhibits inflammatory bone loss induced by TNF

TNF is a potent inducer of inflammation by activating NF-κB. TNF-transgenic (TNFtg) mice develop systemic bone loss and osteoporosis in addition to erosive arthritis by promoting osteoclastogenesis and inhibiting bone formation[157-160]. To further determine whether Wnt4 could directly inhibit inflammation-associated bone loss, we bred TNFtg mice with Wnt4 mice. There was severe paw and joint swelling, often associated with joint deviation in 1-year-old TNFtg mice (**Fig. 3-7A**). μCT (**Fig. 3-7B**) and histological analysis (**Fig. 3-7C**) revealed that there were extensive joint cartilage destruction and bone erosions due to invasion of inflammatory cells. In contrast, there was significantly less joint swelling, bone erosion and inflammation in TNFtg/Wnt4 mice than in TNFtg mice of comparable age.

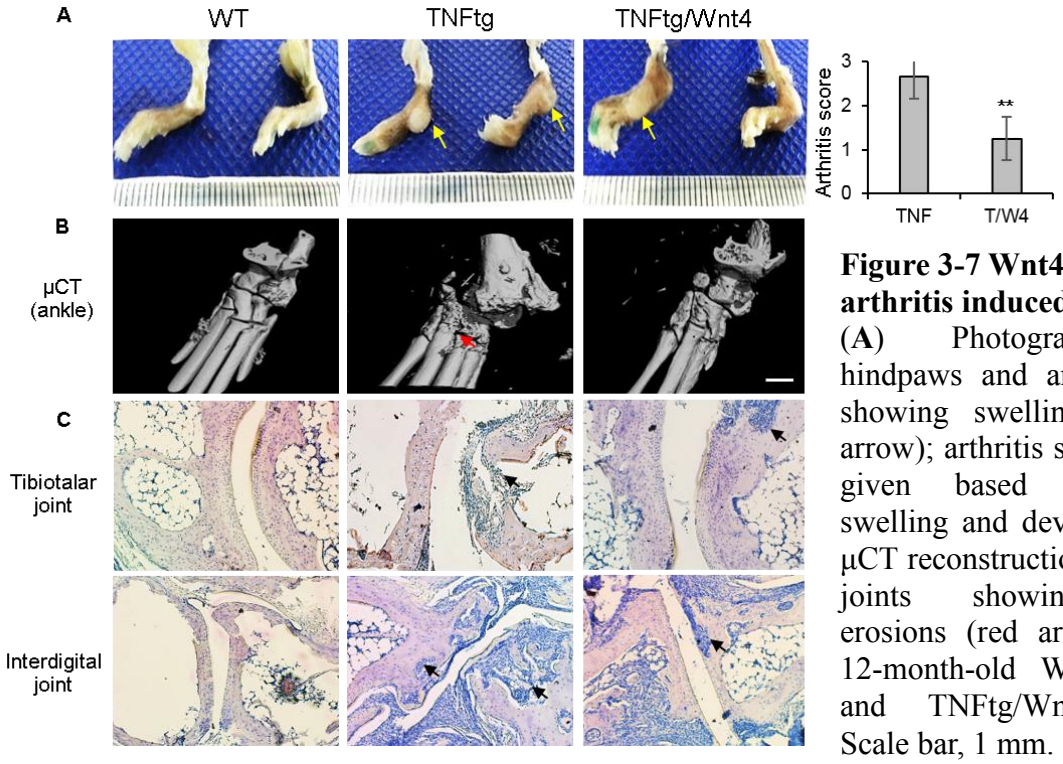

Figure 3-7 Wnt4 alleviates arthritis induced by TNF. (**A**) Photographs of hindpaws and ankle joints showing swelling (yellow arrow); arthritis scores were given based on joint swelling and deviation. (**B**) μCT reconstruction of ankle joints showing bony erosions (red arrow) from 12-month-old WT, TNFtg and TNFtg/Wnt4 mice. Scale bar, 1 mm. (**C**) H&E staining of tibiotalar and interdigital joints showing visible joint cartilage destruction and bone erosions due to invasion of inflammatory cells (black arrows). Scale bar, 200 μm. T/W4: TNFtg/Wnt4 mice. ** $P < 0.01$ by Student's t-test.

Consistent with previous studies, μCT analysis revealed systemic bone loss suffered by 1-year-old TNFtg mice compared with WT mice. However, bone loss in TNFtg/Wnt4 femurs was markedly mitigated (**Fig. 3-8A**). Quantitative measurements revealed that, whereas 31% of BMD and 68% of BV/TV were lost in TNFtg mice compared to WT mice, only 18% of BMD and 28% of BV/TV were lost in TNFtg/Wnt4 mice (**Fig. 3-8B**). As the reduced bone loss could be due to either increased bone formation or slowed bone resorption or both, we examined the effect of Wnt4 on both components of bone homeostasis. The reduction in the BFR and mineral apposition rate (MAR) in TNFtg mice were alleviated in TNFtg/Wnt4 mice (**Fig. 3-8C**). Consistently, histomorphometric analysis also showed 24% greater osteoblast counts in TNFtg/Wnt4 than TNFtg mice (**Fig. 3-8D**). Since it has been shown that osteoclastogenesis and bone resorption were enhanced in TNFtg mice, we then examined the effect of Wnt4 on accelerated bone resorption in TNFtg mice. Histomorphometric analysis also revealed that, while osteoclast activity was higher in TNFtg mice compared to WT controls, it was significantly lower in TNFtg/Wnt4 mice (**Fig. 3-8E**). Consistently, TRAP staining also confirmed the reduction in osteoclasts in TNFtg/Wnt4 mice compared to TNFtg mice (**Fig. 3-9A**). The serum concentrations of OCN were significantly lower in TNFtg mice than that in TNFtg/Wnt4 mice (**Fig. 3-9B**). On the other hand, the serum concentrations of TRAP5b were significantly higher in TNFtg mice than in TNFtg/Wnt4 mice (**Fig. 3-9C**).

We observed that the serum Il-6 concentration in TNFtg/Wnt4 mice was only 55% of that in TNFtg mice (**Fig. 3-10A**). Since TNF is a potent activator of NF-κB which is associated with osteoporosis and skeletal aging[130,136,161], Wnt4 might inhibit TNF-induced NF-κB activation in the TNFtg/Wnt4 mice. Immunostaining of active p65 revealed markedly enhanced NF-κB activity in the proximity of trabecular bones in TNFtg mice, while NF-κB staining was significantly reduced

in TNFtg/Wnt4 mice (**Fig. 3-10B**). Moreover, Wnt4 also inhibited the expression of Cox-2 and Mmp9 in osteoclasts and bone marrow cells induced by TNF *in vivo* (**Fig. 3-10C, D**).

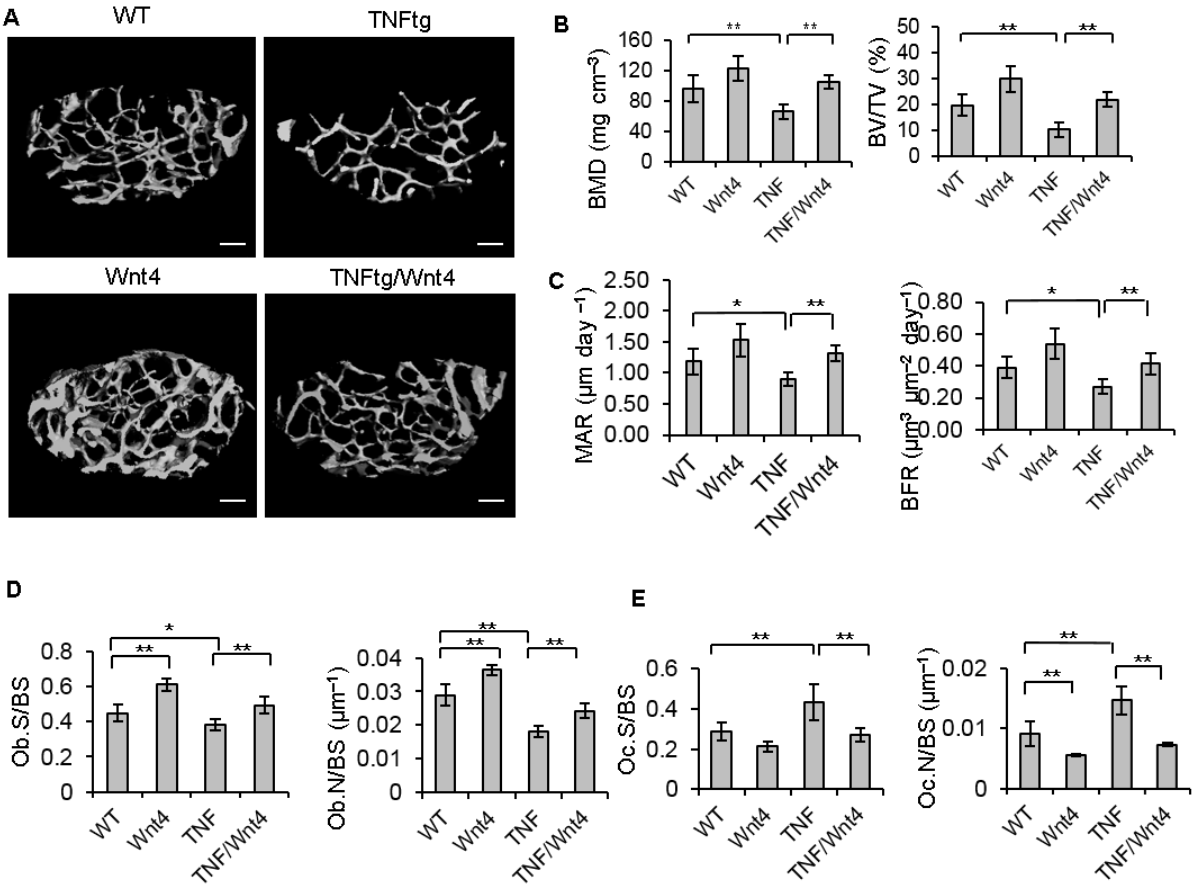

Figure 3-8. Wnt4 inhibits TNF-induced bone loss.

(**A**) μCT reconstruction and (**B**) trabecular BMD and BV/TV of distal femoral metaphysis regions from WT, Wnt4, TNFtg and TNFtg/Wnt4 mice. Scale bars, 200 μm. (**C**) Comparisons of MAR and BFR in TNFtg mice and TNFtg/Wnt4 mice. (**D, E**) Morphometric analysis of osteoblast counts (**D**) and osteoclast counts (**E**) in TNFtg mice and TNFtg/Wnt4 mice. $n = 6$ per group for WT and WNT4 mice; $n = 8$ per group for TNFtg and TNFtg/Wnt mice. *$P < 0.05$, ** $P < 0.01$ by one-way ANOVA.

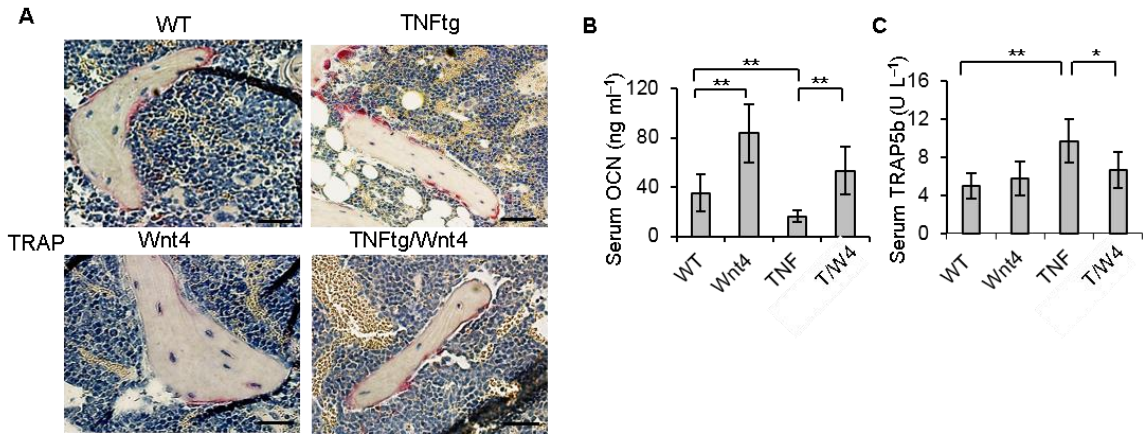

Figure 3-9. Wnt4 suppresses TNF-induced osteoclast activation

(**A**) TRAP staining of osteoclasts surrounding trabecular bones in WT, Wnt4, TNFtg and TNFtg/Wnt4 mice. Scale bars, 40μm. (**B, C**) ELISA of Ocn (**B**) and Trap5b (**C**) concentrations in serum collected from WT, Wnt4, TNFtg and TNFtg/Wnt4 mice. $n = 6$ per group for WT and WNT4 mice; $n = 8$ per group for TNFtg and TNFtg/Wnt mice. *$P < 0.05$, ** $P < 0.01$ by one-way ANOVA.

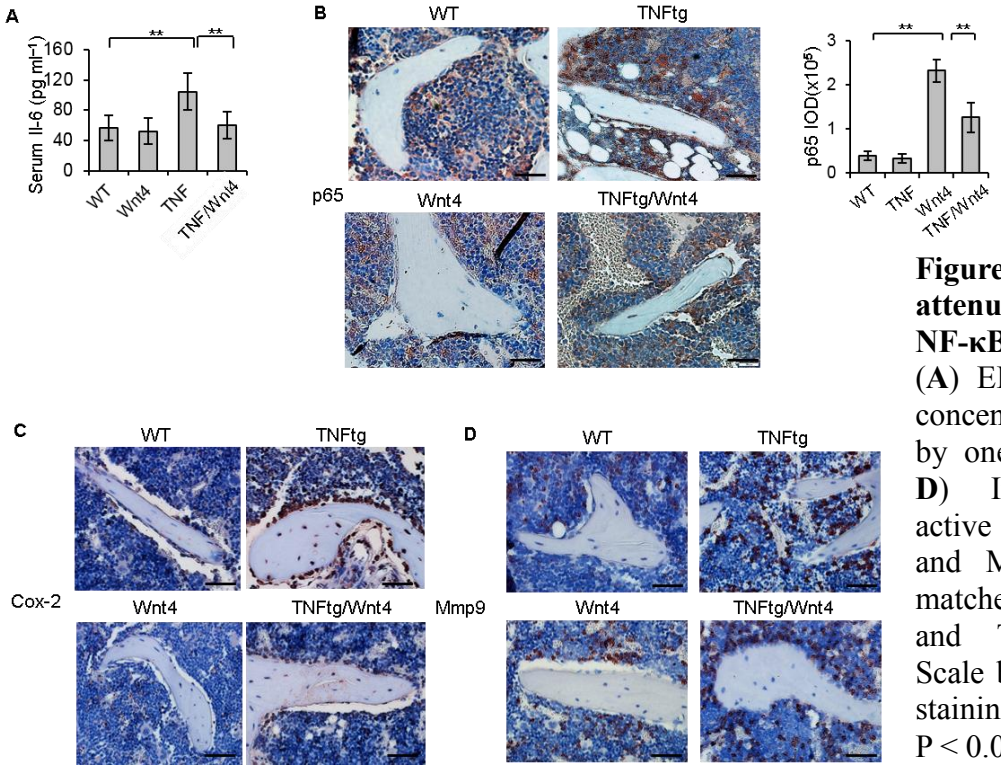

Figure 3-10. Wnt4 attenuated TNF-induced NF-κB signaling.
(**A**) ELISA of serum Il-6 concentrations. **: $P < 0.01$ by one-way ANOVA. (**B-D**) Immunostaining of active p65 (**B**), Cox-2 (**C**) and Mmp9 (**D**) in age-matched WT, Wnt4, TNFtg and TNFtg/Wnt4 mice. Scale bars, 25μm. For p65 staining quantification, **: $P < 0.01$ by Student's test.

3.4 Wnt4 prevents skeletal aging and bone loss

Aging creates a pro-inflammatory environment with elevated levels of cytokines that contribute to various chronic diseases including osteoporosis or osteopenia[115,162,163]. We further examined whether Wnt4 could protect against natural aging-mediated bone loss or osteopenia. μCT analysis revealed that there was a gradual loss of trabecular bone mass with advancing age from 6 to 24 months in WT mice (**Fig. 3-11A**). Based on literature, the most dramatic age-related loss in the femoral trabecular bone of C57BL/6J mice takes place between 6 and 12 months of age; after 12 months, the bone loss is more gradual especially in female mice[164]. Further quantitative analysis showed that the most dramatic loss occurred between 6 and 12 months of age and average BMD dropped 42.7% while BV/TV dropped 51.9%. However, the reduction was significantly less with Wnt4 mice, with 32.0% in BMD and 41.9% in BV/TV respectively (**Fig. 3-11B**). While Wnt4 mice showed higher trabecular bone mass than WT mice across the ages, we wanted to assess if Wnt4 protected against skeletal aging. We performed two-way ANOVA for both trabecular BMD and BV/TV during the period of most dramatic bone loss (between 6 and 12 months), and found significant interaction between genotype and age, thereby confirming age-related trabecular bone loss occurred at a slower rate in Wnt4 mice.

Histological staining also confirmed that aged Wnt4 mice lost less trabecular bone than aged WT mice (**Fig. 3-11C**). Of note, we confirmed that Wnt4 transgene mRNA in bone tissues was still expressed in aged Wnt4 mice using RT-PCR although the levels of Wnt4 mRNA declined over age (**Fig. 3-12A, B**). Immunostaining also demonstrated that Wnt4 proteins in osteoblasts were strongly detected in aged Wnt4 mice, but weakly in aged WT mice (**Fig. 3-12C**).

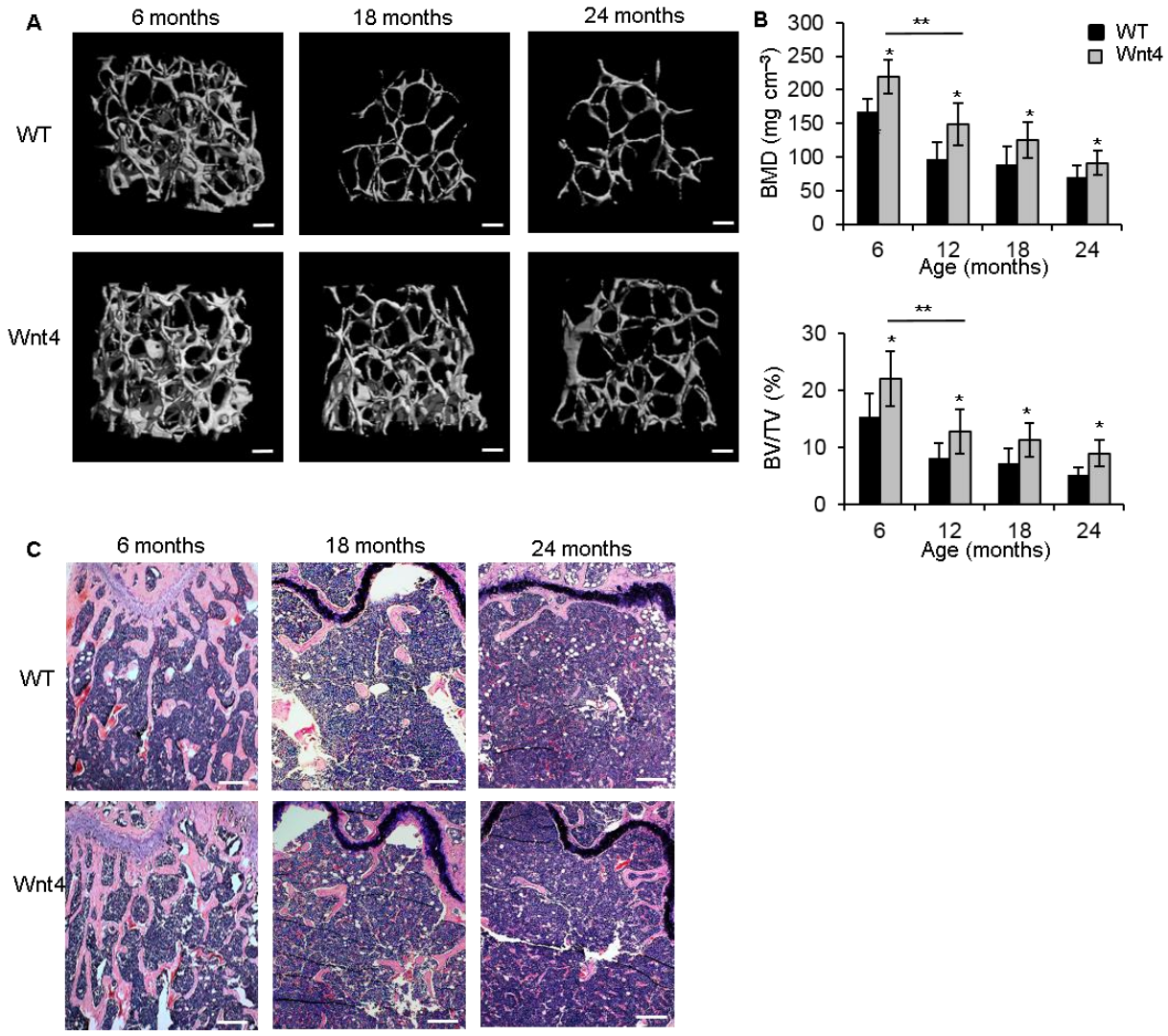

Figure 3-11. Wnt4 protects against age-related bone loss.

(**A**) μCT reconstruction and (**B**) trabecular BMD and BV/TV of distal femoral metaphysis regions from WT and Wnt4 mice at 6,12, 18 and 24 months. Scale bars, 200 μm. (**C**) HE staining of proximal femurs of WT and Wnt4 mice. n = 12 per group. *P < 0.0125 by Student's t-test with Bonferroni adjustment. **: P < 0.05 by two-way ANOVA for interaction between genotype and age.

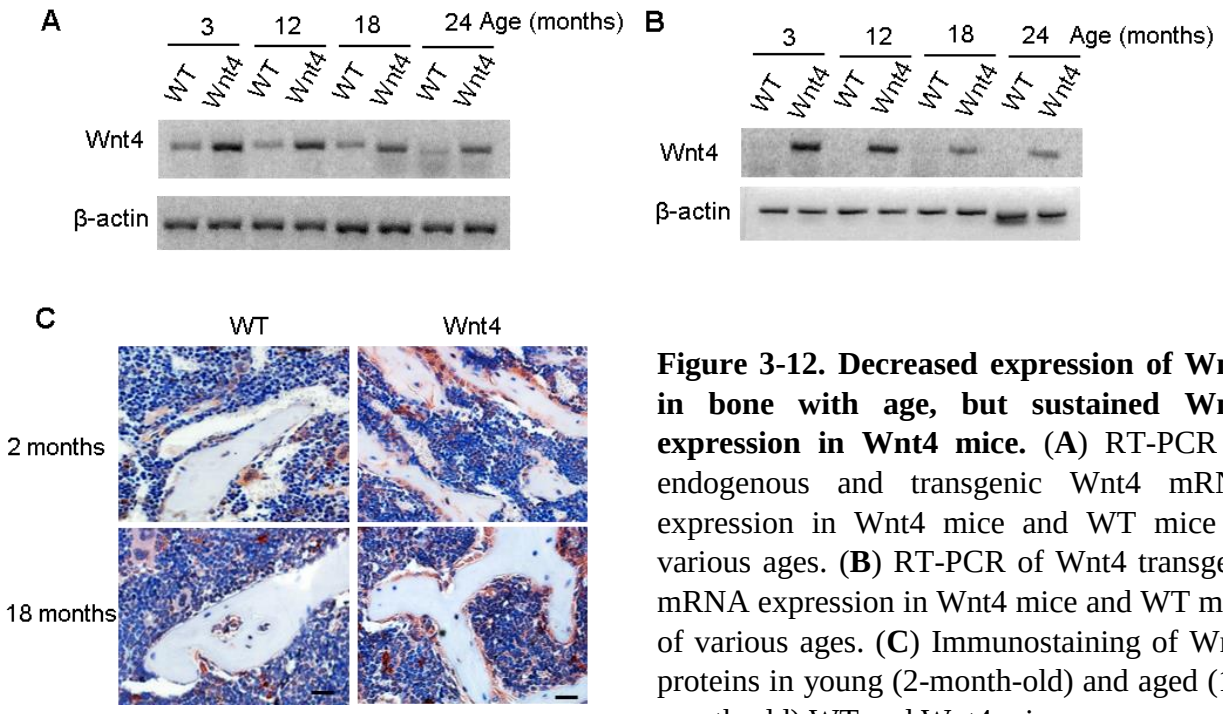

Figure 3-12. Decreased expression of Wnt4 in bone with age, but sustained Wnt4 expression in Wnt4 mice. (**A**) RT-PCR of endogenous and transgenic Wnt4 mRNA expression in Wnt4 mice and WT mice of various ages. (**B**) RT-PCR of Wnt4 transgene mRNA expression in Wnt4 mice and WT mice of various ages. (**C**) Immunostaining of Wnt4 proteins in young (2-month-old) and aged (18-month-old) WT and Wnt4 mice.

Morphometric measurements for osteoblasts (**Fig. 3-13A**), as well as serum Ocn concentrations (**Fig. 3-13B)**, also remained significantly greater in Wnt4 mice than in WT mice across all ages. Osteoclast number rose in aged 18-month-old WT mice compared to 3-month-old mice (**Fig. 3-13C**); however, in aged Wnt4 mice, osteoclast counts became significantly suppressed compared to aged WT mice. Notably, while serum Trap5b concentrations were not significantly different between Wnt4 and WT mice at 3 months of age, they increased drastically at 18 or 24 months in WT mice but not in Wnt4 mice (**Fig. 3-13D**). Furthermore, serum concentrations of Il-6 also showed a similar trend (**Fig. 3-14A**). Finally, we also examined whether natural aging-associated NF-κB activation was suppressed by Wnt4. While immunostaining of active p65 revealed greater NF-κB activity in the vicinity of trabecular bones in aged WT mice, NF-κB appeared less prevalent in aged Wnt4 mice (**Fig. 3-14B, yellow arrow**). Consistently, the

expression of Tnf, Cox-2 and Mmp9 was markedly weaker in aged Wnt4 mice compared with aged WT mice (**Fig. 3-14C-E**).

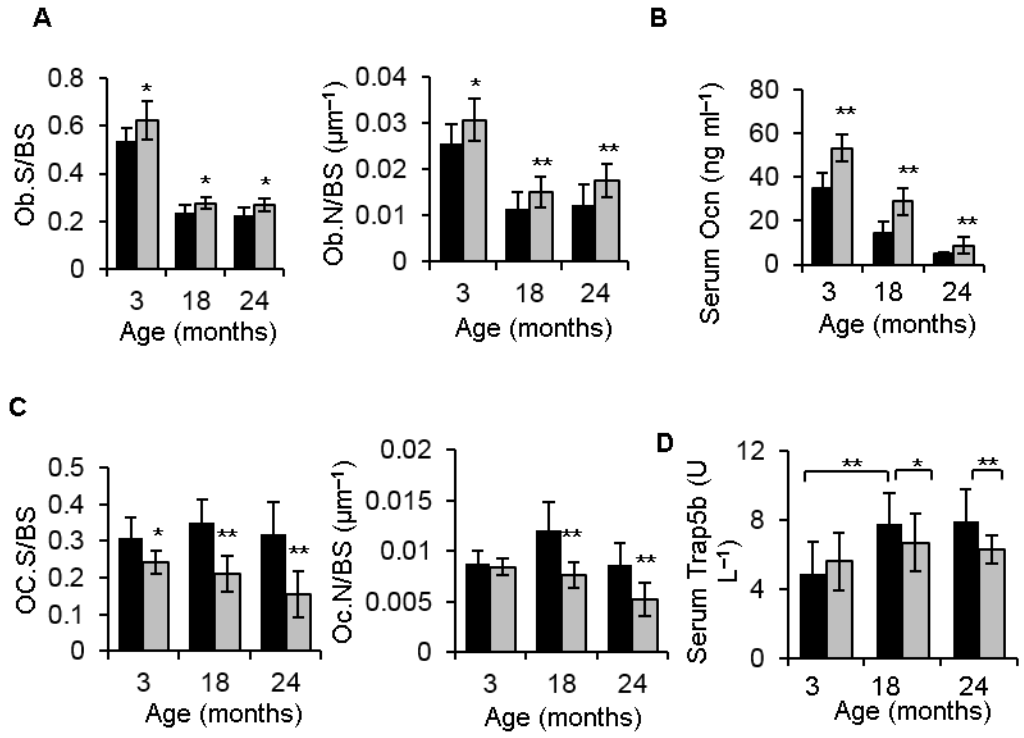

Figure 3-13. Increased osteoblasts and reduced osteoclast formation in aged Wnt4 mice.

(**A**) Morphometric analysis of osteoblast counts in distal femoral metaphysis from 3-, 18- and 24-months-old WT and Wnt4 mice. (**B**) ELISA of Ocn concentrations in serum from 3-, 18- and 24-months-old WT and Wnt4 mice. (**C**) Morphometric analysis of osteoclast counts in distal femoral metaphysis from 3-, 18- and 24-months-old WT and Wnt4 mice. (**D**) ELISA of Trap5b concentrations in serum from 3-, 18- and 24-months-old WT and Wnt4 mice. *: $P < 0.05$; **: $P < 0.01$ by two-tailed Student's t-test comparing WT and Wnt4 mice at each age.

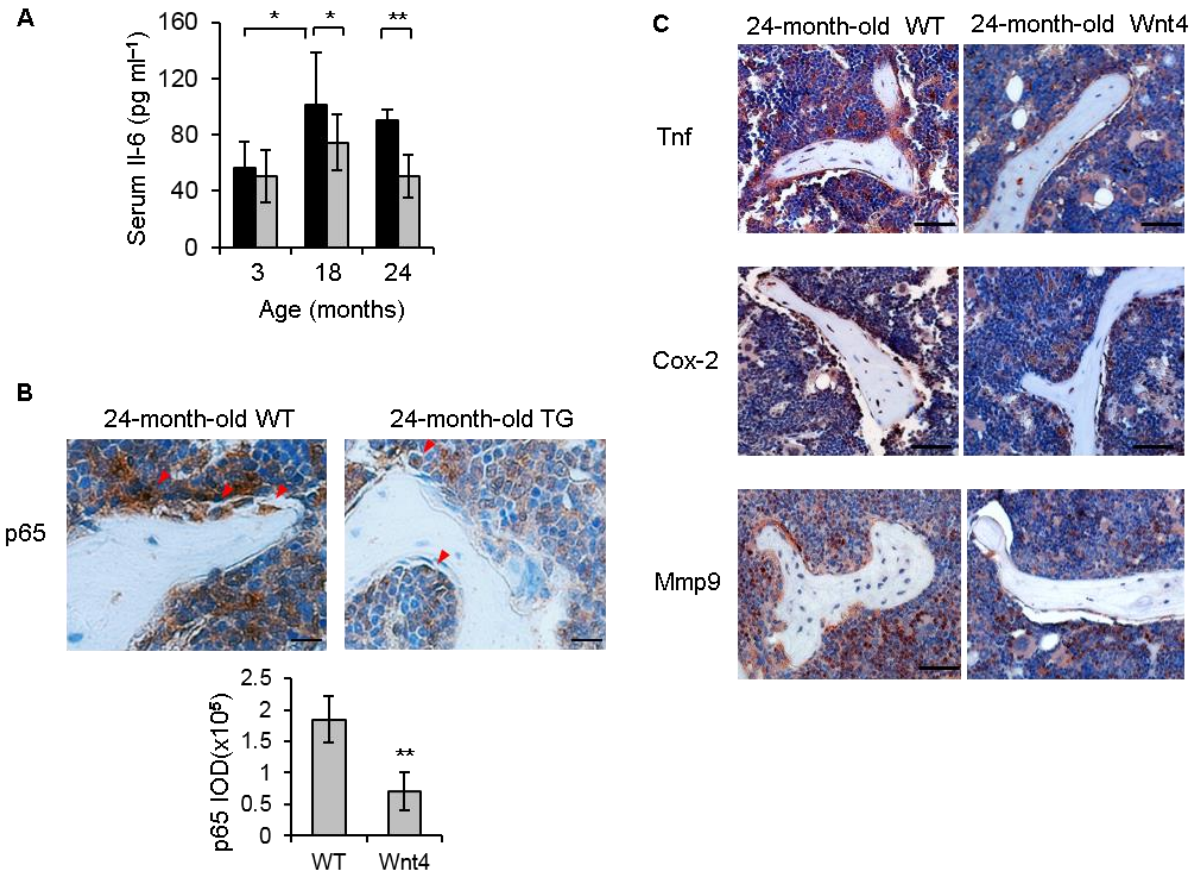

Figure 3-14. Attenuated NF-κB activity in aged Wnt4 mice.

(**A**) ELISA of Il-6 concentrations in serum from 3-, 18- and 24-months-old WT and Wnt4 mice. *: $P < 0.05$; **: $P < 0.01$ by one-way ANOVA. (**B**) Immunostaining and quantification of active p65 in 24-month-old WT and Wnt4 mice. *: $P < 0.05$; **: $P < 0.01$ by Student's t-test. (**C**) Immunostaining of Tnf, Cox-2 and Mmp9 in 24-month-old WT and Wnt4 mice.

3.5 Wnt4 inhibits osteoclast formation *in vitro*

Our *in vivo* results suggest that Wnt-4 secreted by osteoblasts may inhibit osteoclast formation and bone resorption in a paracrine fashion. To confirm our hypothesis, we examined whether Wnt4 could directly inhibit osteoclast differentiation using recombinant Wnt4 proteins (rWnt4). As evidenced by TRAP staining, rWnt4 protein significantly inhibited osteoclast differentiation of primary bone marrow macrophages induced by Rankl (**Fig. 3-15A**). Similarly, the osteoclast-like differentiation of RAW264.7 cells induced by Rankl was also attenuated by Wnt4 (**Fig. 3-15B**).

Real-time RT-PCR confirmed that rWnt4 inhibited the expression of osteoclast marker genes, including *Trap*, *Mmp9* and *ctsk* (*Cathepsin K*), induced by Rankl in bone marrow macrophages and RAW264.7 (**Fig. 3-15C, D**). Since Wnt4 inhibited the expression of NF-κB target genes *in vivo*, we also examined whether rWnt4 inhibited the expression of NF-κB target genes induced by Rankl in bone marrow macrophages and RAW246.7 cells. Real-time RT-PCR revealed that rWnt4 potently inhibited induction of NF-κB-dependent genes *Il6* and *Birc3* by Rankl in bone marrow macrophages (**Fig. 3-16A**) and in RAW264.7 cells (**Fig. 3-16B**). Consistent with our immunostaining *in vivo*, rWnt4 also significantly suppressed NF-κB-dependent genes *Tnf* and *Cox-2* in bone marrow macrophages (**Fig. 3-16C**).

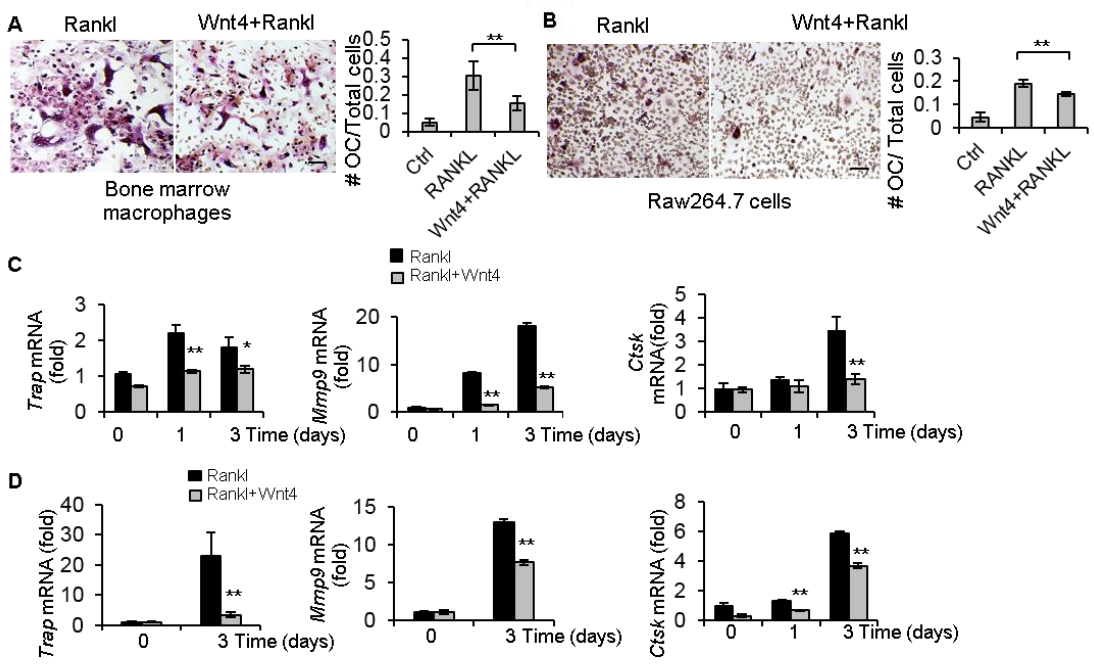

Figure 3-15. rWnt4 inhibited osteoclast formation *in vitro*.

(**A, B**) TRAP staining and quantification of osteoclast cultures formed by bone marrow macrophages (**A**) and Raw264.7 cells (**B**). (**C, D**) mRNA expression of osteoclastogenic marker genes after Rankl stimulation in bone marrow macrophages (**C**) and Raw264.7 cells (**D**) treated with recombinant Wnt4.

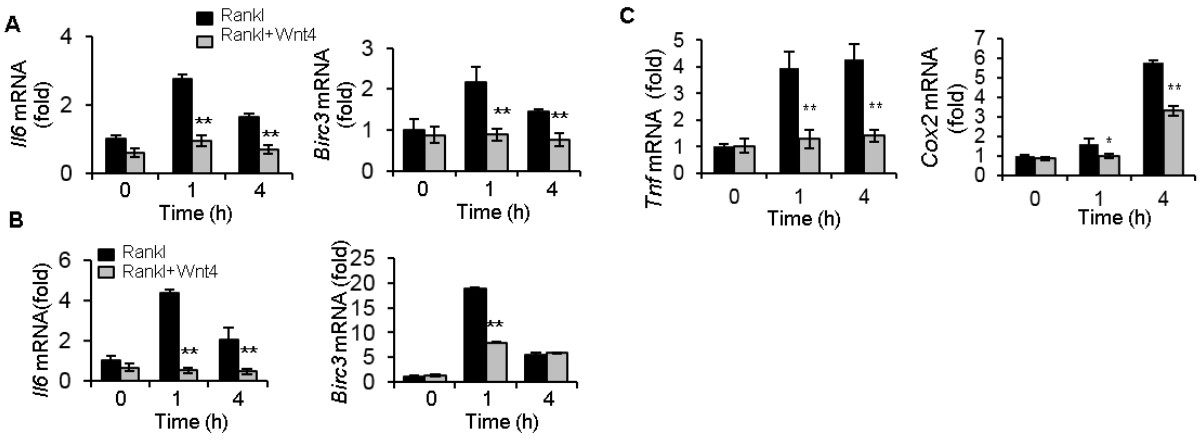

Figure 3-16. rWnt4 inhibited NF-κB signaling in osteoclast progenitors *in vitro*.

(**A, B**) mRNA expression of key NF-κB target genes Il-6 and Birc3 in bone marrow macrophages (**A**) and Raw264.7 cells (**B**) stimulated by Rankl. (**C**) mRNA expression of Tnf and Cox2 after Rankl and Wnt4 stimulation in bone marrow macrophages.

3.6 Wnt4 inhibits TAK1-NF-κB signaling

To further elucidate the molecular mechanism by which Wnt4 inhibited NF-κB and osteoclastogenesis, we examined each key step of NF-κB activation induced by Rankl. Activation of the Rank receptor leads to association of its cytoplasmic domain with Traf6 which is essential in osteoclast differentiation[165,166]. Traf6 forms a complex with TGFβ activated kinase 1 (Tak1) and Tak-binding protein 2 (Tab2), leading to phosphorylation and activation of Tak1[101]. In canonical NF-κB signaling, Tak1 then phosphorylates IKK complex and thereby initiates degradation of IκBα, followed by phosphorylation and nuclear translocation of p65 to activate downstream target genes. Western blot analysis revealed that rWnt4 potently inhibited the apical step of Tak1 phosphorylation, and the subsequent steps of p65 phosphorylation and the phosphorylation and degradation of IκBα induced by Rankl (**Fig. 3-17A**). Furthermore, rWnt4 also suppressed Rankl-induced nuclear translocation of p65 (**Fig. 3-17B**). Moreover, rWnt4 also inhibited NF-κB-

dependent transcription as determined by the NF-κB-dependent luciferase reporter assay (**Fig. 3-17C**).

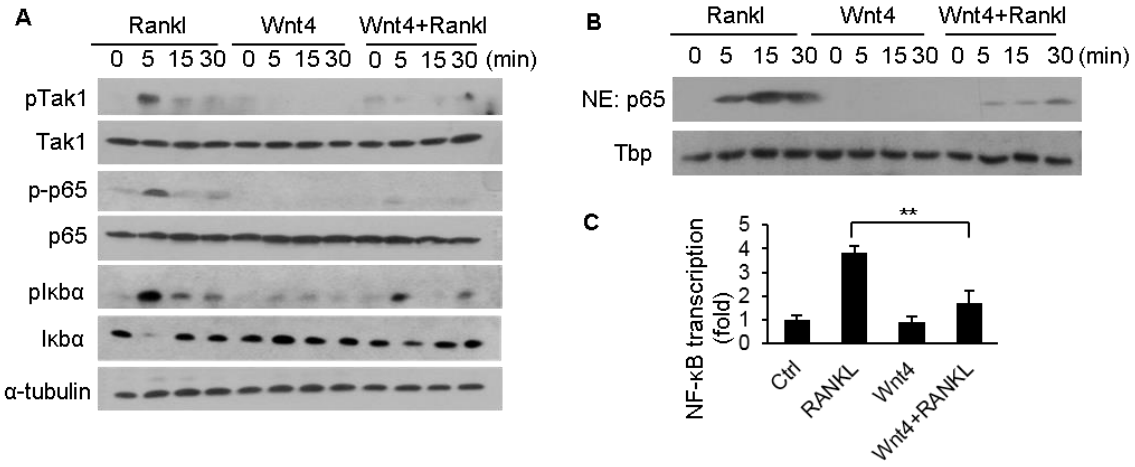

Figure 3-17. rWnt4 inhibited Rankl-induced NF-κB signaling in bone marrow microphages.

(**A**) Western blot analysis of key steps in NF- κB signaling after treatment with Rankl, Wnt4 and Rankl with Wnt4 in bone marrow macrophages. (**B**) Western blot analysis of p65 and Tata-binding protein (Tbp) in the nuclear extract (NE) of bone marrow macrophages after Rankl, Wnt4 and Wnt4 with Rankl treatment. (**C**) Relative NF-κB-dependent luciferase reporter activities in bone marrow macrophages after treatment of Rankl, rWnt4 and rWnt4 with Rankl.

Since Tak1 also forms a complex with Nemo-like kinase (Nlk) and Tab2 in non-canonical Wnt signaling[27,50], we hypothesized that rWnt4 stimulation may interfere with the formation of the Traf6-Tak1-Tab2 complex induced by Rankl. The co-immunoprecipitation (IP) revealed that Rankl induced the formation of the Traf6-Tak1-Tab2 complex using anti-Traf6 antibodies (**Fig. 3-18, lane 1 and 2**). However, addition of rWnt4 drastically inhibited the formation of the Traf6-Tak1-Tab2 complex (**Fig. 3-18, lane 2 and 4**). On the contrary, we observed that rWnt4 stimulation induced the formation of the Tak1-Tab2-Nlk complex, the addition of Rankl partially reduced the formation of the Tak1-Tab2-Nlk complex (**Fig. 3-18, lane 3 and 4**).

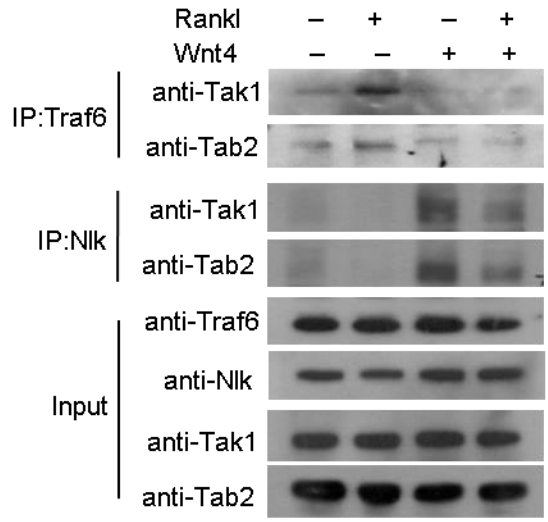

Figure 3-18. rWnt4-induced Nlk/Tak1 competitively inhibited Rankl-induced Tak1/Traf6 complex formation.

Immunoblots showing the Traf6-Tak1-Tab2 complex formation induced by Rankl (5 min) as well as Nlk-Tak1-Tab2 complex induced by Wnt4 (30 min) in bone marrow macrophages.

We next asked how Wnt4 could inhibit osteoclast formation through attenuating NF-κB signaling. As the nuclear factor of associated T-cells c1 (NFATc1) is the key transcription factor for osteoclastogenesis[167], we examined the effect of rWnt4 treatment on its expression following Rankl stimulation in bone marrow macrophages. We found that the induction of Nfatc1 by Rankl was repressed by rWnt4 (**Fig. 3-19A**). Previously, it has been shown that the activation of NF-κB induced the expression of *Nfatc1*, which in turn activated osteoclast differentiation[168]. Both NF-κB and NFAT consensus binding sites exist at the *Nfatc1* promoter. Upon induction by Rankl, p65 is recruited to the *Nfatc1* promoter to activate its transcription and subsequently the newly-generated Nfatc1 can auto-amplify itself. ChIP assays revealed that rWnt4 significantly suppressed

the Rankl-induced p65 binding to the *Nfatc1* promoter (**Fig. 3-19B**). Consequently, rWnt4 also potently reduced Nfatc1 binding at its own promoter induced by Rankl (**Fig. 3-19C**).

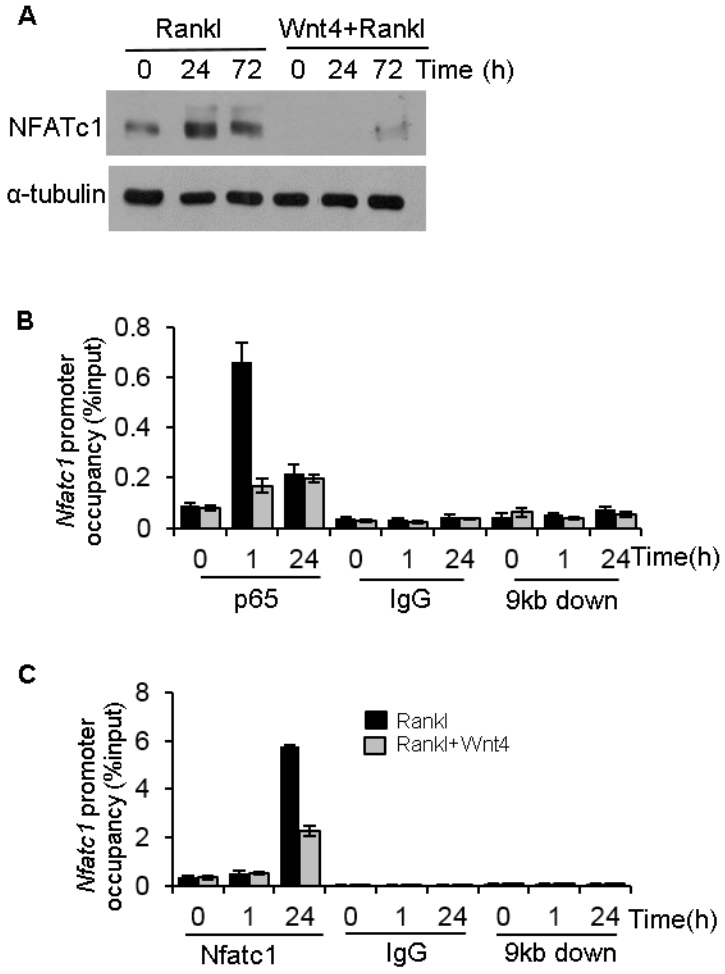

Figure 3-19. rWnt4 suppressed Rankl-induced Nfatc1 transcription and autoamplification by inhibiting p65 binding to *Nfatc1* promoter.

(**A**) Immunoblots showing the induction of Nfatc1 in bone marrow macrophages after treatment of Rankl, and rWnt4 with Rankl. (**B**) ChIP assays of the recruitment of p65 to the *Nfatc1* promoter induced by Rankl. Anti-IgG and primers designed at 9kb downstream of transcription start site (TSS) were used as negative control. (**C**) ChIP assays of Nfatc1 binding to the *Nfatc1* promoter.

While we previously found that Wnt4 activates non-canonical Wnt signaling in MSCs, Wnt4 might stimulate canonical Wnt signaling by stabilizing β-catenin. To rule out this possibility, we examined whether rWnt4 proteins increased the levels of cytosolic and nuclear β-catenin in bone marrow macrophages. Subcellular fractionation revealed that, while rWnt3a increased the levels of cytosolic and nuclear β-catenin, rWnt4 did not induce in the accumulation of β-catenin (**Fig. 3-20A**). Moreover, we also examined whether rWnt4 induced β-catenin-dependent transcription using a Topflash luciferase reporter. rWnt3a, but not rWnt4, significantly activated the luciferase reporter in bone marrow macrophages (**Fig. 3-20B**). In addition, two well-known Wnt/β-catenin target genes, including *Axin2* and *Dkk1*, were induced by rWnt3a, but not by rWnt4 (**Fig. 3-20C**).

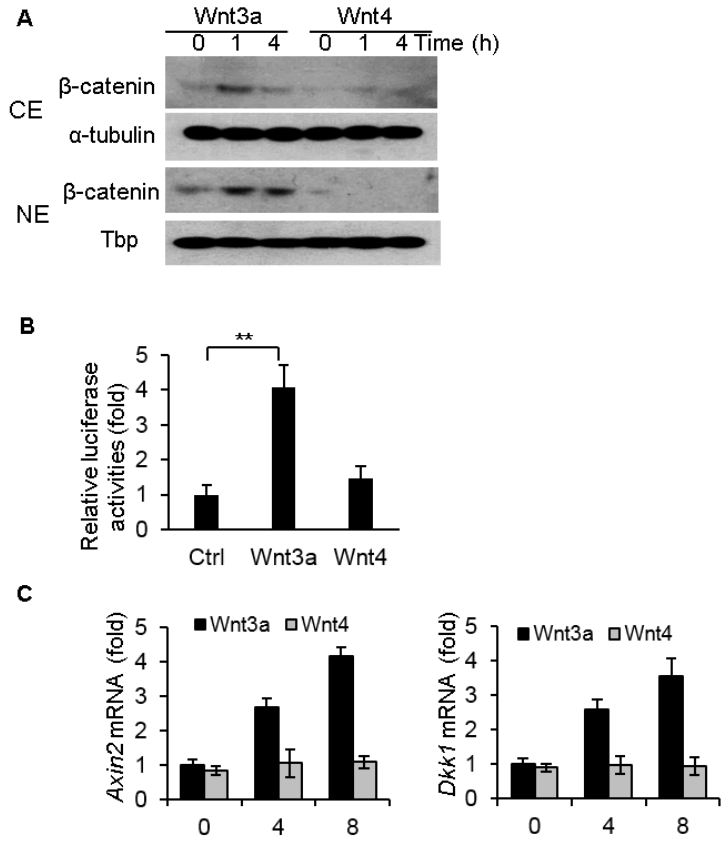

Figure 3-20. Wnt4 signals through a β-catenin-independent pathway in osteoclast progenitors.

(**A**) Immunoblots of β-catenin in cytosolic extract (CE) and nuclear extract (NE) of bone marrow macrophages after Wnt3a and Wnt4 stimulation. (**B**) Relative Topflash luciferase activities in bone marrow macrophages treated with Wnt3a or Wnt4. (**C**) Real-time RT-PCR of *Axin2* and *Dkk1* in bone marrow macrophages treated with Wnt3a or Wnt4. $n = 3$; * $P < 0.05$; ** $P < 0.01$; unpaired two-tailed t-test

3.7 Preventive injections of rWnt4 protein inhibit osteoporosis

To explore the potential clinical utilization of Wnt4, we first tested whether rWnt4 prevented osteoporotic bone loss by inhibiting NF-κB. 3 month-old mice were ovariectomized and intraperitoneally administered with rWnt4 once a day for three weeks. μCT analysis revealed that, while mice that underwent OVX suffered marked loss in trabecular BMD and BV/TV one month after OVX, mice injected with rWnt4 had significantly less bone loss (**Fig. 3-21A, B**). Dynamic histomorphometric analysis revealed that rWnt4 significantly enhanced bone formation due to OVX using calcein labeling (**Fig. 3-21C**). Histological staining also confirmed that rWnt4 significantly inhibited trabecular bone loss induced by OVX (**Fig. 3-21D**). TRAP staining (**Fig. 3-21E)** and morphometric analysis (**Fig. 3-21F)** revealed that rWnt4 significantly inhibited osteoclast formation induced by OVX. Moreover, rWnt4 also significantly reduced serum TRAP5b levels (**Fig. 3-21G**). Immunostaining showed that rWnt4 significantly inhibited NF-κB activity in osteoclasts and adjacent inflammatory cells upon OVX and the expression of TNF, Cox-2 and MMP9 (**Fig. 3-22A**). Consistently, we found that serum levels of IL-6 and TNF induced by OVX were significantly reduced by rWnt4 (**Fig. 3-22B**).

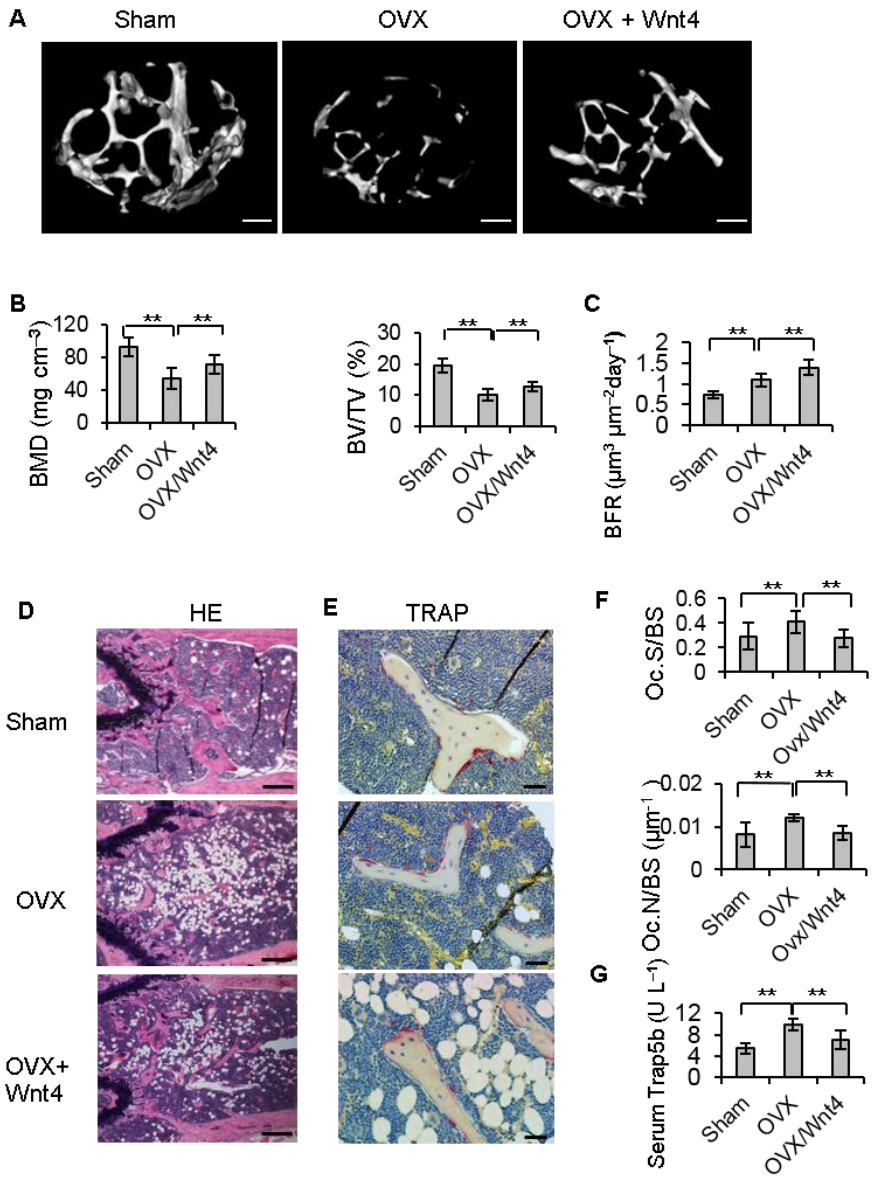

Figure 3-21. rWnt4 prevents estrogen-deficiency induced osteoporosis.

(**A**) μCT reconstruction and (**B**) trabecular BMD and BV/TV of distal femoral metaphysis regions from mice after sham operation, OVX and OVX immediately followed by rWnt4 injection (preventive model). (**C**) BFR measurement from dual calcein labeling of mice after sham, OVX or OVX with preventive rWnt4 injection. (**D**) H&E staining and (**E**) TRAP staining in distal metaphysis of mice after sham, OVX or OVX with preventive rWnt4 injection. (**F**) Morphometric analysis of osteoclast counts in distal femoral metaphysis. (**G**) ELISA of Trap5b concentrations in serum from mice after sham operation, OVX and OVX with preventive rWnt4 injection. $n = 8$ mice for sham group; $n = 12$ mice per group for mice receiving OVX and OVX with preventive rWnt4 injection. *$P < 0.05$, ** $P < 0.01$ by one-way ANOVA. Scale bars, 200 μm (**A**); 300 μm (**D**) and (**E**).

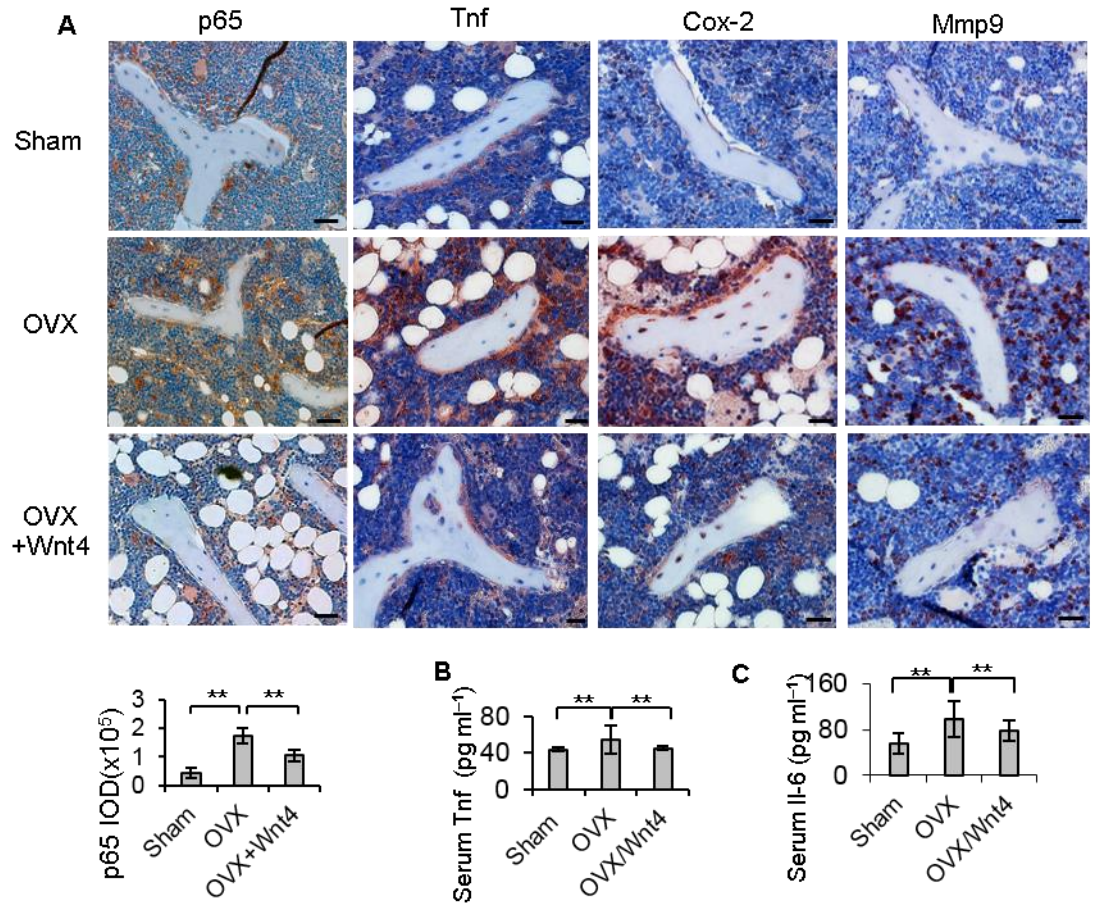

Figure 3-22. rWnt4 injection attenuated local and systemic NF-κB activity in mice after OVX. (**A**) Immunostaining and quantification of active p65 as well as NF- κB target genes Tnf, Cox-2 and Mmp9 in trabecular regions of mice after sham operation, OVX and OVX immediately followed by Wnt4 injections. Scale bars, 25μm. (**B,C**) ELISA of serum concentrations of Tnf (**B**) and Il-6 (**C**) after OVX and OVX followed by Wnt4 injection. *: P<0.05, **: P<0.01 by one-way ANOVA. *n=8* mice for sham group; *n*=12 mice for OVX and OVX+Wnt4 groups.

3.8 rWnt4 protein could reverse established bone loss in OVX-induced osteoporosis

To further evaluate the therapeutic value of rWnt4 proteins, we examined whether rWnt4 could reverse established bone loss in mice induced by OVX. We began administering rWnt4 to mice one month after OVX. μCT analysis revealed that rWnt4 significantly reversed OVX-induced reduction in trabecular BMD and BV/TV (**Fig. 3-23A**). Histological staining confirmed that rWnt4 significantly reduced trabecular bone loss induced by OVX (**Fig. 3-23B**). Histomorphometric analysis also showed that rWnt4 significantly increased osteoblast number and surface counts induced by OVX (**Fig. 3-23C**). In contrast, rWnt4 significantly inhibited osteoclast formation induced by OVX (**Fig. 3-23D).** Consistently, rWnt4 significantly reduced serum Trap5b concentrations induced by OVX (**Fig. 3-23E**) while it modestly increased serum Ocn concentrations (**Fig. 3-23F**). Immunostaining revealed that rWnt4 potently inhibited NF-κB activity in osteoclasts and adjacent bone marrow cells as well as the expression of Tnf, Cox-2 and Mmp9 (**Fig. 3-24A**). rWnt4 also significantly reduced serum concentrations of Il-6 and Tnf induced by OVX (**Fig. 3-24B**).

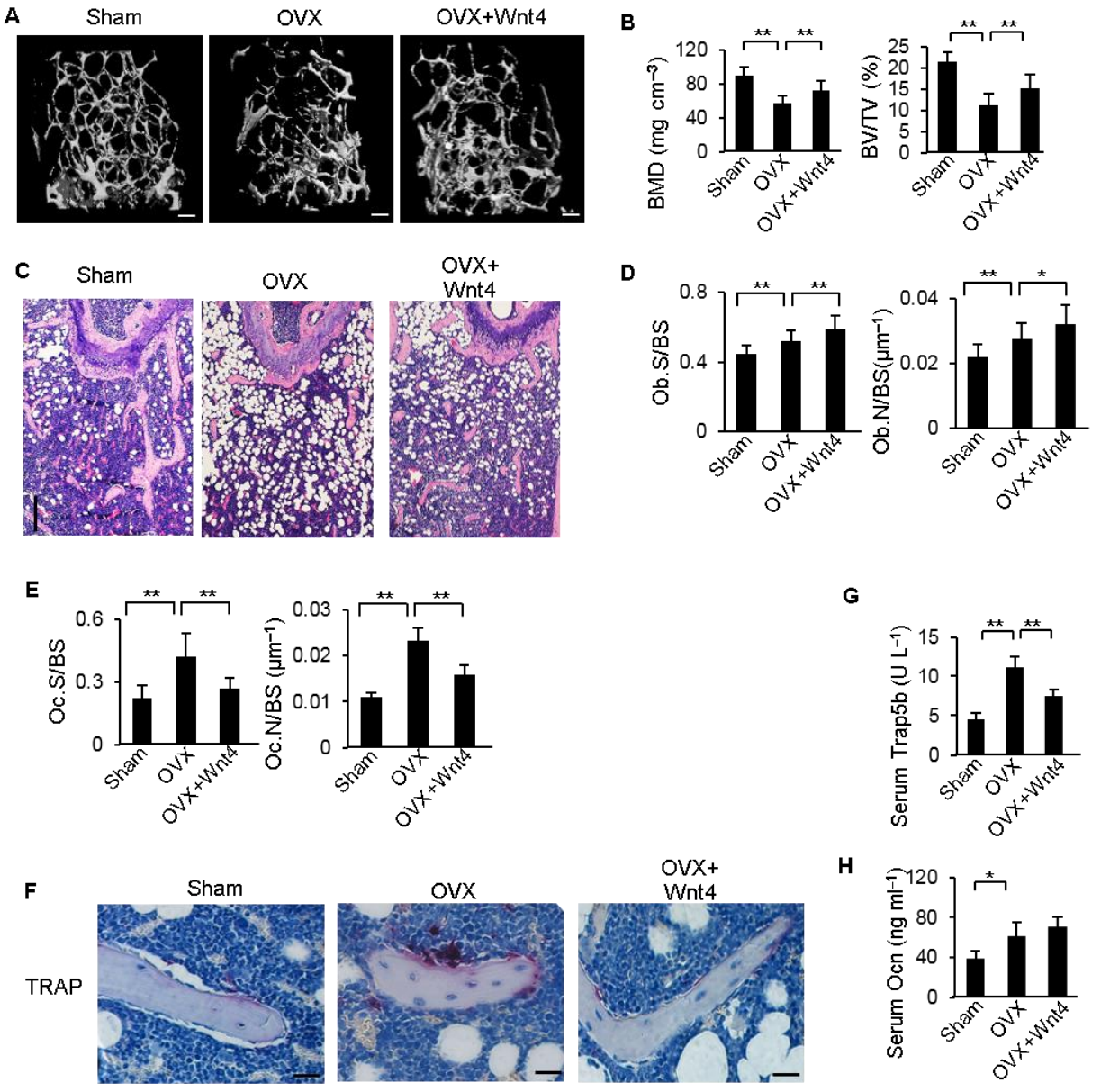

Figure 3-23. rWnt4 protein injections could reverse bone loss induced by OVX.
(**A**) μCT reconstruction and (**B**) trabecular BMD and BV/TV as well as (**C**) H&E staining of distal femoral metaphysis regions from mice after sham operation, OVX and OVX with rWnt4 injection. Scale bars, 200 μm (**A**); 300 μm (**C**). (**D, E**) Morphometric analysis of osteoblast (**D**) and osteoclast (**E**) counts in distal femoral metaphysis from mice after sham operation, OVX and OVX with rWnt4 injection. (**F**) TRAP staining showing osteoclasts surrounding trabecular bones in mice after sham operation, OVX and OVX with rWnt4 injection. Scale bars, 30μm. (**G, H**) ELISA of Trap5b (**G**) and Ocn (**H**) concentrations in serum from mice after sham operation, OVX and OVX with rWnt4 injection. *: $P < 0.05$; **: $P < 0.01$ by one-way ANOVA. $n = 8$ mice for sham group; $n = 12$ mice per group for mice receiving OVX and OVX with rWnt4 injection.

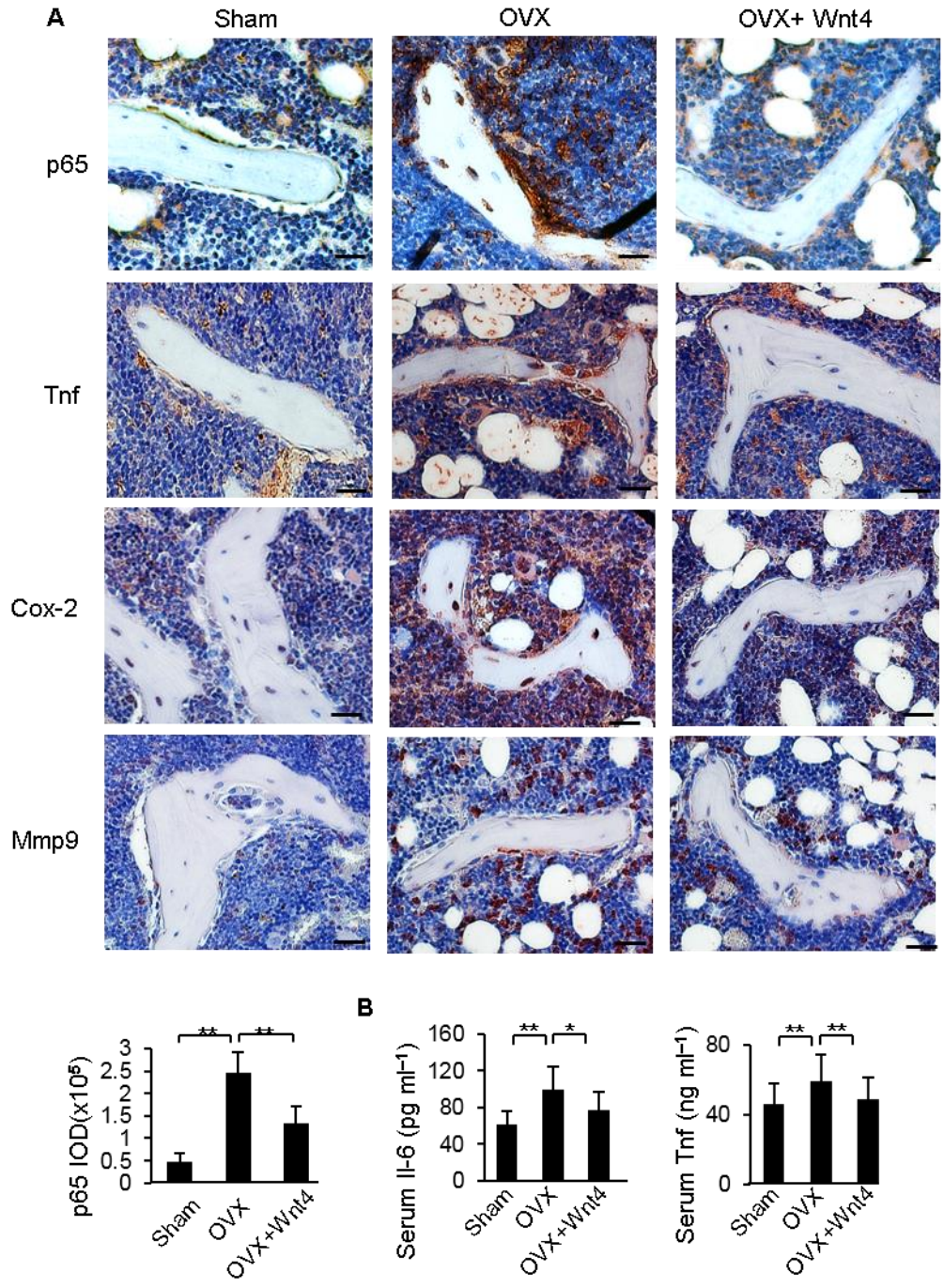

Figure 3-24. rWnt4 injection (therapeutic model) attenuated local and systemic NF-κB activity in mice after OVX.

(**A**) Immunostaining and quantification of active p65 as well as NF- κB target genes Tnf, Cox-2 and Mmp9 in trabecular regions of mice after sham operation, OVX and OVX immediately followed by Wnt4 injections. Scale bars, 25μm. (**B**) ELISA of serum concentrations of Tnf and Il-6 after OVX and OVX followed by Wnt4 injection. *: P<0.05, **: P<0.01 by one-way ANOVA. *n=8* mice for sham group; *n*=12 mice for OVX and OVX+Wnt4 groups.

3.9 Discussion

In the bone marrow, multiple factors act upon osteoblasts and osteoclasts to regulate bone remodeling. Growing evidence suggests that NF-κB is chronically activated in osteoporosis and skeletal aging as well as other age-related diseases [161,169-171]. Chronic activation of NF-κB induces the expression of pro-inflammatory cytokines which interferes with normal bone homeostasis and promotes bone loss [124,130,133]. Because less is known about the role of non-canonical Wnt proteins in bone remodeling, our initial study was to examine the functional role of Wnt4 in bone formation *in vivo* based on our previous work on osteoblast differentiation. Unexpectedly, we found that Wnt4, as a novel non-canonical signaling ligand, not only enhanced bone formation, but also inhibited osteoclastogenesis and bone resorption *in vivo*. Intriguingly, Wnt4 suppressed NF-κB activation and the expression of pro-inflammatory cytokines independent of β-catenin. Using three different, but complimentary animal models, we demonstrated that Wnt4 could prevent osteoporosis and age-related bone loss by inhibiting NF-κB, unraveling a novel crosstalk between non-canonical Wnt signaling and NF-κB pathways. While the physiological level of Wnt4 expressed by osteoblasts or bone marrow cells is likely low to exert strong anabolic effects, the delivery of recombinant Wnt4 proteins in mice significantly prevented osteoporosis, revealing the potential of Wnt4 as a therapeutic agent.

3.9.1 Non-canonical Wnt signaling in osteoclasts

Canonical Wnt/β-catenin signaling plays an essential role in skeletal development and bone formation. The gain- or loss-of-function mutations of Wnt signaling components have been identified in a variety of human bone disorders. On the other hand, while it is well established that

canonical Wnt/β-catenin signaling in osteoblasts induced OPG and inhibited osteoclast formation[105], few studies have been performed to examine Wnt signaling in osteoclasts. Recently, Wnt5a has been found to enhance osteoclast formation and bone resorption by activating the non-canonical JNK signaling pathway. Wnt5a enhanced osteoclastogenesis induced by RANKL through the Ror2 receptor[107], suggesting that targeting Wnt5a may prevent bone destruction. However, Wnt5a was also found to enhance osteogenic differentiation and inhibit adipogenesis in bone marrow. Wnt5a-haploinsufficient mice had a bone-loss phenotype with increased adipogenesis in bone marrow[27]. On the contrary, we found that Wnt4 inhibited osteoclastogenesis and bone resorption in vitro and in vivo while promoting bone formation, thereby holding more promising potential as a therapeutic agent for preventing skeletal aging and osteoporosis compared to inhibiting Wnt5a. Another recent study reported that Wnt16, another osteoblast-derived Wnt ligand, could suppress osteoclast differentiation via a non-canonical pathway in osteoclasts[108]. Intriguingly, Rankl-induced NF-κB transactivation was reduced in osteoclasts following Wnt16 treatment, thereby suggesting a potentially similar mechanism by another Wnt ligand to modulate osteoclastogenesis.

More importantly, recent evidence has suggested that the crosstalk between osteoblasts and osteoclasts is critical for the regulation of bone resorption. M-CSF and Wnt5a represent key osteoclastogenic signaling ligands generated by osteoblasts. On the other hand, osteoblast-produced OPG is a classical signal that inhibits osteoclastogenesis. In our study, we identified a promising therapeutic target that is involved in the well-orchestrated crosstalk between osteoblasts and osteoclasts. As a non-canonical Wnt ligand secreted by osteoblasts, Wnt4 directly modulates RANKL-induced osteoclast differentiation, but also exerts substantial anabolic effect on osteoblasts.

3.9.2 Tak1 and its key role in non-canonical Wnt signaling

Our results also highlighted the complexity of non-canonical Wnt signaling pathway. Various Wnt ligands can elicit different responses depending on the receptors. Wnt5a acts via Ror2 receptors to enhance the expression of RANK in osteoclast precursors by stimulating AP-1 activation and promoted Rankl-induced osteoclast formation[107]. However, unlike Wnt5a, we did not observe Wnt4- induced AP-1 activation in osteoclast precursors, which could be due to Wnt4 binding to different receptors. Notably, we found that Wnt4 suppressed Tak1 activation induced by Rankl, resulting in the inhibition of IKK/NF-κB activation in osteoclast precursors. Rankl induces the interaction between Traf6 and Tak1 which results in the activation of Tak1[101]. Intriguingly, Wnt4 potently blocked the Traf6/Tak1 complex formation induced by Rankl. While Tak1 plays a role in a non-canonical Wnt signaling by interacting with Nlk[172], it also modulates canonical Wnt signaling[173]. The definitive role of Tak1 in both canonical and non-canonical signaling may depend on cell contexts and the specific Wnt ligands. Based on our results, Wnt4 might activate its receptors to promote Tak1-mediated non-canonical Wnt signaling in osteoclasts, and subsequently sequester Tak1 from effectively binding with Traf6 to induce NF-κB signaling cascade. Aside from Tak1-Nlk interaction, Wnt4 might also promote the interaction between Tak1 and other Wnt signaling components, since it has been reported that Ror2 interacted with Tak1 during noncanonical Wnt signaling[173].

3.9.3 Wnt4 signaling and inflammatory bone loss

Alterations in Wnt signaling have been associated with rheumatoid arthritis and osteoarthritis. Dysregulation in canonical Wnt signaling directly affects the balance between bone formation and resorption, leading to exacerbated bone loss in the inflamed joints[174,175]. While Wnt4 is expressed

in developing joints, interestingly, Wnt4 is down-regulated in the synovium during the early phase of mouse collagenase-induced osteoarthritis[175]. Crossing arthritic TNF model with Wnt4 mice significantly alleviated systemic bone loss and contained localized inflammation induced by TNF, suggesting that Wnt4 could reduce the deleterious effects of chronic inflammation and aging.

3.9.4 Wnt4 signaling, inflammation and NF-κB

On the systemic level, the functions of osteoclasts and osteoblasts are modulated by the immune system and hormone levels. Proinflammatory cytokines not only positively regulates osteoclastogenesis, but they can also potently control osteoblast function and differentiation[176]. Chronic activation of NF-κB has been found to play an important role in aging and metabolic diseases, including osteoporosis and arthritis[125]. IL-6 secreted from bone marrow increases with aging[177]. While OPG in the marrow is markedly lower in older subjects, RANKL expression is significantly increased in bone marrow cells isolated from older postmenopausal women[115]. Osteoporosis was once thought to be due to gonadal failure and estrogen withdrawal. Recently, growing body of evidence has associated estrogen deficiency with increased production of pro-inflammatory cytokines including IL6, IL7 and TNF[178], and several theories arise to explain the possible inhibition of NF-κB signaling by estrogen[154]. The view of osteoporosis has shifted to a disease characterized by overwhelming bone resorption culminated by gradual accumulation of inflammatory responses. The inhibition of NF-κB has been found to block bone resorption and to promote bone formation in osteoporosis and arthritis[124]. Consistently, Wnt4 mitigated the inhibitory effect on bone formation by chronic inflammation associated with aging by inhibiting NF-κB activities in MSCs (unpublished observation).

3.9.5 Wnt4 signaling and age-related bone loss

While OVX acutely induced estrogen deficiency and osteoporosis, aged mice experience an increase in bone resorption due to the proinflammatory environment and the rise in production of RANKL, M-CSF by osteoblasts[179]. Of note, while Wnt4 slowed trabecular bone loss during the period of most dramatic age-related bone loss, bone mass in Wnt4 mice still underwent significant decline at advanced age. This could be due to other mechanisms associated with aging that overwhelm the protective effect of Wnt4. Furthermore, bone metabolism and remodeling conditions vary based on the existing bone mass. The rate of bone loss may also depend on the amount of bone remaining, as evidenced by the very slow trabecular bone loss in WT mice after 12 months of age compared to before. The higher peak bone mass in Wnt4 mice may also contribute to increased susceptibility to bone remodeling and resorption associated with aging, despite the protective effect of Wnt4. Finally, the expression of both endogenous and transgenic Wnt4 decreased over age, which could attribute to the reduced protective effect of Wnt4 in older mice.

Using the complimentary models of OVX and aging, we showed that Wnt4 inhibited chronic inflammation and prevented bone loss. Moreover, we found that Wnt4 also significantly inhibited TNF-induced bone loss. Since chronic diseases such as diabetes and inflammatory bowel diseases also suffer bone loss due to chronic inflammation, our results suggest that Wnt4 may be able to prevent bone loss mediated by chronic diseases[115,180].

3.9.6 Therapeutic potential of Wnt4

Most drugs currently used for osteoporosis are inhibitors of bone resorption, but cannot restore the significant bone loss that has already occurred at the time of diagnosis. Therefore, a better

treatment module for osteoporosis should be able to not only address issues with bone homeostasis, but also to control local inflammation[5]. Multiple Wnt proteins, including Wnt4, have been detected in bone tissues or bone marrow[181,182]. Although the inhibition of age-associated bone loss and inflammation was mainly based on transgenic overexpression of Wnt4, and that physiological level of Wnt4 may not exert a strong anabolic effect, we showed that recombinant Wnt4 proteins effectively protected from OVX-induced osteoporosis. While canonical Wnt proteins have potential therapeutic values for treating osteoporosis by promoting bone formation, the constitutive activation of β-catenin might also increase the risk for cancer development which is associated with aging[50,51]. Since Wnt4 did not activate β-catenin in either osteoblasts or osteoclasts, our results suggest that recombinant Wnt4 proteins may be a better therapeutic agent for preventing skeletal aging and for treating inflammatory bone diseases by inhibiting NF-κB.

4 EPIGENETIC REGULATION OF MESENCHYMAL STEM CELLS BY KDM4B and KDM6B

4.1 Induction of KDM4B and KDM6B by BMP-4/7 through Smad in MSCs

BMP-4/7 are potent inducers of osteogenic differentiation of MSCs, offering a great promise for bone regeneration and repair. To investigate potential roles of histone demethylases in osteogenic differentiation of MSCs, we profiled expression of 28 histone demethylases in BMP4/7-induced MSCs. RT-PCR revealed that KDM4B and KDM6B were most strongly induced by BMP4/7 (**Fig. 4-1A**). KDM4B and KDM6B are histone demethylases that remove H3K9me3 and H3K27me3, respectively[81,183-187]. Both H3K9me3 and H3K27me3 mark for gene silencing. Previously, KDM6B was identified as an early response gene induced by LPS through NF-κB signaling in macrophages[84]. Since BMPs mainly induce gene expression through SMAD signaling (Chen et al., 2004; Kang et al., 2005; Feng and Derynck, 2005; Attisano and Wrana, 2002; Massagué et al., 2005), we examined whether the inductions of KDM4B and KDM6B was dependent on SMAD signaling. Lentiviruses expressing *SMAD4* shRNA were generated to knock-down SMAD4. Western blot analysis showed that more than 85% SMAD4 was depleted in MSCs expressing *SMAD4* shRNA (MSC/SMAD4sh) compared with MSCs expressing scramble shRNA (MSC/Scrsh) (**Fig. 4-1B**). Real-time RT-PCR revealed that knock-down of SMAD4 significantly reduced the expression of *KDM4B* and *KDM6B* in MSCs induced by BMP4/7 (**Fig. 4-1C, D**). Since SMAD4 is the shared mediator of BMP signaling and TGF-β signaling, we went on to assess if SMAD1, which is specific to BMP signaling, also played a role in mediating the induction of KDM4B and KDM6B. Knockdown of SMAD1 also significantly inhibited the induction of KDM4B and KDM6B by BMP4/7 (**Fig. 4-1E-G**).

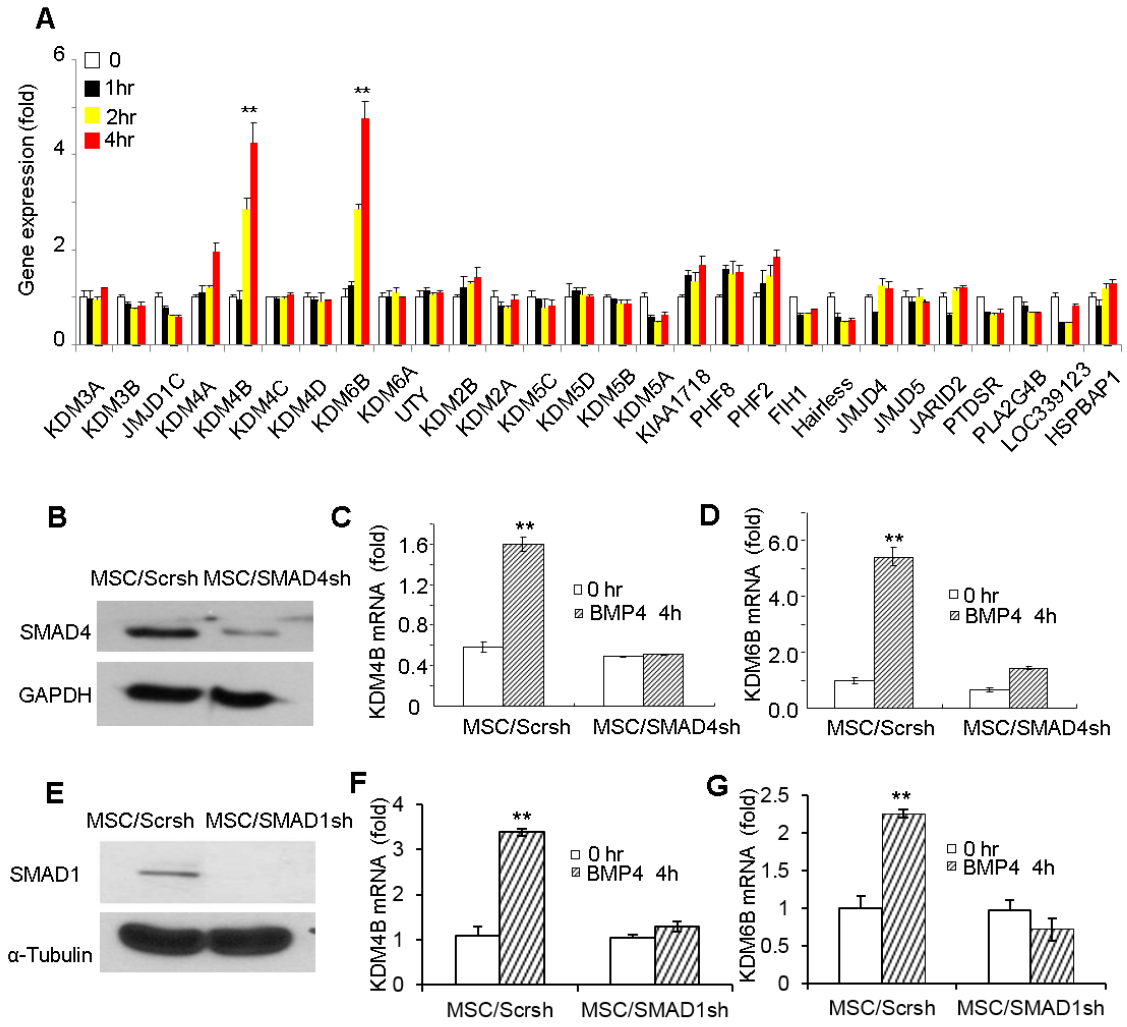

Figure 4-1. KDM4B and KDM6B Were Induced by BMP/SMAD Signaling in MSCs.
(**A**) BMP4/7-induced histone demethylases in MSC by gene expression profiling. The mRNAexpression of histone demethylases was assessed by real-time RT-PCR. (**B**) The knockdown of SMAD4 by shRNA. SMAD4 expression was examined by western blot analysis. (**C**) The knockdown of SMAD4 inhibited KDM4B in MSCs. KDM4B mRNA was examined by real-time RT-PCR. (**D**) The knockdown of SMAD4 inhibited KDM6B expression in MSCs. KDM6B mRNA was assessed by real-time RT-PCR. ** $P < 0.01$. (**E**) The knockdown of SMAD1 by siRNA. (**F**) The knockdown of SMAD1 inhibited KDM4B in MSCs. (**G**) The knockdown of SMAD1 inhibited KDM6B expression in MSCs. ** $P < 0.01$ by two-tailed Student's t-test.

4.2 KDM4B and KDM6B are required for osteogenic differentiation of MSCs

Since KDM4B and KDM6B were induced by BMP4/7, we explored whether they played a role in MSC cell fate determination. MSCs can be differentiated into osteoblasts, chondrocytes and adipocytes *in vitro* depending on the culture conditions. When stimulated by culture medium containing dexamethasone, β-glycerophosphate, and inorganic phosphate, MSCs can be induced to undergo osteogenic differentiation *in vitro*[79,188,189]. Using a retroviral approach, we over-expressed KDM6B in human MSCs (**Fig. 4-2A**). After osteogenic induction, we found that over-expression of KDM6B significantly increased ALP activity, an early marker of osteoblast differentiation (**Fig. 4-2B**). Consistently, over-expression of KDM6B enhanced mineralization in vitro, as assessed by Alizarin Red staining (**Fig. 4-2C**). Similarly, we found that over-expression of KDM4B also enhanced ALP activity and mineralization in MSCs (**Fig. 4-3**).

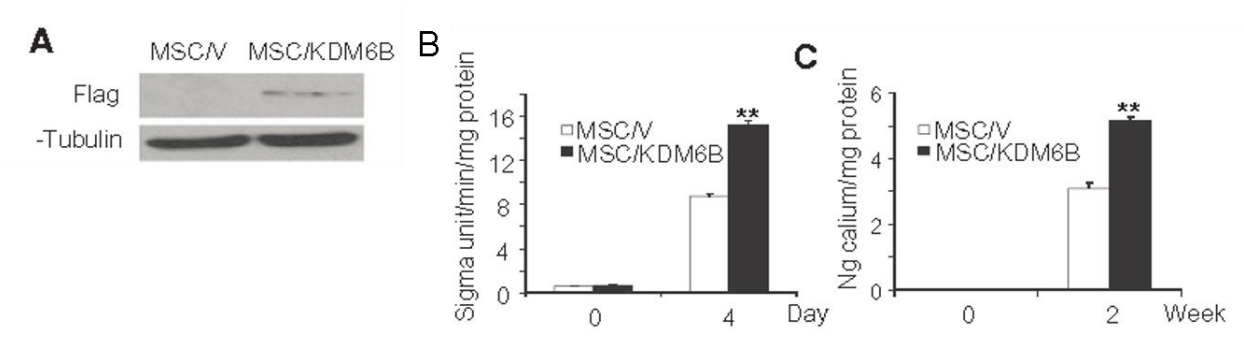

Figure 4-2. Overexpression of KDM6B promoted osteogenic differentiation of MSCs.
(**A**) Over-expression of KDM6B in MSCs. MSCs were transduced with retroviruses expressing Flag-KDM6B. Western blot analysis was performed using anti-Flag antibodies. (**B**) Over-expression of KDM6B enhanced ALP activities in MSC differentiation. Both MSCs expressing KDM6B (MSC/KDM6B) and MSCs expressing empty vector (MSC/V) were grown in osteogenic inducing media for 4 days. ALP activities were qualitatively measured. Values are mean ± s.d for triplicate samples from a representative experiment. **P < 0.01. (**C**) The over-expression of KDM6B enhanced mineralization in MSC differentiation. Mineralization was stained with Alizarin Red and qualitatively measured. **P < 0.01.

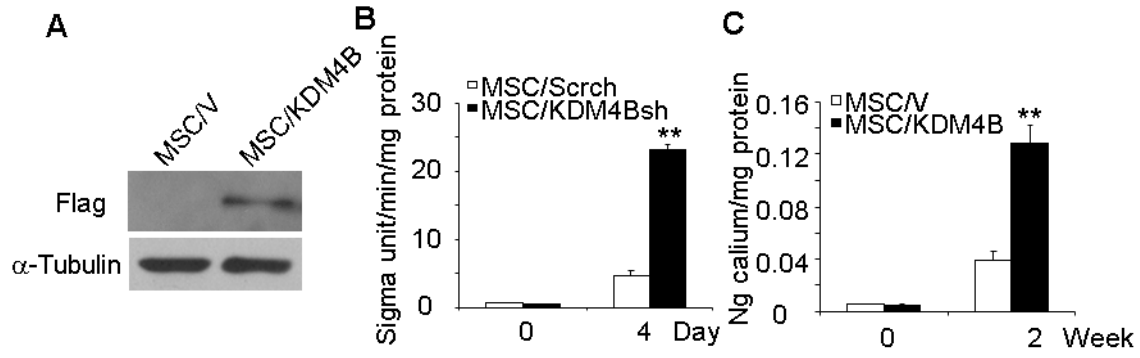

Figure 4-3. Overexpression of KDM4B promoted osteogenic differentiation of MSCs.
(**A**) Immunoblot of MSCs overexpressing Flag-tagged KDM4B and empty vector, using anti-Flag antibodies. (**B**) Over-expression of KDM4B enhanced ALP activities in MSC differentiation. Both MSCs expressing KDM4B (MSC/KDM4B) and MSCs expressing empty vector (MSC/V) were grown in osteogenic inducing media for 4 days. ALP activities were qualitatively measured. Values are mean ± s.d for triplicate samples from a representative experiment. **P < 0.01. (**C**) The over-expression of KDM4B enhanced mineralization in MSC differentiation. Mineralization was stained with Alizarin Red and qualitatively measured. **P < 0.01.

To confirm whether KDM4B and KDM6B played important roles in osteogenic differentiation of MSCs, we generated lentiviruses expressing KDM4B or KDM6B shRNA. The knock-down of *KDM6B* in MSCs was confirmed using Real-time RT-PCR (**Fig. 4-4A**). After treating MSCs with osteogenic inducing media for 4-5 days, ALP activity of differentiating MSCs was significantly suppressed by knocking down *KDM6B* (**Fig. 4-4B**). Moreover, *KDM6B* knock-down also reduced formation of mineralized nodules, as assessed by Alizarin Red staining after prolonged treatment with inducing media for 2 weeks (**Fig. 4-4C**). To confirm that *KDM6B* depletion inhibited osteogenic differentiation in MSCs, we assessed the mRNA expression of several osteogenic markers 7, 10, and 14 days after induction. The knock-down of *KDM6B* significantly inhibited the expression of bone sialoprotein (IBSP), osteopontin (SPP1) and

osteocalcin (BGLAP) (**Fig. 4-4D**). Moreover, to rule out off-target effects, we made another vector targeting a different region of *KDM6B* and obtained similar results (**Fig. 4-5**).

We next want to confirm the effect of on osteogenic differentiation was indeed due to KDM6B, using a rescue experiment to restore KDM6B expression. In mouse MSC/Kdm6bsh, the over-expression of human *KDM6B*, which was resistant to mouse *Kdm6sh* shRNA, restored osteogenic differentiation of MSCs (**Fig. 4-6**).

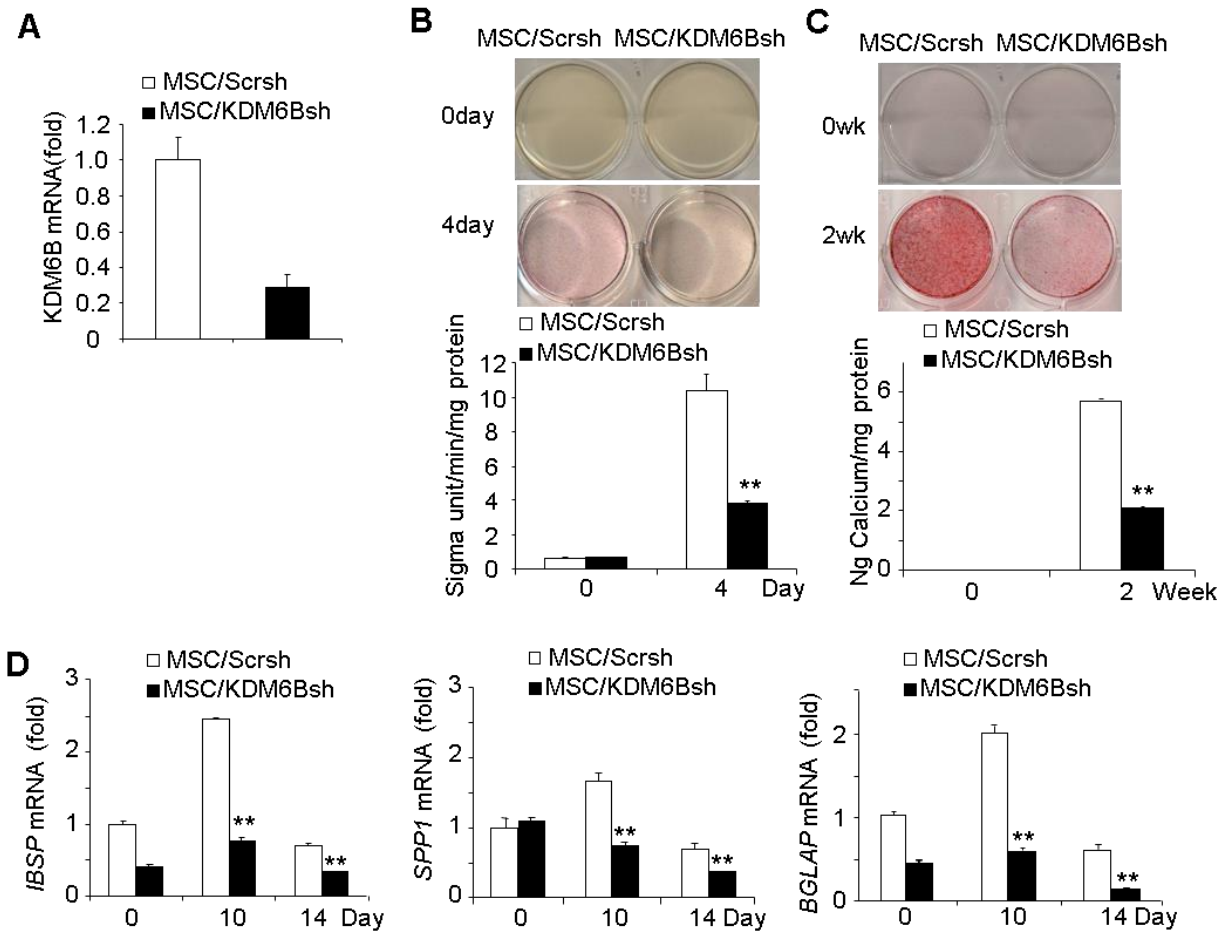

Figure 4-4. Depletion of KDM6B in MSCs inhibited osteogenic differentiation.
(**A**) The knock-down of KDM6B by shRNA. MSC/KDM6Bsh, MSCs expressing KDM6B shRNA; MSC/Scrsh, MSCs expressing scramble shRNA. (**B**) The knock-down of KDM6B inhibited ALP activities in MSCs. Values are mean ± s.d for triplicate samples from a representative experiment. **P < 0.01. (**C**) The knock-down of KDM6B inhibited mineralization in MSCs. **P < 0.01. (**D**) mRNA expression of osteogenic marker genes IBSP, SPP1 and BGLAP in KDM6B-depleted MSCs and scramble control. **P < 0.01.

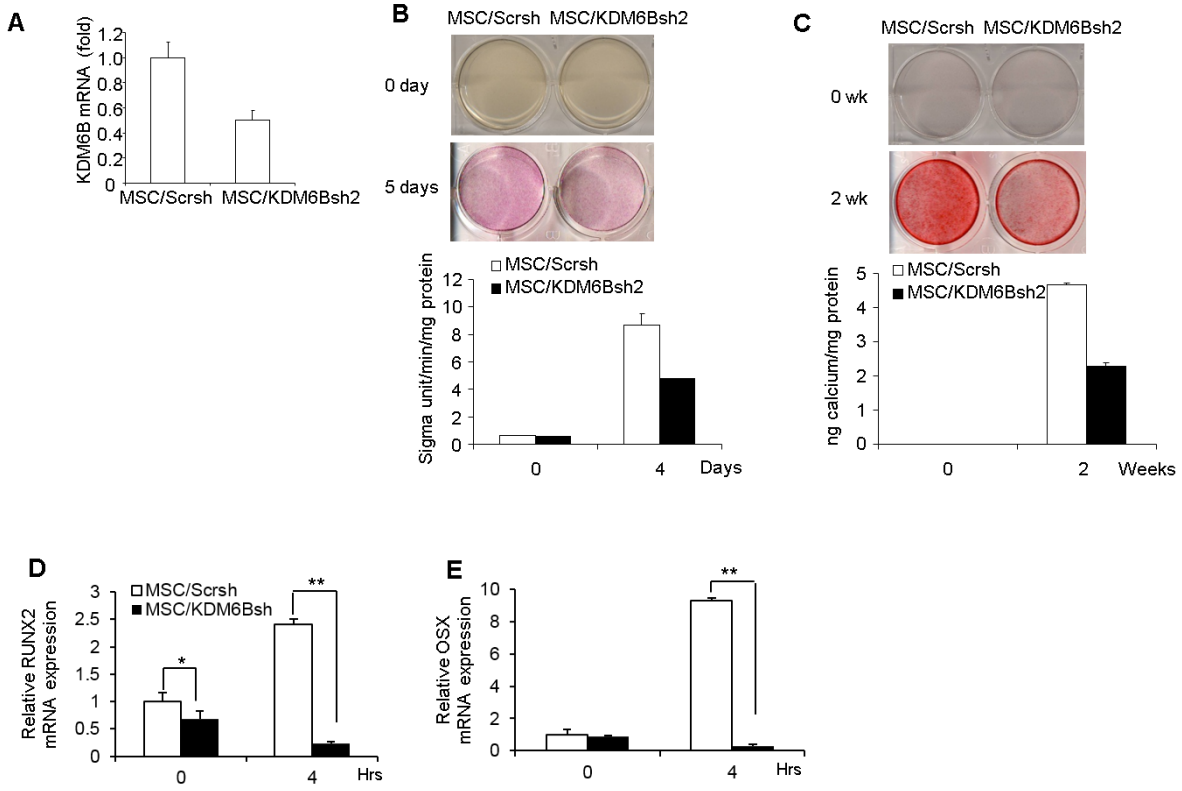

Figure 4-5. Depletion of KDM6B using another shRNA sequence in MSCs inhibited osteogenic differentiation.

(**A**) The knock-down of KDM6B by another shRNA sequence. MSC/KDM6Bsh2, MSCs expressing a different KDM6B shRNA; MSC/Scrsh, MSCs expressing scramble shRNA. (**B**) The knock-down of KDM6B inhibited ALP activities in MSCs. Values are mean ± s.d for triplicate samples from a representative experiment. **P < 0.01. (**C**) The knock-down of KDM6B inhibited mineralization in MSCs. **P < 0.01. (**D**) mRNA expression of osteogenic master regulators *RUNX2* and *SP7* in KDM6B-depleted MSCs and scramble control. **P < 0.01.

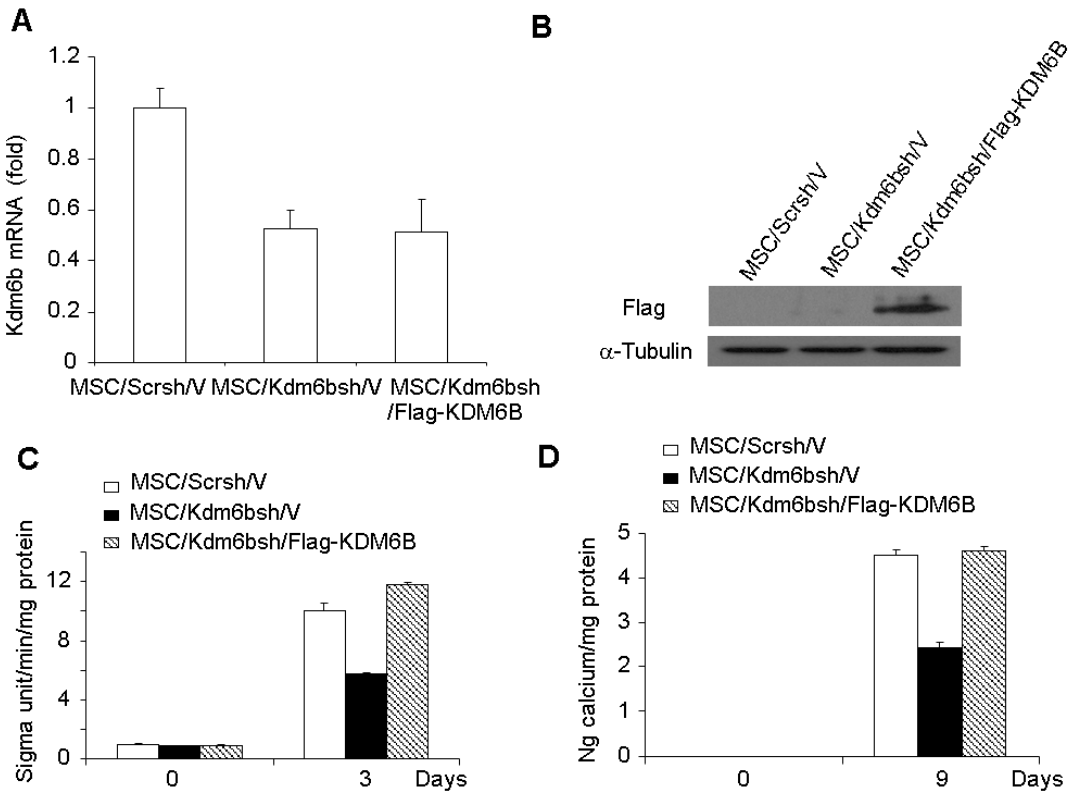

Figure 4-6. Restoration of KDM6B in mouse MSCs restored osteogenic differentiation. (**A**) Examination of *KDM6B* mRNA by Real-time RT-PCR. Kdm6b in mouse MSCs were knocked down and subsequently transduced with retroviruses expressing human Flag-KDM6B. MSC/Srcsh/V, MSC/Scrsh expressing empty vector; MSC/Kdm6bsh/V, MSC/Kdm6bsh expressing empty vector; MSC/Kdm6bsh/Flag-KDM6B, MSC/Kdm6bsh expressing human Flag-KDM6B. (**B**) The restoration of KDM6B in *Kdm6b* knock-down MSCs by Western blot analysis. (**C**) The restoration of *KDM6B* in MSC increased ALP activities. (**D**) The restoration of *KDM6B* in MSCs increased mineralization as assessed by ARS staining.

KDM6B may function independently from its demethylase activity to achieve chromatin remodeling of its target genes in T cell commitment[190]. To test this possibility, we generated a catalytically-dead KDM6B mutant construct in which histidin 1390 was changed to alanine, disrupting the non-heme center essential for its demethylase activity. However, the over-expression of KDM6B, but not the catalytically mutant KDM6B, in mouse MSC/Kdm6sh rescued

osteogenic differentiation of MSCs (**Fig. 4-7**), indicating that KDM6B demethylase activity is required for MSC differentiation.

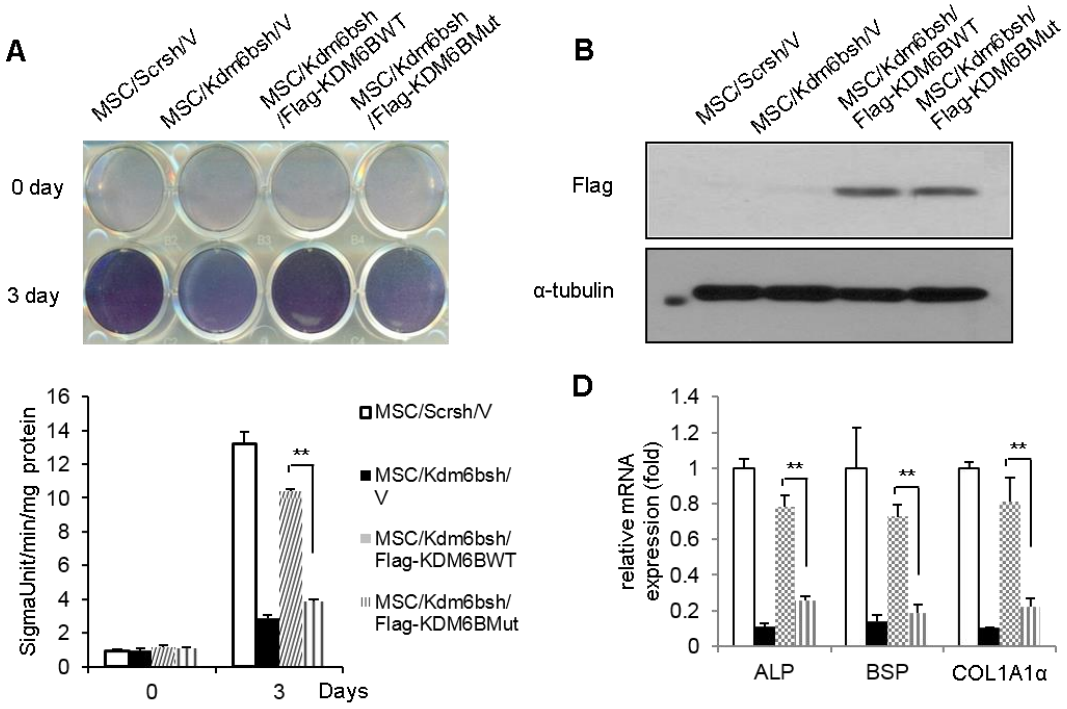

Figure 4-7. Demethylase activity of KDM6B is required for promoting osteogenic differentiation of MSCs.
(**A**) Mouse MSCs with depleted Kdm6b restored ALP acitivty following overexpression of WT KDM6B. However, overexpression of catalytically inactive KDM6B (KDM6BMut) could not restore ALP activities in MSCs. (**B**) The restoration of KDM6B and mutant KDM6B in Kdm6b knock-down MSCs by Western blot analysis. (**C**) The catalytically mutant KDM6B could not restore the expression of osteoblast marker genes in MSCs.

It is well known that addition of exogenous BMPs enhances osteogenic differentiation in MSCs. More importantly, since *KDM6B* was induced by BMP4, we examined whether the depletion of KDM6B would affect BMP4/7-induced osteogenesis. The knock-down of *KDM6B* significantly suppressed osteogenic differentiation of MSC induced by BMP4/7. Consistently, the knock-down of *KDM6B* inhibited the expression of RUNX2 and OSX induced by BMP4/7 (**Fig 4-8**).

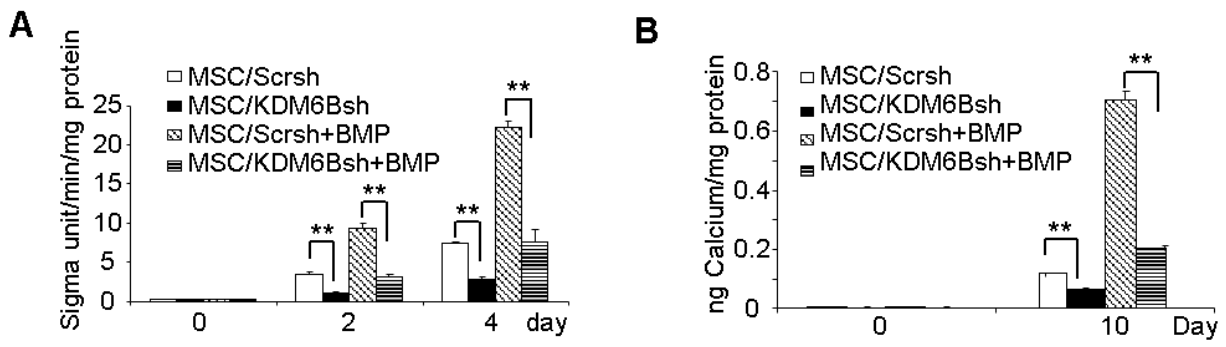

Figure 4-8. Depletion of KDM6B suppressed the osteogenic induction by BMP4/7.
(A) The knock-down of KDM6B inhibited BMP-enhanced ALP activities in MSCs. Cells were treated with osteogenic inducing media in the presence or absence of BMP4/7 for 4 days and ALP activities were qualitatively measured. **P < 0.01. (B) The knock-down of KDM6B inhibited BMP-enhanced mineralization in MSCs. **P < 0.01.

We also utilized shRNA to knock-down KDM4B in MSCs. The depletion of KDM4B inhibited ALP activity, mineralization and expression of extracellular matrix proteins in MSCs stimulated with osteogenic inducing media (**Fig. 4-9**). To rule out off-target effects, we made another vector targeting different region of *KDM4B* and obtained similar results (**Fig. 4-10**). We also created a Flag-KDM4B construct that was resistant to *KDM4B* shRNA. The restoration of *KDM4B* in MSC/KDM4Bsh cells reinstated osteogenic differentiation of MSCs (**Fig. 4-11**). The knock-down of KDM4B also inhibited osteogenic differentiation of MSCs enhanced by BMP4/7 (**Fig. 4-12**).

Taken together, our results suggest that KDM4B and KDM6B might be associated with osteoblastic lineage commitment of MSCs.

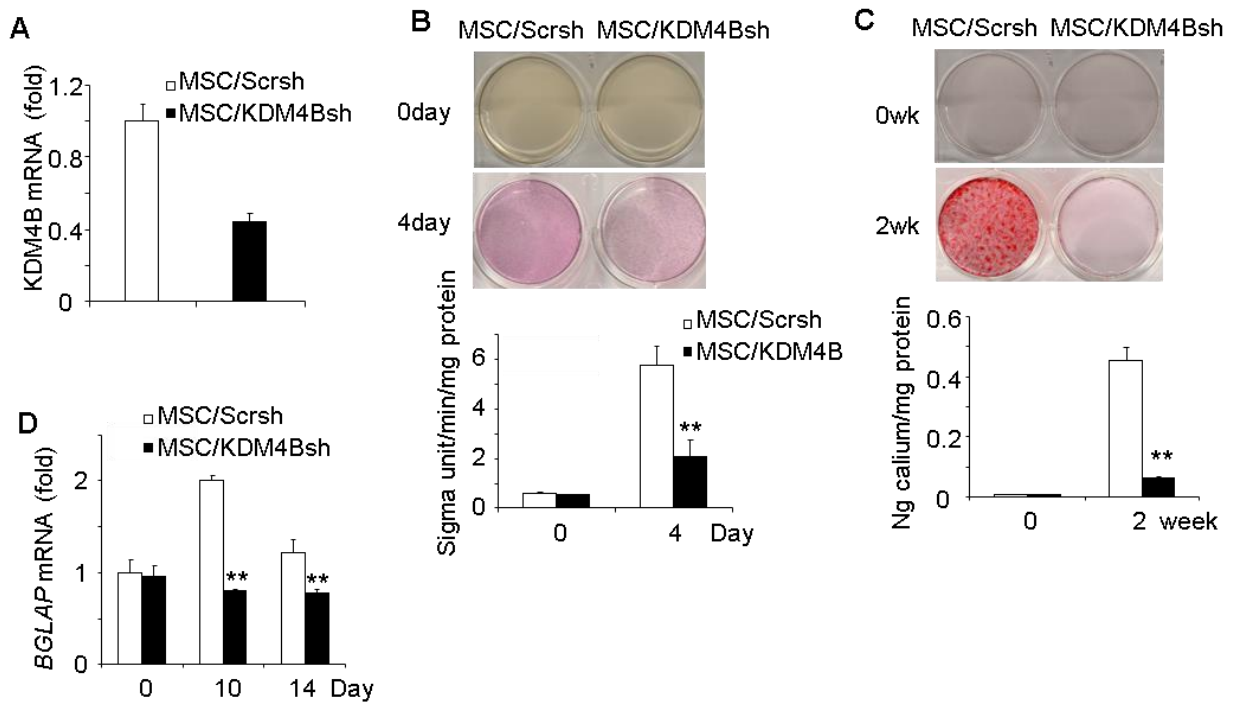

Figure 4-9. Depletion of KDM4B in MSCs inhibited osteogenic differentiation.
(**A**) The knock-down of KDM4B by shRNA. MSC/KDM4Bsh, MSCs expressing KDM4B shRNA; MSC/Scrsh, MSCs expressing scramble shRNA. (**B**) The knock-down of KDM4B inhibited ALP activities in MSCs. Values are mean ± s.d for triplicate samples from a representative experiment. **P < 0.01. (**C**) The knock-down of KDM4B inhibited mineralization in MSCs. **P < 0.01. (**D**) mRNA expression of osteogenic marker genes BGLAP in KDM4B-depleted MSCs and scramble control. **P < 0.01.

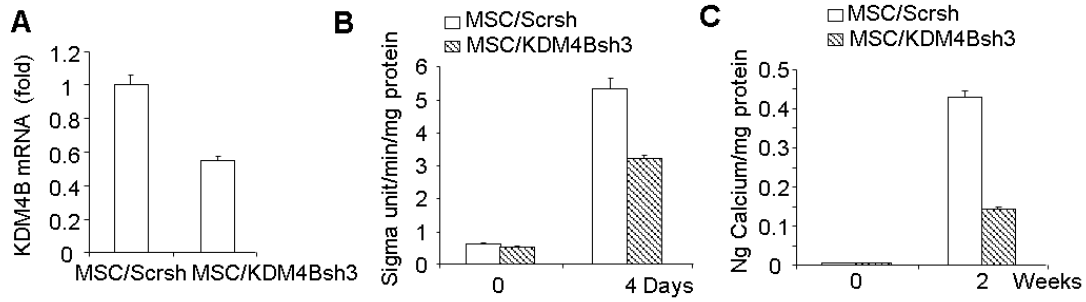

Figure 4-10. Depletion of KDM4B using a different shRNA sequence in MSCs inhibited osteogenic differentiation.
(**A**) The knock-down of KDM4B by another shRNA sequence. MSC/KDM6Bsh3, MSCs expressing a different KDM6B shRNA; MSC/Scrsh, MSCs expressing scramble shRNA. (**B**) The knock-down of KDM4B inhibited ALP activities in MSCs. (**C**) The knock-down of KDM4B inhibited mineralization in MSCs. **P < 0.01.

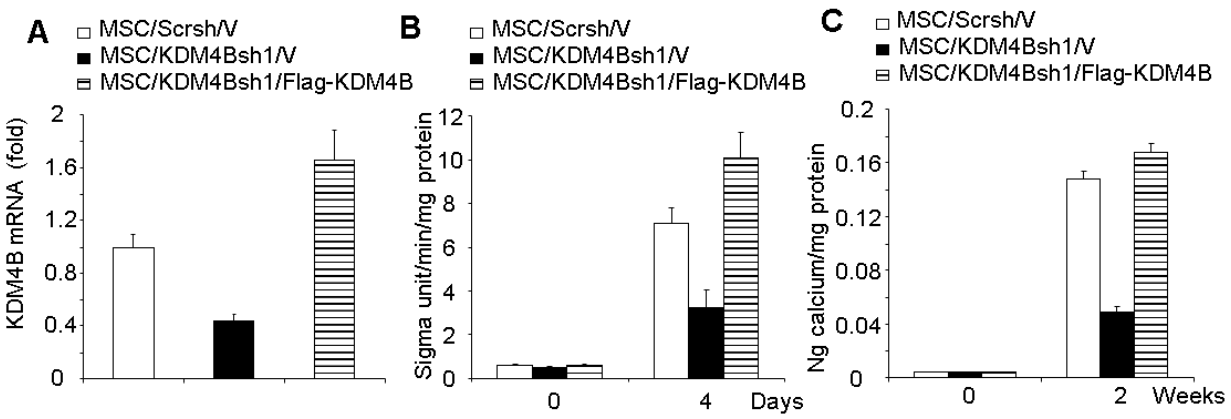

Figure 4-11. Restoration of KDM4B in human MSCs restored osteogenic differentiation.
(**A**) *KDM4B* mRNA by Real-time RT-PCR. KDM4B in mouse MSCs were knocked down and subsequently transduced with retroviruses expressing a variant Flag-KDM4B protected from knockdown. MSC/Srcsh/V, MSC/Scrsh expressing empty vector; MSC/KDM4Bsh1/V, MSC/KDM4Bsh expressing empty vector; MSC/KDM4Bsh/Flag-KDM4B, MSC/KDM4Bsh expressing Flag-KDM4B. (**B**) The restoration of *KDM6B* in MSC increased ALP activities. (**C**) The restoration of *KDM6B* in MSCs increased mineralization as assessed by ARS staining.

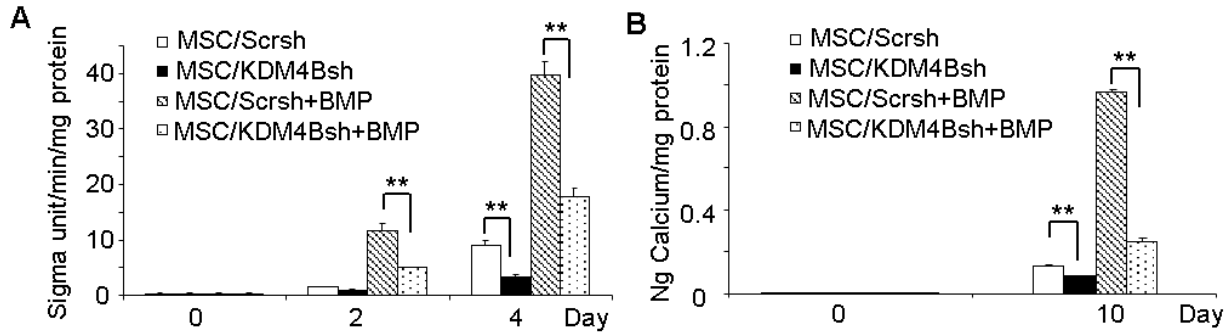

Figure 4-12. Depletion of KDM4B suppressed the osteogenic induction by BMP4/7.
(A) The knock-down of KDM4B inhibited BMP-enhanced ALP activities in MSCs. Cells were treated with osteogenic inducing media in the presence or absence of BMP4/7 for 4 days and ALP activities were qualitatively measured. **P < 0.01. (B) The knock-down of KDM4B inhibited BMP-enhanced mineralization in MSCs. **P < 0.01.

4.3 KDM4B and KDM6B are required for MSC-mediated bone formation *in vivo*

To verify our *in vitro* findings, we examined whether the knock-down of KDM4B and KDM6B affected MSC-mediated bone formation *in vivo*. MSC/KDM4Bsh, MSC/KDM6Bsh and MSC/Scrsh were mixed with hydroxyapatite/tricalcium phosphate (HA/TCP) carriers, and then transplanted subcutaneously into the dorsal side of 10-week old nude mice. After 8 weeks, transplants were harvested and prepared for histological analysis. H&E staining showed that MSC/KDM4Bsh and MSC/KDM6Bsh cells formed less bone tissues than MSC/Scrsh cells (**Fig. 4-13A and C**). Quantitative measurement of mineralized tissue areas revealed a greater than 50% decrease in bone formation by MSC/KDM4Bsh or MSC/KDM6Bsh cells compared with MSC/Scrsh cells (**Fig. 4-13B and D**). Interestingly, although it was difficult to perform qualitative measurement, we noted that adipose tissue formation in some regions was increased in MSC/KDM4B or MSC/KDM6B transplants as compared with MSC/Scrch transplants, suggesting that KDM4B and KDM6B may inhibit adipogenic differentiation of MSCs.

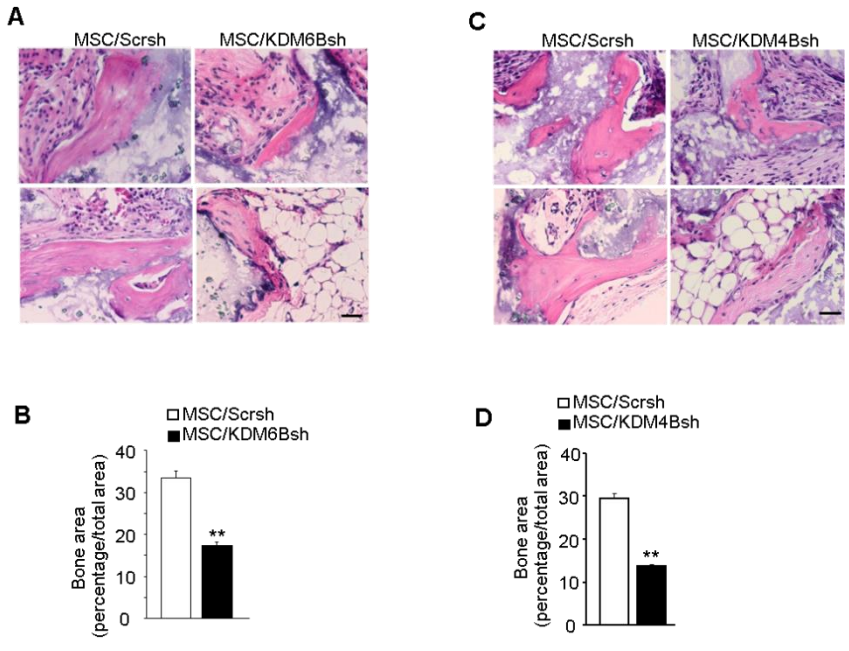

Figure 4-13. KDM4B and KDM6B are required for MSC-mediated bone formation *in vivo*.

(**A**) HE staining and (**B**) quantification of bone volume in subcutaneous transplant with MSC/Scrsh and KDM6B-depleted MSCs after 8 weeks of transplantation. (**C**) HE staining and (**D**) quantification of bone volume in subcutaneous transplant with MSC/Scrsh and KDM4B-depleted MSCs after 6 weeks of transplantation. Scale bar, 100 μm. $n = 5$. **$P < 0.01$.

4.4 Inhibition of adipocyte lineage commitment of MSCs by KDM4B and KDM6B

As normal bone homeostasis relies on the dynamic balance between osteogenesis and adipogenesis in differentiating MSCs, an osteogenic lineage commitment could be coupled with an inhibition of adipogenic differentiation. To explore whether KDM4B and KDM6B regulated adipogenic differentiation of MSCs, we assessed phenotypical changes of MSC/KDM4Bsh and MSC/KDM6Bsh cultured with adipogenic inducing medium. Oil-red-O staining revealed significant enhancement of adipogenesis in MSC/KDM6B cells as compared with MSC/Scrsh cells (**Fig. 4-14A**). To examine if the early onset of adipogenesis was influenced by KDM6B, we quantified the mRNA levels of the master adipogenic transcription factor PPAR-γ. The depletion of *KDM6B* significantly enhanced PPAR-γ expression (**Fig. 4-14B**). CD36, also known as fatty acid translocase, is highly expressed in adipocytes and is important in fatty acid uptake and lipid accumulation. Its expression is induced by PPAR-γ. The depletion of KDM6B significantly increased CD36 expression over a longer period (**Fig. 4-14C**). Consistently, we found that the knock-down of KDM4B also enhanced adipogenic differentiation of MSCs (**Fig. 4-14D and E**). Collectively, these results suggest that KDM4B and KDM6B inhibit adipogenic differentiation of MSCs.

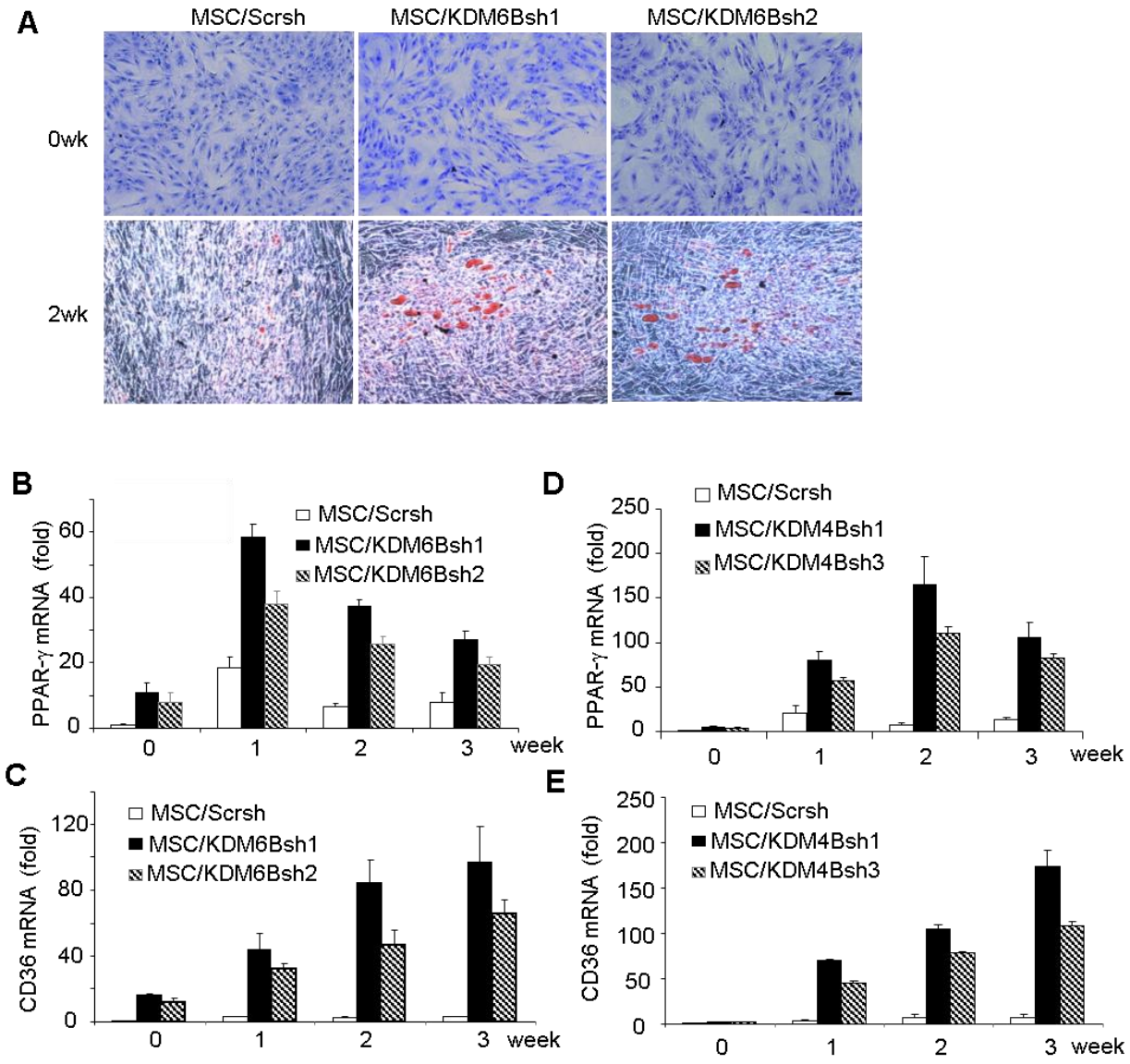

Figure 4-14. KDM6B and KDM4B depletion promoted adipogenic differentiation in MSCs.

(**A**) Oil-Red-O staining of MSCs infected with lentiviruses expressing two different shRNA sequences against KDM6B. MSC/Scrsh, MSCs expressing scramble shRNA; MSC/KDM6Bsh1, MSCs expressing KDM6B shRNA1; MSC/KDM6Bsh2, MSCs expressing KDM6B shRNA2. Cells were treated with adipogenic inducing medium for 3 weeks . (**B**) Knock-down of KDM6B promoted PPAR-γ expression as determined by Real-time RT-PCR. (**C**) Knock-down of KDM6B promoted CD36 expressing as determined by Real-time RT-PCR. (**D**) Knock-down of KDM4B promoted PPAR-γ expression as determined by Real-time RT-PCR. KDM4B was knocked down by lentiviruses expressing two different KDM4B shRNAs. Cells were treated with adipogenic inducing medium for 3 weeks. (**E**) Knock-down of KDM4B promoted CD36 expressing as determined by Real-time RT-PCR.

4.5 KDM4B and KDM6B epigenetically target distinct transcription factors to induce MSC cell lineage commitment

4.5.1 KDM6B epigenetically regulates transcription of BMP and HOXC6 genes

Previously, it was shown that KDM6B regulates the expression of homeobox (*HOX*) and *BMP* genes in embryonic stem cell differentiation through the removal of H3K27me3[187,191]. Since *HOX* and *BMP* genes are implicated in osteogenic differentiation, we tested whether the depletion of KDM6B affected the endogenous expression of *BMP* and *HOX* genes. Interestingly, in MSC/KDM6Bsh cells, the basal levels of endogenous BMP2 and BMP4 were significantly suppressed (**Fig. 4-15A and B**). Consistently, the induction of RUNX2 was inhibited upon induction of osteogenic differentiation (**Fig. 4-15C**). *HOX* genes encode a large family of homeodomain-containing transcription factors that are implicated in anterior-posterior axis patterning in embryonic development[81,187]. Moreover, HOX transcription factors were found to activate *RUNX2* transcription and can also mediate osteoblastogenesis in a RUNX2-independent manner[77]. Real-time RT-PCR revealed that the depletion of KDM6B significantly inhibited the expressions of *HOXC6-1*, *HOXA10*, *HOXB2* and *HOXC10* (**Fig. 4-15D**), implying that these HOX transcription factors may be regulated by KDM6B, thereby playing roles in promoting the osteogenic differentiation of MSCs.

To further examine how KDM6B globally controlled MSC differentiation, we also performed microarray analysis on KDM6Bsh MSCs. KDM6B knock-down significantly inhibited the expression of 1867 genes at the basal level and 638 genes induced by BMP4/7, including BMP2 and BMP4 as well as members of HOX family (**Fig. 4-16**). A gene ontology (GO) analysis revealed that KDM6B controls the pathways associated with skeletal system development, development

process, cell morphogenesis, BMP signaling and extracellular matrix organization (**Tables 4-1 and 4-2**).

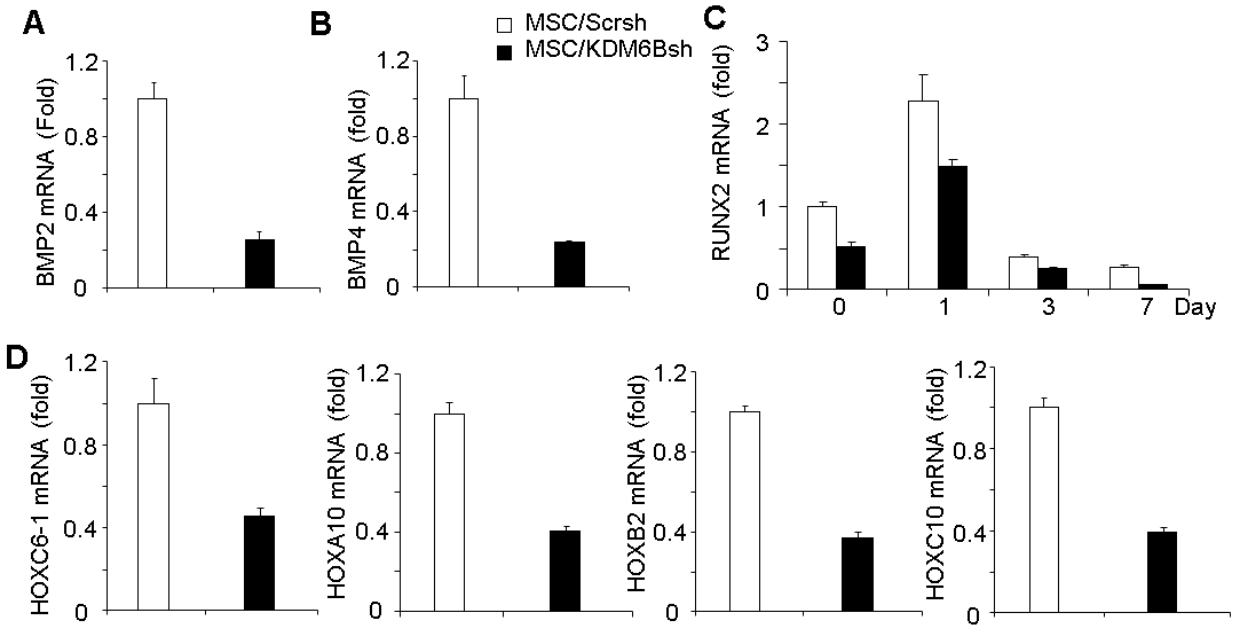

Figure 4-15. KDM6B is required for BMP and HOX gene expression in MSCs .

(**A** and **B**) Knock-down of *KDM6B* inhibited the basal levels of *BMP2* and *BMP4* expression as determined by Real-time RT-PCR. (**C**) Knock-down of *KDM6B* inhibited *RUNX2* expression during MSC differentiation, as determined by Real-time RT-PCR. (**D**) Knock-down of *KDM6B* inhibited the basal levels of HOX gene expression in MSCs as assessed Real-time RT-PCR.

Table 4-1. GO Analysis of KDM6B-dependent Genes at Basal Level (selected terms)

GO Term	Count	PValue
GO:0007010~cytoskeleton organization	52	0.006803
GO:0001501~skeletal system development	41	0.004973
GO:0008610~lipid biosynthetic process	38	0.025516
GO:0007398~ectoderm development	27	0.012716
GO:0007517~muscle organ development	26	0.041665
GO:0026664~regulation of cellular morphogenesis	19	0.021706
GO:0051216~cartilage development	12	0.0392

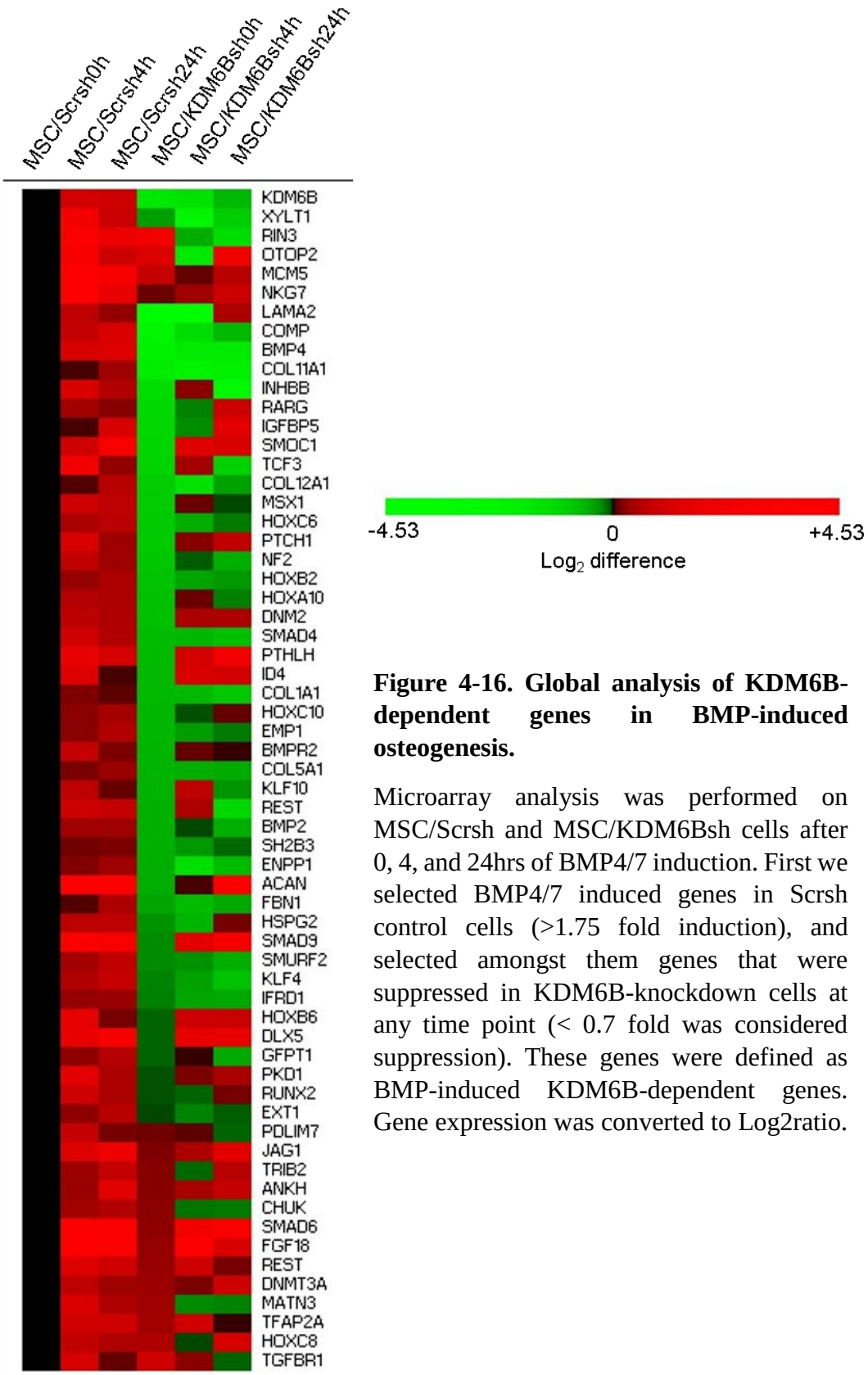

Figure 4-16. Global analysis of KDM6B-dependent genes in BMP-induced osteogenesis.

Microarray analysis was performed on MSC/Scrsh and MSC/KDM6Bsh cells after 0, 4, and 24hrs of BMP4/7 induction. First we selected BMP4/7 induced genes in Scrsh control cells (>1.75 fold induction), and selected amongst them genes that were suppressed in KDM6B-knockdown cells at any time point (< 0.7 fold was considered suppression). These genes were defined as BMP-induced KDM6B-dependent genes. Gene expression was converted to Log2ratio.

Table 4-2. GO Analysis of KDM6B-dependent Genes induced by BMP4/7 (selected terms)

GO Term	Count	PValue
GO:0001501~skeletal system development	29	2.77E-07
GO:0007389~pattern specification process	15	0.02777
GO:0045597~positive regulation of cell differentiation	13	0.03983
GO:0048729~tissue morphogenesis	13	0.00729
GO:0048705~skeletal system morphogenesis	13	1.16E-04
GO:0045165~cell fate commitment	11	0.00827
GO:0022604~regulation of cell morphogenesis	11	0.0055
GO:0051216~cartilage development	11	6.06E-05
GO:0048562~embryonic organ morphogenesis	10	0.01724
GO:0060348~bone development	10	0.01075
GO:0001503~ossification	10	0.00705
GO:0016055~Wnt receptor signaling pathway	9	0.0438
GO:0030509~BMP signaling pathway	9	3.80E-05
GO:0048706~embryonic skeletal system development	8	0.00763
GO:0030278~regulation of ossification	7	0.02774
GO:0042476~odontogenesis	7	0.00502
GO:0048704~embryonic skeletal system morphogenesis	6	0.02626
GO:0045667~regulation of osteoblast differentiation	5	0.03755
GO:0042475~odontogenesis of dentine-containing tooth	5	0.02742
GO:0070167~regulation of biomineral formation	5	0.01407
GO:0030500~regulation of bone mineralization	5	0.01123
GO:0045669~positive regulation of osteoblast differentiation	5	0.00582
GO:0050994~regulation of lipid catabolic process	4	0.04033
GO:0045778~positive regulation of ossification	4	0.03278
GO:0060349~bone morphogenesis	4	0.02013
GO:0001502~cartilage condensation	4	0.01749
GO:0002062~chondrocyte differentiation	4	0.01505
GO:0060350~endochondral bone morphogenesis	4	0.01079
GO:0001958~endochondral ossification	4	0.00463
GO:0060391~positive regulation of SMAD protein nuclear translocation	3	0.01209
GO:0060390~regulation of SMAD protein nuclear translocation	3	0.01209

In order to examine if KDM6B epigenetically regulated MSC differentiation by demethylating H3K27me3, we performed ChIP assay to assess the changes in histone methylation status at the promoter regions of those master differentiation genes. Indeed, we found that KDM6B were bound to the promoter regions of *BMP2* and *BMP4* (**Fig. 4-17A and B**). Since our gain- and loss-of-function analysis revealed that HOXC6-1 played a critical role in osteogenic differentiation of MSCs (**Fig. 4-18**), we also examined the epigenetic status of the *HOXC6-1* promoter. KDM6B occupancy on the promoters of *BMP2, BMP4, and HOXC6-1* was reduced in MSC/KDM6B cells (**Fig. 4-17C**). Consistently, decreased binding of KDM6B at the promoter regions was associated with increased occurrence of its substrate, H3K27me3, which is a hallmark of gene silencing (**Fig. 4-17D, E, F**). As a control, we could not detect KDM6B occupancy 3 to 4kb downstream of the transcription start sites, and the knock-down of KDM6B did not affect H3K27me3 on that region. Importantly, we found that knock-down of KDM6B decreased H3 acetylation and the recruitment of RNA polymerase II on the promoter of BMP2 and HOXC6-1 (**Fig. 4-19**), further suggesting that KDM6B is required for transcription activation of key osteogenic genes in MSCs. However, despite our repeated efforts, we could not detect KDM6B on the *RUNX2* and *OSX* promoter, suggesting that KDM6B does not directly regulate the *RUNX2* and *OSX* expression.

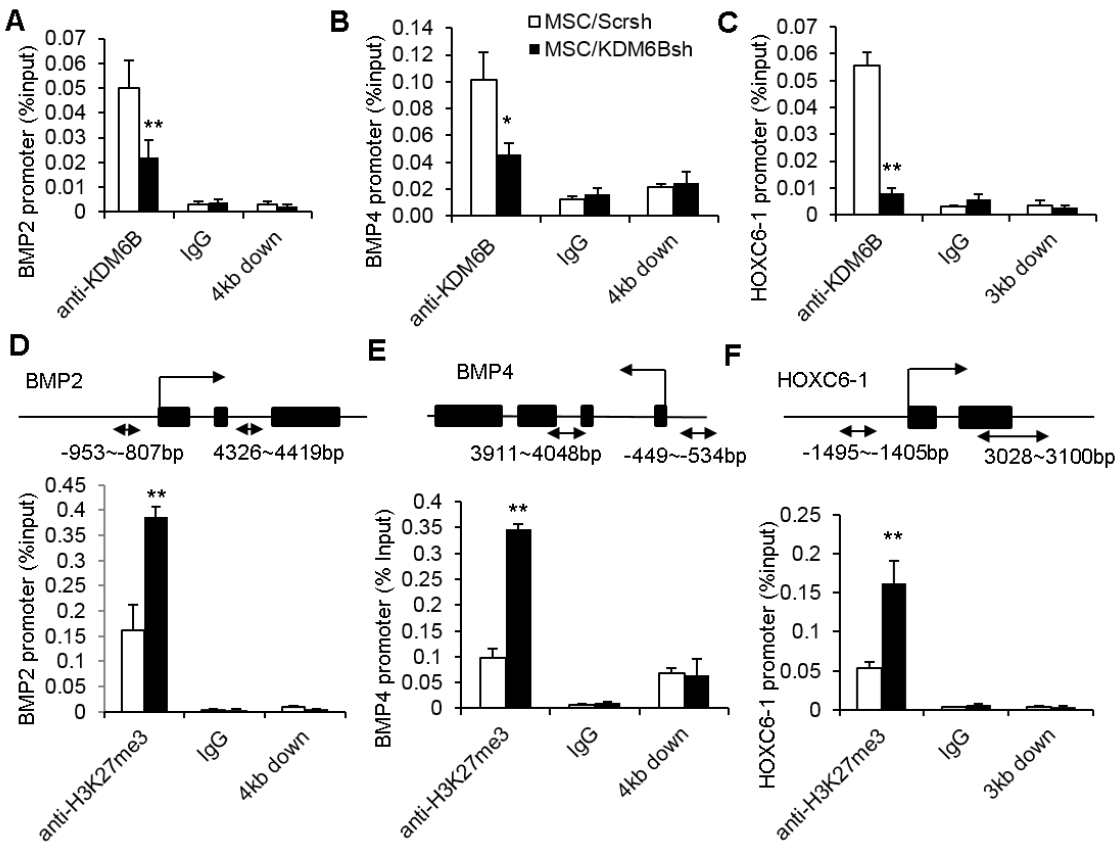

Figure 4-17. KDM6B epigenetically regulates BMP and HOX gene expression in MSCs .

(**A-C**) Knock-down of *KDM6B* reduced KDM6B binding to the promoters of *BMP2*, *BMP4* and *HOXC6-1* in MSCs. The promoters of *BMP2*, *BMP4* and *HOXC6-1* were ChIP-ed with anti-KDM6B antibodies or IgG control. The 3 to 4 kb downstream of the transcriptional start site was also ChIPed with anti-KDM6B. Schematics of the primers corresponding to gene promoter are shown. (**D-F**) Knock-down of *KDM6B* increased H3K27me3 levels at the promoters of *BMP2*, *BMP4* and *HOXC6-1*. The promoters of *BMP2*, *BMP4* and *HOXC6-1* were ChIP-ed with anit-H3K27me3 antibodies or IgG control. The 3 to 4 kb downstream of the transcriptional start site was also ChIP-ed with anti-H3K27me3. **P < 0.01.

.

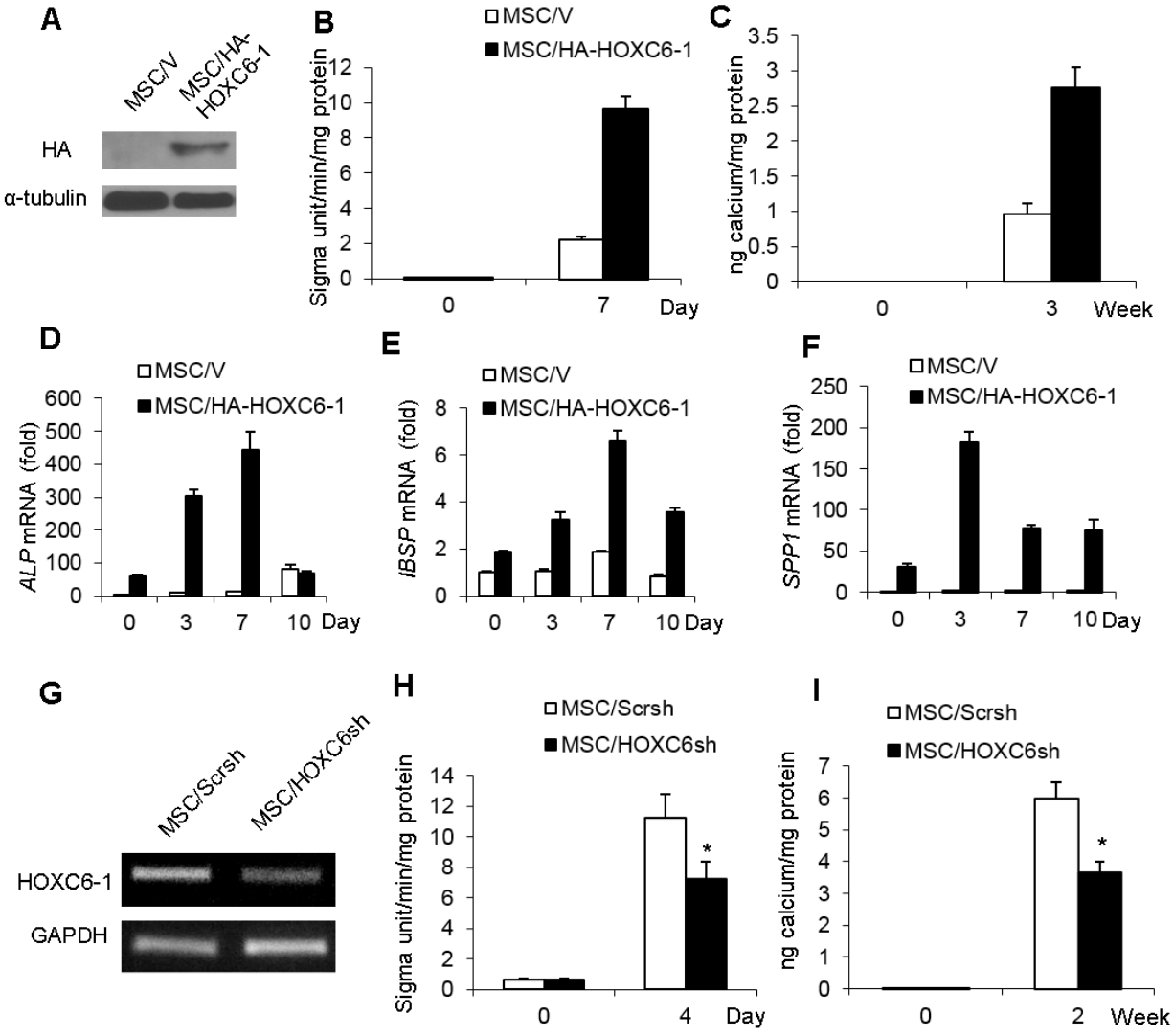

Figure 4-18. HOXC6-1 plays a functional role in osteogenic differentiation of MSCs.

(**A**) Over-expression of HOXC6-1 in MSCs. (**B**) Over-expression of HOXC6-1 increased ALP activities in MSCs. (**C**) Over-expression of HOXC6-1 increased mineralization in MSCs. (**D**) Over-expression of HOXC6-1 enhanced ALP expression. (**E**) Over-expression of HOXC6-1 enhanced *IBSP* expression (**F**) Over-expression of HOXC6-1 enhanced *SPP1* expression. (**G**) The knock-down of *HOXC6-1* in MSCs by shRNA. (**H**) The knock-down of *HOXC6-1* attenuated ALP activities in MSCs. (**I**) The knock-down of *HOXC6-1* attenuated mineralization in MSCs.

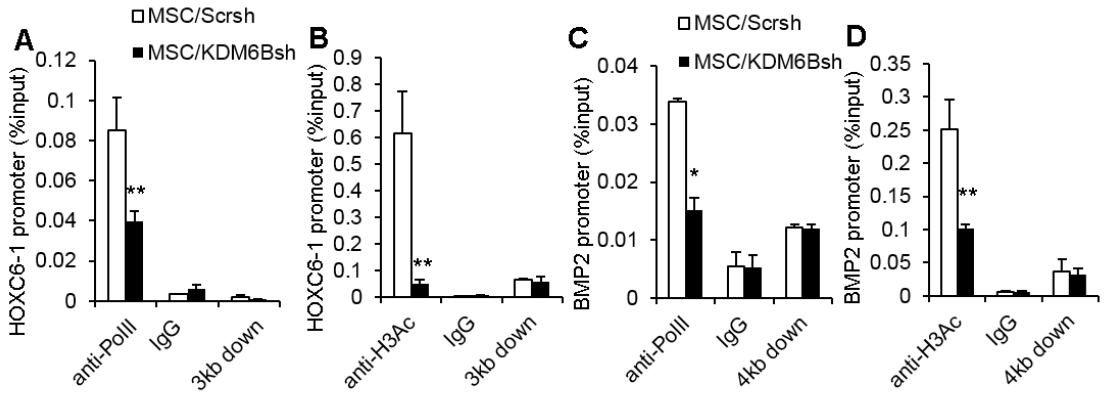

Figure 4-19. The demethylation of H3K27me3 by KDM6B promotes H3 acetylation and recruits RNA polymerase II (Pol II) to the target gene promoters.

(**A**) The knock-down of KDM6B reduced H3 acetylation on the *HOXC6-1* promoter. (**B**) The knock-down of KDM6B reduced the recruitment of Pol II to the *HOXC6-1* promoter. (**C**) The knock-down of KDM6B reduced H3 acetylation on the *BMP2* promoter. (**D**) The knock-down of KDM6B reduced the recruitment of Pol II to the *BMP2* promoter.

4.5.2 KDM4B epigenetically regulates DLX genes in MSCs

To explore the molecular mechanisms underlying the regulation of osteogenic differentiation by KDM4B, we performed Real-Time RT-PCR analysis to assess the expression of key genes associated with osteogenic differentiation of MSCs. In contrast to *KDM6B*, we found that the depletion of *KDM4B* did not affect the basal levels of *HOX* genes (data not shown). Interestingly, we observed that the depletion of *KDM4B* significantly reduced *DLX5* expression that was induced by BMP4/7 (**Fig. 4-20A**). The depletion of *KDM4B* also repressed expression of *DLX2* and *DLX3* induced by BMP4/7 (**Fig. 4-20B and C**). Additionally, we found that *KDM4B* depletion also inhibited *OSX* expression, although *OSX* induction was slower than that that of *DLX5* (**Fig. 4-20D**).

We also examined how KDM4B globally controlled gene expression profile during MSC differentiation using microarray analysis. KDM4B knock-down inhibited the expression of 2448 genes at the basal level and 643 genes induced by BMP4/7. Unlike the results from KDM6Bsh cells, the DLX family genes, including DLX2, DLX3, DLX5 and DLX6, were mainly dependent

on KDM4B (**Fig. 4-21**). The GO analysis also indicated that KDM4B globally controls the expression of genes associated with skeletal development and osteoblast differentiation (**Tables 4-3 and 4-4**). Of note, we found that there were some overlaps between KDM4B- and KDM6B-depenent genes. The demethylation of both H3K27me3 and H3K9me3 might be required for their transcription. However, it also could be due to secondary effects because KDM4B or KDM6B knock-down impaired MSC differentiation through master regulators and subsequently affected common genes associated with osteogenesis.

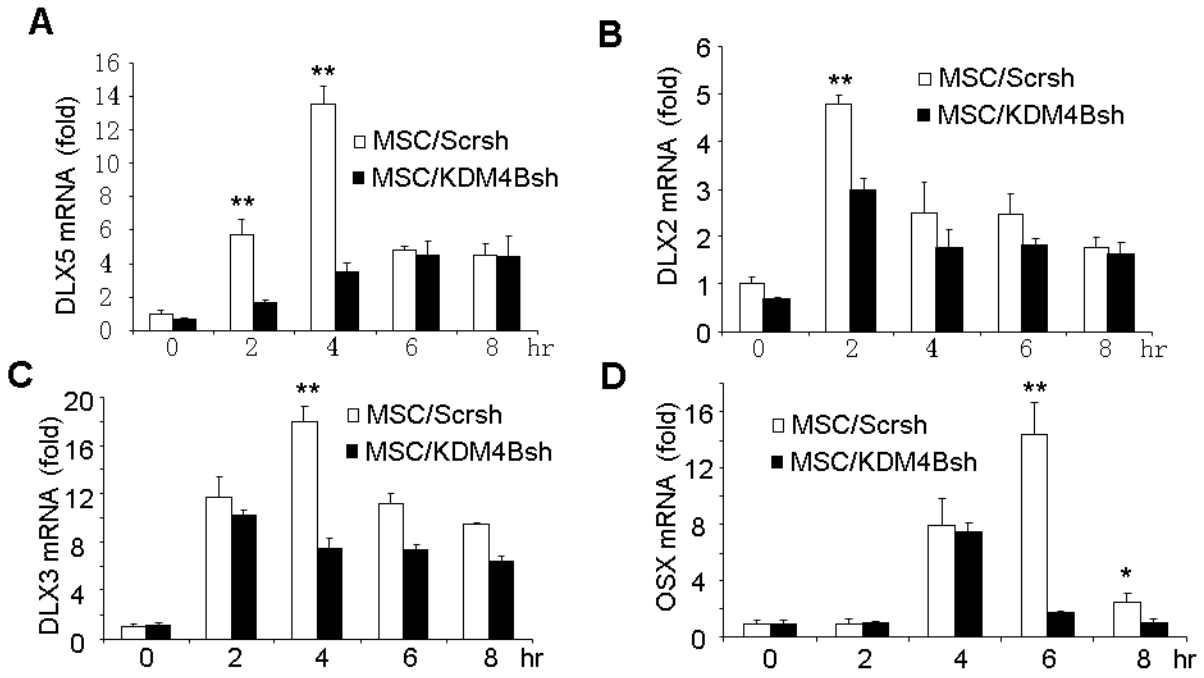

Figure 4-20. KDM4B is required for *DLX* family gene expression in MSCs.

(**A**-**C**) Knock-down of *KDM6B* inhibited the BMP4/7 induction of *DLX5* (**A**), *DLX2* (**B**) *and DLX3* (**C**) expression as determined by Real-time RT-PCR. (**D**) Knock-down of *KDM6B* inhibited the induction of *SP7(OSX)* expression during MSC differentiation, as determined by Real-time RT-PCR. *: P<0.05; **: P<0.01.

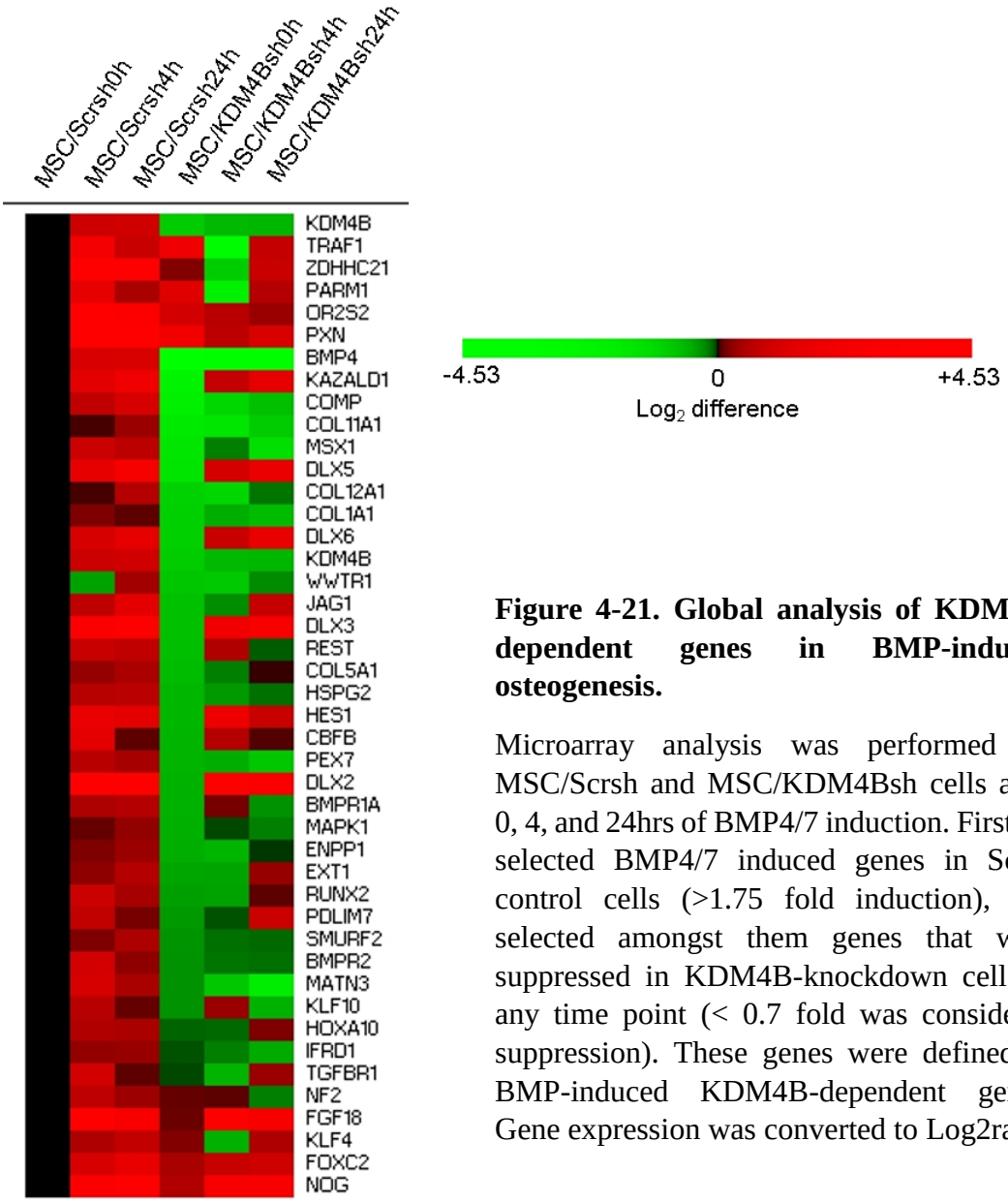

Figure 4-21. Global analysis of KDM4B-dependent genes in BMP-induced osteogenesis.

Microarray analysis was performed on MSC/Scrsh and MSC/KDM4Bsh cells after 0, 4, and 24hrs of BMP4/7 induction. First we selected BMP4/7 induced genes in Scrsh control cells (>1.75 fold induction), and selected amongst them genes that were suppressed in KDM4B-knockdown cells at any time point (< 0.7 fold was considered suppression). These genes were defined as BMP-induced KDM4B-dependent genes. Gene expression was converted to Log2ratio.

Table 4-3. GO Analysis of KDM4B-dependent Genes at Basal Level (selected terms)

GO Term	Count	PValue
GO:0007010~cytoskeleton organization	71	1.01E-04
GO:0001501~skeletal system development	49	0.00449
GO:0030198~extracellular matrix organization	32	2.81E-08
GO:0022604~regulation of cell morphogenesis	29	1.32E-04
GO:0051493~regulation of cytoskeleton organization	22	0.03801
GO:0001503~ossification	19	0.04634
GO:0045444~fat cell differentiation	12	0.01741

Table 4-4. GO Analysis of KDM4B-dependent Genes Induced by BMP4/7 at 4hr (selected terms)

GO Term	Count	PValue
GO:0001501~skeletal system development	25	3.10E-05
GO:0007010~cytoskeleton organization	23	0.01134
GO:0048598~embryonic morphogenesis	19	0.00498
GO:0032990~cell part morphogenesis	14	0.04354
GO:0060348~bone development	13	3.03E-04
GO:0001503~ossification	13	1.61E-04
GO:0048705~skeletal system morphogenesis	13	1.25E-04
GO:0048729~tissue morphogenesis	11	0.04323
GO:0051216~cartilage development	11	6.45E-05
GO:0030198~extracellular matrix organization	10	0.00384
GO:0035107~appendage morphogenesis	8	0.02831
GO:0035108~limb morphogenesis	8	0.02831
GO:0035113~embryonic appendage morphogenesis	8	0.01499
GO:0030326~embryonic limb morphogenesis	8	0.01499
GO:0030278~regulation of ossification	7	0.02864
GO:0030509~BMP signaling pathway	7	0.00182
GO:0045667~regulation of osteoblast differentiation	6	0.00869
GO:0001649~osteoblast differentiation	6	0.00787
GO:0060349~bone morphogenesis	6	2.45E-04
GO:0060350~endochondral bone morphogenesis	6	7.62E-05
GO:0001958~endochondral ossification	6	1.52E-05
GO:0048332~mesoderm morphogenesis	5	0.02579
GO:0045669~positive regulation of osteoblast differentiation	5	0.00598
GO:0002062~chondrocyte differentiation	5	0.0017
GO:0014013~regulation of gliogenesis	4	0.02343
GO:0001502~cartilage condensation	4	0.01784
GO:0002063~chondrocyte development	4	8.40E-04
GO:0060391~positive regulation of SMAD protein nuclear translocation	3	0.01226
GO:0060390~regulation of SMAD protein nuclear translocation	3	0.01226
GO:0060395~SMAD protein signal transduction	3	0.01226

DLX family genes play critical roles in osteoblast differentiation[77,78]. Importantly, *DLX5* has been found to control *OSX* expression[192]. Since *DLX5* was dramatically induced by BMP4/7, we examined whether KDM4B directly regulated *DLX5* expression by removing H3K9me3 silencing marks. ChIP assays revealed that H3K9me3 levels were significantly reduced, while KDM4B was induced to bind to the promoter of DLX5 in MSCs following BMP4/7 treatment (**Fig. 4-22A and B**). Moreover, we found that the knock-down of *KDM4B* reduced KDM4B binding to the *DLX5* promoter induced by BMP4/7. Consistently, H3K9me3 levels on the *DLX5* promoter were elevated in MSC/KDM4Bsh cells as compared with MSC/Scrsh cells (**Fig. 4-22C and D**). As a control, KDM4B did not occupy DNA4kb downstream of the transcription start site, and the knock-down of KDM4B did not affect H3K9me3 on that region. Since KDM4 family demethylases might help to remove H3K36me3 marks, we also examined the levels of H3K36me3 on the DLX5 promoter. ChIP assays showed that KDM4B knock-down did not affect H3K36me3 levels on the DLX5 promoter (data not shown). Importantly, knock-down of KDM4B decreased H3 acetylation and the recruitment of RNA polymerase II on the DLX5 promoter, further implicating that KDM4B is required for DLX5 gene transcription (**Fig. 4-22E and F**). Taken together, our results revealed that KDM4B and KDM6B target key transcription factors to control osteogenic differentiation by demethylating H3K9me3 and H3K27me3 silencing marks, respectively.

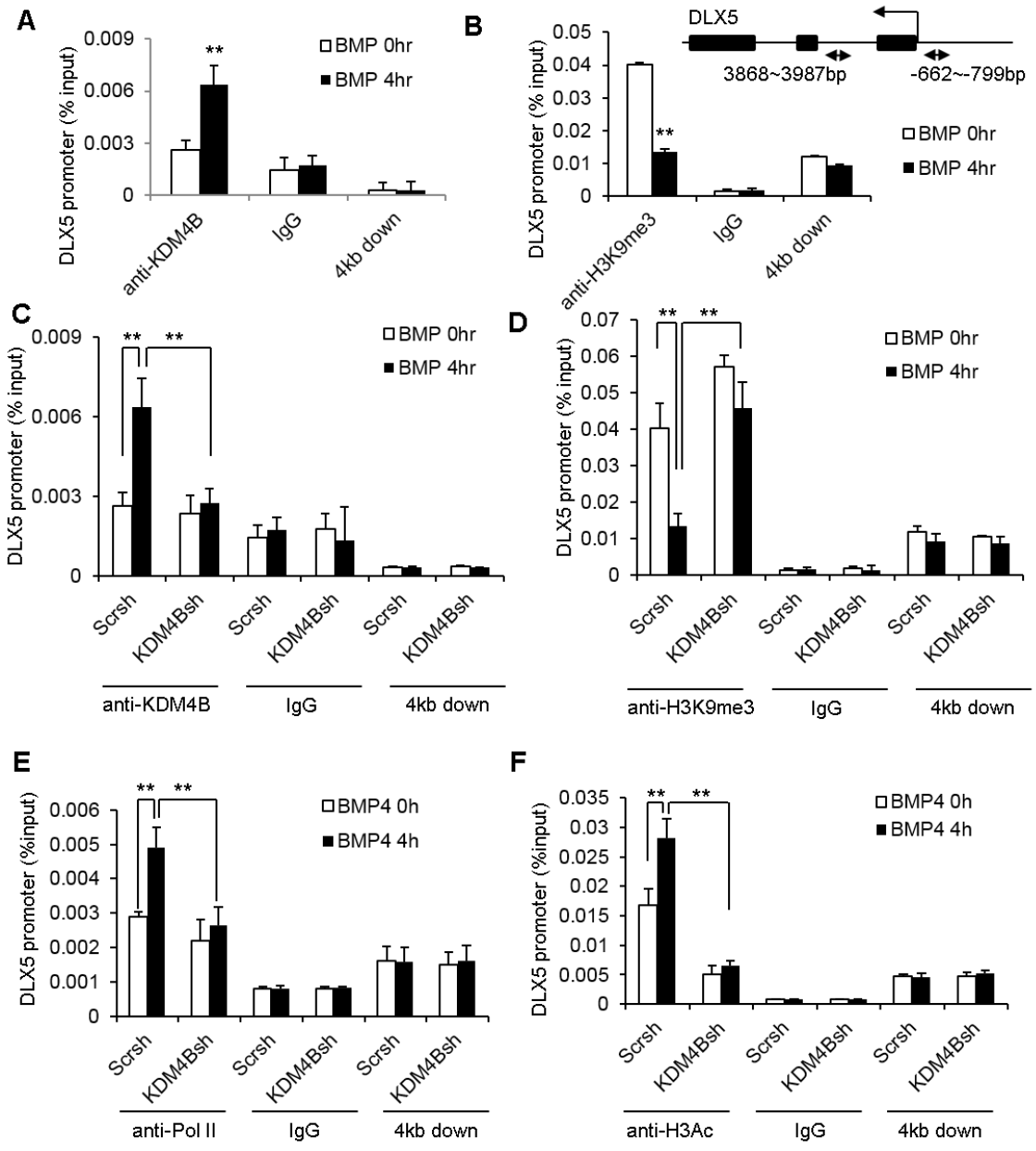

Figure 4-22. KDM4B epigenetically regulates *DLX5* expression in MSCs.

(**A**) BMP4/7 induced KDM4B binding to the *DLX5* promoter. MSCs were treated with BMP4/7 for 4 hr and the *DLX5* promoter was ChIP-ed with anti-KDM4B or IgG control. The 4 kb downstream of the transcriptional start site was also ChIPed with anti-KDM4B. (**B**) BMP4/7 promoted the removal of H3K9me3 in the *DLX5* promoter. (**C**) Knock-down of *KDM4B* inhibited the recruitment of KDM4B to the *DLX5* promoter. (**D**) Knock-down of *KDM4B* abolished BMP-induced removal of H3K9me3 marks at the *DLX5* promoter. Schematics of the primers corresponding to gene promoter are shown. (**E**) Knock-down of *KDM4B* abolished BMP-induced RNA PolII recruitment to the *DLX5* promoter. (**F**) Knock-down of *KDM4B* abolished BMP-induced histone 3 acetylation at the *DLX5* promoter. **P < 0.01.

4.6 H3K27me3 and H3K9me3 are elevated in MSCs of osteoporotic bone marrow.

An inverse relationship exists between osteogenesis and adipogenesis in MSC differentiation[27,29,172,193]. Excessive adipogenic differentiation has been observed in bone marrow of osteoporotic postmenopausal women[194-196]. Our results suggest that the methylation status of H3K9me3 and H3K27me3 may be a critical epigenetic factor that determines MSC fate in bone marrow. Previously, we showed that the adipogenesis was significantly increased in the bone marrow of mice with osteoporosis induced by OVX[130]. Based on our *in vitro* studies, it is possible that H3K9me3 and H3K27me3 might be abnormally elevated in bone marrow MSCs of OVX-ed mice. To test this possibility *in vivo*, we performed immunofluorescence double labeling to examine the status of H3K9me3 and H3K27me3 in bone marrow MSCs of OVX-ed mice using anti-nestin antibodies and anti-H3K9me3 or anti-H3K27me3 antibodies. Very recently, elegant studies showed that mouse MSCs expressed nestin which can be utilized to directly detect MSCs in mouse bone marrow[23]. The total number of cells positive for both nestin and H3K9me3 or H3K27me3 were counted and compared with the total number of nestin-positive cells. Double immunofluorescence labeling revealed that the percentage of H3K9me3- and H3K27me3-positive MSCs was significantly increased in ovariectomized mice compared with sham-operated mice (**Fig. 4-23**).

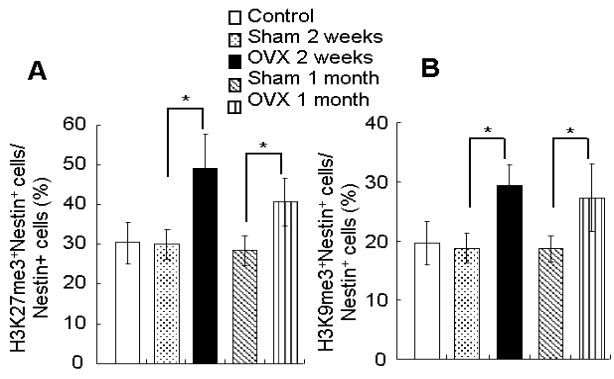

Figure 4-23. Enhanced H3K9me3 and H3K27me3 expression in osteoporotic bone marrow MSCs.

The percentage of H3K27me3-positive MSCs (**A**) and H3K9me3-positive MSCs (**B**) were increased in bone marrow after OVX. The total number of double nestin- and H3K27me3-positive MSCs from 5 different fields were counted per mouse and compared with the total number of nestin-positive MSCs. $n = 6$ mice per group; *$P<0.05$.

4.7 H3K27me3 and H3K9me3 are elevated in MSCs of aged bone marrow.

In aged mice, adipogenesis is increased in bone marrow whereas osteoblastogenesis is reduced. To further confirm that H3K9me3 and H3K27me3 are associated with MSC fate commitments, we also examined their status in bone marrow MSCs of aging mice. μCT showed that the trabecular bone was significantly reduced in 18-month-old mice as compared with 2-month-old mice (**Fig. 4-24A and C**). Compared with younger, 2-month-old mice, we observed that adipose tissues were significantly increased in the bone marrows of 18-month-old mice (**Fig. 4-24B**). Immunofluorescence double labeling revealed that the percentage of H3K9me3- and H3K27me3-positive MSCs was significantly higher in 18 month-old mice than in 2 month-old mice (**Fig. 4-25A and B**). Due to the lack of effective commercial antibodies for KDM4B and KDM6B at the time of study, we isolated MSC from both young and old mice. Real-time RT-PCR revealed that the expression of KDM4B and KDM6B was significantly reduced in primary MSCs from old mice compared to those from young mice (**Fig. 4-25C**). Taken together, our results suggest that H3K9me3 and H3K27me3 epigenetically determine the osteogenic and adipogenic differentiation of MSCs in osteoporosis and skeletal aging.

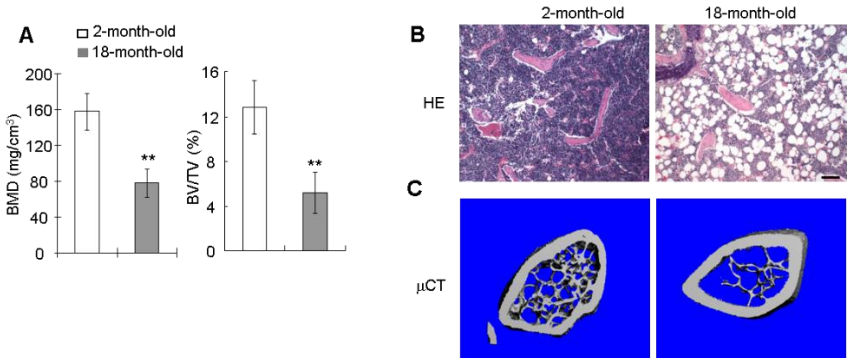

Figure 4-24. Adipogenesis is enhanced while osteogenesis is inhibited in aged mice.

(**A**) μCT analysis of trabecular BMD and BV/TV in distal femurs of 2- and 18-month-old mice. *n*=8 mice per group. (**B**) HE staining of trabecular bone region in 2- and 18-month-old mice, revealing increased adiposity in aged mice. (**C**) Reconstruction of μCT scanning of distal femurs of 2- and 18-month-old mice, indicating reduced bone mass in aged mice.

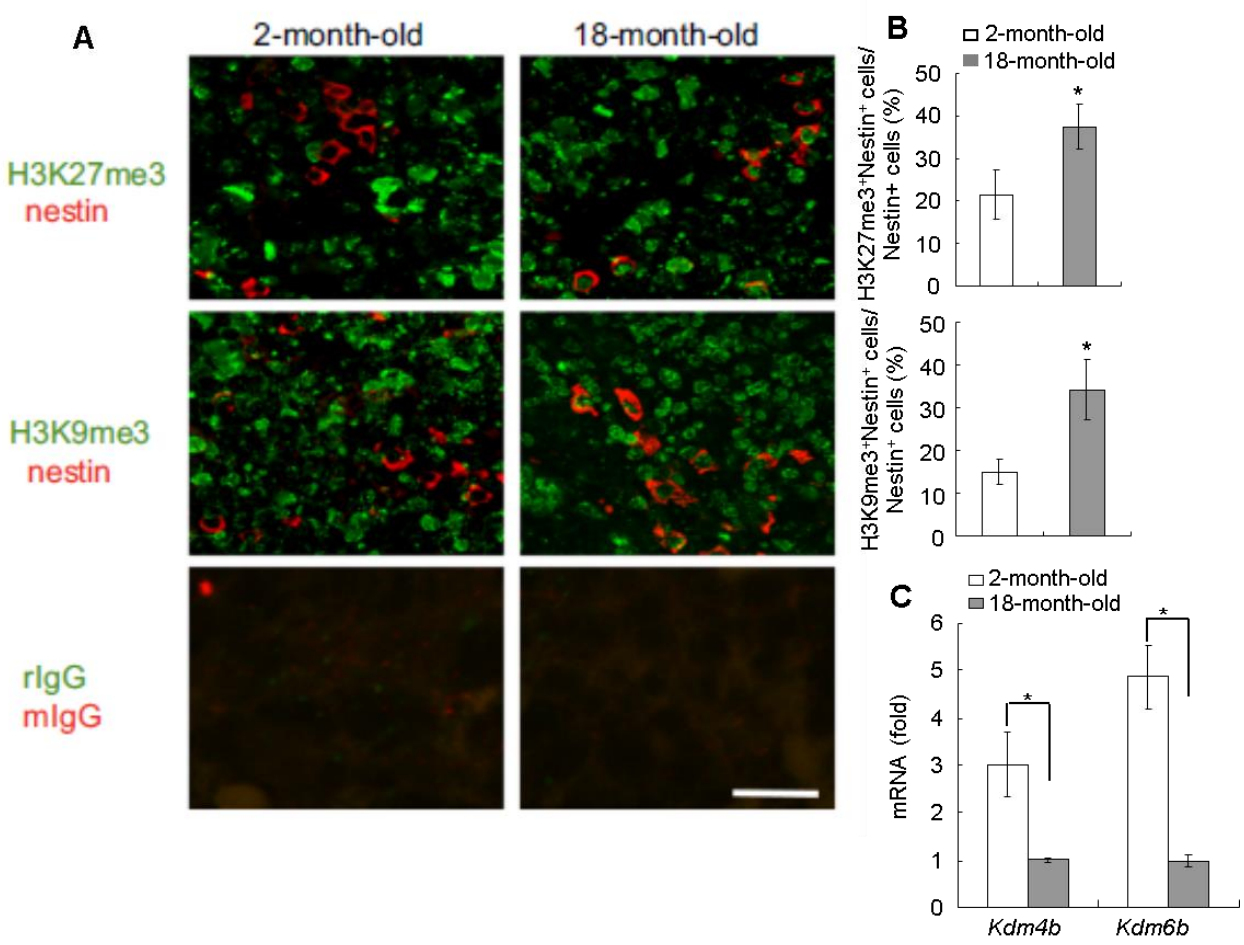

Figure 4-25. H3K27me3 and H3K9me3 marks were increased in MSCs of bone marrow in aged mice.

(**A**) Double immunofluorescent staining of H3K27me3 /H3K9me3 (green) and nestin (red) in distal femur sections of 2- and 18-month-old mice. Scale bar, 40μm. (**B**) Ratio of H3K27me3/H3K9me3-nestin double positive cells in nestin positive cells in bone marrow of young and aged mice. 5 random images were quantified at 40X per mouse; *n* = 6 mice per group. (**C**) mRNA expression of Kdm4b and Kdm6b in MSCs isolated from young and aged mouse bone marrow. *n* = 3 mice per group. *: $P < 0.05$.

4.7 Discussion

MSCs have multiple differentiation potentials and can be induced to differentiate into osteoblasts or adipocytes. However, both lineages are mutually exclusive[29]. The activation of *RUNX2, OSX* and *DLX5* has been found to inhibit adipogenesis. Conversely, forced expression of PPAR-γ inhibits osteogenic differentiation of MSCs[172,197,198]. The commitment of MSCs to an osteogenic lineage requires coordinated inhibition of differentiation toward other lineages, including the adipogenic lineage. The activation of multiple transcription factors has been identified to be associated with MSC differentiation[197,199,200]. To differentiate into osteoblastic or adipogenic lineages, in theory, the chromatin of those genes needs to be reprogrammed or modified. However, very few studies have focused on the epigenetic regulatory mechanisms involved in the activation of master differentiation genes or histone modifications involved in MSC fate determination[26,79,201]. In this study, using gene expression profiling, we identified that KDM4B and KDM6B played largely independent roles in MSC cell fate commitment by removing H3K9me3 and H3K27me3 on different sets of lineage specific genes. The *HOX* and *DLX* genes that play essential roles in MSC osteogenic differentiation were found to be epigenetically regulated by KDM6B and KDM4B through the removal of H3K27me3 and H3K9me3 respectively. More importantly, given the inverse relationship between osteogenic and adipogenic lineage commitment, we found that H3K9me3 and H3K27me3 marks were abnormally elevated in MSCs of osteoporotic bone marrow *in vivo*. Our results provide the first demonstration that histone demethylation controls the imbalance between osteogenesis and adipogenesis in metabolic bone diseases.

BMPs are potent inducers of osteogenic differentiation of MSC that stimulate master transcription factors[202]. In this study, we provide novel epigenetic insights into BMP-stimulated MSC differentiation. The H3K27me3 gene silencing function is essential for maintaining the

balance between embryonic stem cell (ESC) self-renewal and differentiation[81,187]. Decrease of H3K27me3 marks is associated with embryonic development and ESC differentiation. It is possible that chromatins of master differentiation genes in MSCs are enriched with repressive H3K27me3 marks prior to lineage commitment. Recently, H3K27 methyltransferase EZH2 was found to play an important role in the inhibition of MSC differentiation. Interestingly, they found that EZH2 directly binds to the promoter of *RUNX2*[26]. The inactivation of EZH2 by CDK1-dependent phosphorylation reduced the levels of H3K27me3 and promoted osteogenic differentiation of MSC by inducing RUNX2. In addition, another histone demethylase KDM6A could also promote osteogenesis *in vitro* and *in vivo*[80]. Although the knock-down of KDM6B inhibited RUNX2 expression, we found that KDM6B did not directly bind to the promoter of RUNX2. As in the case of ESCs, we found that KDM6B directly regulated the expression of BMP and HOX genes by removing H3K27me3 marks. Therefore, it is likely that KDM6B indirectly controls RUNX2 expression through BMPs and HOX genes. Given the fact that KDM6B is also induced by BMPs, our results suggest a possible feedback system and that MSC fate commitment can be regulated at multiple levels by modulating the levels of H3K27me3.

KDM4B has been characterized as being capable of selectively reducing chromosomal H3K9me3 marks to H3K9me1 with the H3K9me2 state remaining unaltered[183-186]. H3K9me3 marks are generally associated with gene repression. The majority of H3K9me3 marks are found in inactive regions of the genome, such as constitutive heterochromatin. Whereas in some reports these marks are enriched in actively transcribed regions of the genome, they are never at the promoter regions of expressed genes[203,204]. Depletion of KDM4B homolog in *C. elegans* led to a global increase in H3K9me3 levels and activated p53-mediated apoptosis[186]. However, we found that the knock-down of *KMD4B* did not affect MSC apoptosis. Unlike KDM6B, *KDM4B* knock-

down mainly inhibited the expression of *DLX genes*. Our results suggest that KDM4B and KDM6B may target different transcription factors by removing H3K9me3 or H3K27me27 marks, respectively. DLX family transcription factors have been found to play a critical role in the induction of *RUNX2* and *OSX* [78,192,205,206]. Although knock-down of *KDM4B* inhibited *OSX* expression, our ChIP assay was unable to detect KDM4B binding to the *OSX* promoter, thereby implying an indirect regulation of *OSX* expression through DLX. Importantly, recent evidence suggested that DLX5 could inhibit adipogenesis by binding with CEBP, thereby sequestering it from activating PPARγ transcription, a master regulator of adipogenesis[207]. Hence, KDM4B, through epigenetic activation of DLX5, could promote osteogenic differentiation over adipogenesis.

Our results suggest that the levels of H3K27me3 and H3K9me3 determine MSC cell lineage commitment. Since osteoporosis is one of the most common bone metabolic diseases that are associated with a shift in MSC lineage commitment, we examined whether the levels of H3K27me3 and H3K9me3 were changed in OVX-ed mice in which bone loss is accompanied by increased adipose tissues in the bone marrow cavity. The MSC differentiation potential in aged or diseased skeletal system may undergo significant changes. After establishing the roles of KDM4B and KDM6B in promoting osteogenesis and inhibiting adipogenesis in healthy MSCs, we observed a consistent trend that persists in pathogical conditions, which shed light to their potential involvement in diseased and aging system. Our immunostaining revealed a significant higher percentage of H3K27me3- and H3K9me3-positive MSCs in bone marrow of OVX-ed mice as compared with sham-operated mice. Moreover, we found that the percentage of H3K27me3- and H3K9me3-positive MSCs in bone marrow of aging mice was also significantly increased as compared with young mice. Taken together, these results suggest that increased H3K27me3 and

H3K9me3 levels might play an important role in the development of osteoporosis by influencing determination of MSC fate choices in bone marrow. As a chemically modifiable enzyme, KDM4B and KDM6B could be activated or deactivated to regulate specific lineage decisions of MSCs, thereby holding promising potentials as a therapeutic target for stem cell-mediated regenerative medicine as well as the treatment of human metabolic bone diseases such as osteoporosis.

5 SUMMARY AND CONCLUSION

Bone remodeling is under tight regulation by the complex molecular signaling initiated by factors in the bone microenvironment, including locally secreted factors from stromal cells and bone cells, immune cytokines from lymphocytes and macrophages, and systemically delivered hormones. The coordination and balance between osteoblasts and osteoclasts, as well as the lineage decisions for MSCs between adipogenesis and osteogenesis, play a critical role in maintaining homeostasis in health, and in pathogenesis of metabolic, inflammatory and age-related bone loss.

In Chapter 3, we used three complimentary bone loss models with transgenic mice expressing Wnt4 in osteoblasts, and reported a non-canonical Wnt4 signaling that could not only promote osteoblasts, but also inhibit osteoclasts via attenuating NF-κB. Here we will highlight several novel findings which contribute to our understanding of the molecular regulatory networks of bone cells:

1) Wnt4 expressed by osteoblasts, in addition to promoting bone formation *in vivo*, acts upon osteoclasts to inhibit bone resorption. This exemplifies the cell-cell interaction between two types of bone cells.
2) Wnt4 signaling takes place without accumulation of β-catenin in neither osteoblasts nor osteoclasts. This adds another dimension to the poorly understood mechanisms by which non-canonical Wnt signaling regulates bone cell differentiation and functions.
3) Wnt4 signaling effectively attenuated NF-κB activity both locally and systemically. This revealed a novel crosstalk between two major pathways affecting bone cells. As most bone pathologies are associated with chronic inflammation and the proinflammatory bone environment, Wnt4 may play a significant role in the osteoimmune interactions between bone cells and the immune system.

4) From a therapeutic perspective, Wnt4 recombinant protein holds significant value as Wnt4 injection was able to restore established bone loss in osteoporotic mouse model, via simultaneously enhancing bone formation and slowing bone resorption. In addition, the non-canonical Wnt signaling would not lead to carcinogenic concerns from β-catenin accumulation.

In Chapter 4, we explored the epigenetic regulation of MSC lineage decisions, specifically the choice between osteoblastogenesis and adipogenesis. The shift from osteogenesis towards adipogenesis is manifested in both age-related bone loss and osteoporosis. However, the epigenetic links that lead to these lineage decisions were previously poorly defined.

1) Using gain- and loss-of-functions studies, we discovered two novel histone demethylases KDM4B and KDM6B that could promote osteoblastic differentiation and inhibit adipogenic differentiation of MSCs.
2) KDM4B and KDM6B targets different sets of osteogenic transcription factors, activating them by removing gene silencing marks H3K9me3 and H3K27me3 respectively.
3) H3K27me3- and H3K9me3-positive MSCs were elevated in osteoporotic and aged bone marrow, which correlated with a decrease in KDM4B and KDM6B expression in aged mice, implicating these demethylases could be potential therapeutic targets for treatment of metabolic bone diseases.

In summary, our findings supported the following model: in undifferentiated MSCs, gene silencing marks are enriched on the promoters of osteogenic transcription factors. Upon BMP4/7 signaling or osteogenic induction, KDM4B and KDM6B expression is induced via SMAD, thereby removing gene silencing marks from BMP, HOX and DLX

genes and resulting in their activation. These genes in turn promote osteoblastogenesis and inhibit adipogenesis of MSCs.

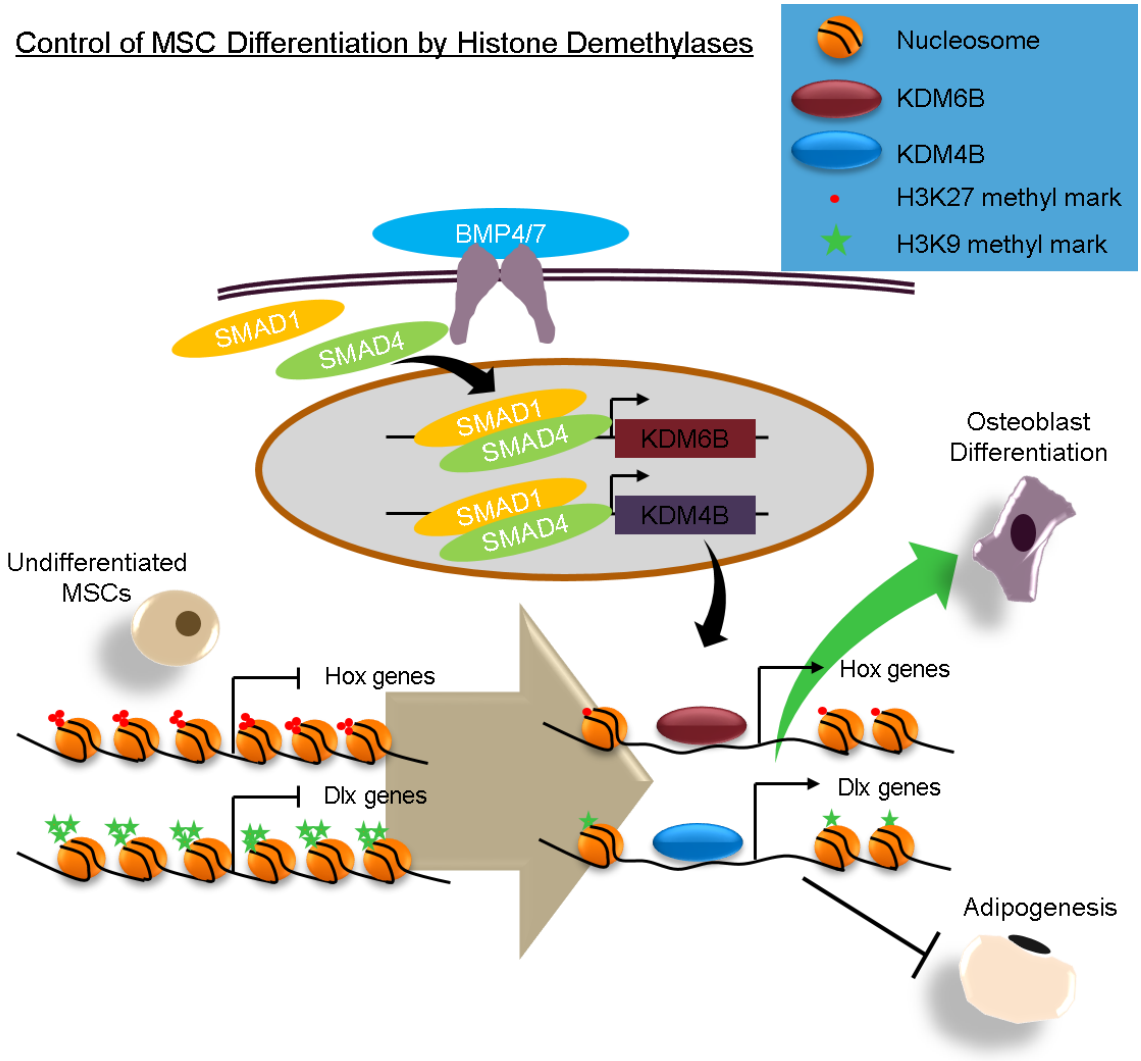

Figure 5-1 Schematics of epigenetic regulation of MSC cell fate decisions by KDM4B and KDM6B.

BIOBLIOGRAPHY

1. Manolagas, S. & Jilka, R. Bone marrow, cytokines, and bone remodeling. Emerging insights into the pathophysiology of osteoporosis. *The New England journal of medicine* **332**, 305 - 311 (1995).
2. Zaidi, M. Skeletal remodeling in health and disease. *Nature medicine* **13**, 791-801 (2007).
3. Teitelbaum, S.L. Bone resorption by osteoclasts. *Science* **289**, 1504-1508 (2000).
4. Del Fattore, A., Teti, A. & Rucci, N. Bone cells and the mechanisms of bone remodelling. *Front Biosci (Elite Ed)* **4**, 2302-2321 (2012).
5. Raisz, L.G. Pathogenesis of osteoporosis: concepts, conflicts, and prospects. *The Journal of clinical investigation* **115**, 3318-3325 (2005).
6. Riggs, B.L., Khosla, S. & Melton, L.J., 3rd. Better tools for assessing osteoporosis. *The Journal of clinical investigation* **122**, 4323-4324 (2012).
7. Syed, F. & Khosla, S. Mechanisms of sex steroid effects on bone. *Biochemical and biophysical research communications* **328**, 688-696 (2005).
8. Sun, L., *et al.* FSH directly regulates bone mass. *Cell* **125**, 247-260 (2006).
9. Yasui, T., Hirose, J., Aburatani, H. & Tanaka, S. Epigenetic regulation of osteoclast differentiation. *Annals of the New York Academy of Sciences* **1240**, 7-13 (2011).
10. Benayahu, D., Shefer, G. & Shur, I. Insights into the transcriptional and chromatin regulation of mesenchymal stem cells in musculo-skeletal tissues. *Annals of anatomy = Anatomischer Anzeiger : official organ of the Anatomische Gesellschaft* **191**, 2-12 (2009).
11. Sinha, K.M. & Zhou, X. Genetic and molecular control of osterix in skeletal formation. *Journal of cellular biochemistry* **114**, 975-984 (2013).

12. Michalakis, K., Peitsidis, P. & Ilias, I. Pregnancy- and lactation-associated osteoporosis: a narrative mini-review. *Endocrine regulations* **45**, 43-47 (2011).

13. Sinaki, M. Exercise for patients with osteoporosis: management of vertebral compression fractures and trunk strengthening for fall prevention. *PM & R : the journal of injury, function, and rehabilitation* **4**, 882-888 (2012).

14. Frenkel, B., *et al.* Regulation of adult bone turnover by sex steroids. *Journal of cellular physiology* **224**, 305-310 (2010).

15. Johnell, O. & Kanis, J.A. An estimate of the worldwide prevalence and disability associated with osteoporotic fractures. *Osteoporosis international : a journal established as result of cooperation between the European Foundation for Osteoporosis and the National Osteoporosis Foundation of the USA* **17**, 1726-1733 (2006).

16. Lopez-Otin, C., Blasco, M.A., Partridge, L., Serrano, M. & Kroemer, G. The hallmarks of aging. *Cell* **153**, 1194-1217 (2013).

17. Uccelli, A., Moretta, L. & Pistoia, V. Mesenchymal stem cells in health and disease. *Nat Rev Immunol* **8**, 726-736 (2008).

18. da Silva Meirelles, L., Chagastelles, P.C. & Nardi, N.B. Mesenchymal stem cells reside in virtually all post-natal organs and tissues. *Journal of cell science* **119**, 2204-2213 (2006).

19. Sacchetti, B., *et al.* Self-renewing osteoprogenitors in bone marrow sinusoids can organize a hematopoietic microenvironment. *Cell* **131**, 324-336 (2007).

20. Rosset, P., Deschaseaux, F. & Layrolle, P. Cell therapy for bone repair. *Orthopaedics & traumatology, surgery & research : OTSR* **100**, S107-112 (2014).

21. Kolf, C.M., Cho, E. & Tuan, R.S. Mesenchymal stromal cells. Biology of adult mesenchymal stem cells: regulation of niche, self-renewal and differentiation. *Arthritis research & therapy* **9**, 204 (2007).

22. Phinney, D.G. & Prockop, D.J. Concise review: mesenchymal stem/multipotent stromal cells: the state of transdifferentiation and modes of tissue repair--current views. *Stem cells* **25**, 2896-2902 (2007).

23. Mendez-Ferrer, S., *et al.* Mesenchymal and haematopoietic stem cells form a unique bone marrow niche. *Nature* **466**, 829-834 (2010).

24. Gomez-Barrena, E., *et al.* Bone fracture healing: Cell therapy in delayed unions and nonunions. *Bone* (2014).

25. Hernigou, P., *et al.* Osteonecrosis repair with bone marrow cell therapies: State of the clinical art. *Bone* (2014).

26. Wei, Y., *et al.* CDK1-dependent phosphorylation of EZH2 suppresses methylation of H3K27 and promotes osteogenic differentiation of human mesenchymal stem cells. *Nature cell biology* **13**, 87-94 (2011).

27. Takada, I., Kouzmenko, A.P. & Kato, S. Wnt and PPARgamma signaling in osteoblastogenesis and adipogenesis. *Nat Rev Rheumatol* **5**, 442-447 (2009).

28. Kawai, M. & Rosen, C.J. Bone: adiposity and bone accrual-still an established paradigm? *Nature reviews. Endocrinology* **6**, 63-64 (2010).

29. McCauley, L.K. c-Maf and you won't see fat. *The Journal of clinical investigation* **120**, 3440-3442 (2010).

30. Muruganandan, S., Roman, A.A. & Sinal, C.J. Adipocyte differentiation of bone marrow-derived mesenchymal stem cells: cross talk with the osteoblastogenic program. *Cellular and molecular life sciences : CMLS* **66**, 236-253 (2009).

31. Gaur, T., *et al.* Canonical WNT signaling promotes osteogenesis by directly stimulating Runx2 gene expression. *The Journal of biological chemistry* **280**, 33132-33140 (2005).

32. Ducy, P., *et al.* A Cbfa1-dependent genetic pathway controls bone formation beyond embryonic development. *Genes & development* **13**, 1025-1036 (1999).

33. Karsenty, G., *et al.* Cbfa1 as a regulator of osteoblast differentiation and function. *Bone* **25**, 107-108 (1999).

34. Ducy, P. & Karsenty, G. Two distinct osteoblast-specific cis-acting elements control expression of a mouse osteocalcin gene. *Molecular and cellular biology* **15**, 1858-1869 (1995).

35. Otto, F., *et al.* Cbfa1, a candidate gene for cleidocranial dysplasia syndrome, is essential for osteoblast differentiation and bone development. *Cell* **89**, 765-771 (1997).

36. Komori, T., *et al.* Targeted disruption of Cbfa1 results in a complete lack of bone formation owing to maturational arrest of osteoblasts. *Cell* **89**, 755-764 (1997).

37. Nakashima, K., *et al.* The novel zinc finger-containing transcription factor osterix is required for osteoblast differentiation and bone formation. *Cell* **108**, 17-29 (2002).

38. Okamoto, M., Murai, J., Yoshikawa, H. & Tsumaki, N. Bone morphogenetic proteins in bone stimulate osteoclasts and osteoblasts during bone development. *Journal of bone and mineral research : the official journal of the American Society for Bone and Mineral Research* **21**, 1022-1033 (2006).

39. Mishina, Y., *et al.* Bone morphogenetic protein type IA receptor signaling regulates postnatal osteoblast function and bone remodeling. *The Journal of biological chemistry* **279**, 27560-27566 (2004).

40. Gazzerro, E., *et al.* Conditional deletion of gremlin causes a transient increase in bone formation and bone mass. *The Journal of biological chemistry* **282**, 31549-31557 (2007).

41. Derynck, R. & Zhang, Y.E. Smad-dependent and Smad-independent pathways in TGF-beta family signalling. *Nature* **425**, 577-584 (2003).

42. Chen, G., Deng, C. & Li, Y.P. TGF-beta and BMP signaling in osteoblast differentiation and bone formation. *International journal of biological sciences* **8**, 272-288 (2012).

43. Lee, K.S., *et al.* Runx2 is a common target of transforming growth factor beta1 and bone morphogenetic protein 2, and cooperation between Runx2 and Smad5 induces osteoblast-specific gene expression in the pluripotent mesenchymal precursor cell line C2C12. *Molecular and cellular biology* **20**, 8783-8792 (2000).

44. Javed, A., *et al.* Specific residues of RUNX2 are obligatory for formation of BMP2-induced RUNX2-SMAD complex to promote osteoblast differentiation. *Cells, tissues, organs* **189**, 133-137 (2009).

45. Javed, A., *et al.* Structural coupling of Smad and Runx2 for execution of the BMP2 osteogenic signal. *The Journal of biological chemistry* **283**, 8412-8422 (2008).

46. Bae, J.S., *et al.* Reconstitution of Runx2/Cbfa1-null cells identifies a requirement for BMP2 signaling through a Runx2 functional domain during osteoblast differentiation. *Journal of cellular biochemistry* **100**, 434-449 (2007).

47. Afzal, F., *et al.* Smad function and intranuclear targeting share a Runx2 motif required for osteogenic lineage induction and BMP2 responsive transcription. *Journal of cellular physiology* **204**, 63-72 (2005).

48. Matsubara, H., Tsuchiya, H., Watanabe, K., Takeuchi, A. & Tomita, K. Percutaneous nonviral delivery of hepatocyte growth factor in an osteotomy gap promotes bone repair in rabbits: a preliminary study. *Clinical orthopaedics and related research* **466**, 2962-2972 (2008).

49. Hata, K., *et al.* Differential roles of Smad1 and p38 kinase in regulation of peroxisome proliferator-activating receptor gamma during bone morphogenetic protein 2-induced adipogenesis. *Molecular biology of the cell* **14**, 545-555 (2003).

50. Anastas, J.N. & Moon, R.T. WNT signalling pathways as therapeutic targets in cancer. *Nature reviews. Cancer* **13**, 11-26 (2013).

51. MacDonald, B.T., Tamai, K. & He, X. Wnt/beta-catenin signaling: components, mechanisms, and diseases. *Developmental cell* **17**, 9-26 (2009).

52. Koay, M.A. & Brown, M.A. Genetic disorders of the LRP5-Wnt signalling pathway affecting the skeleton. *Trends in molecular medicine* **11**, 129-137 (2005).

53. Kato, M., *et al.* Cbfa1-independent decrease in osteoblast proliferation, osteopenia, and persistent embryonic eye vascularization in mice deficient in Lrp5, a Wnt coreceptor. *The Journal of cell biology* **157**, 303-314 (2002).

54. Hu, H., *et al.* Sequential roles of Hedgehog and Wnt signaling in osteoblast development. *Development* **132**, 49-60 (2005).

55. Day, T.F., Guo, X., Garrett-Beal, L. & Yang, Y. Wnt/beta-catenin signaling in mesenchymal progenitors controls osteoblast and chondrocyte differentiation during vertebrate skeletogenesis. *Developmental cell* **8**, 739-750 (2005).

56. Holmen, S.L., *et al.* Essential role of beta-catenin in postnatal bone acquisition. *The Journal of biological chemistry* **280**, 21162-21168 (2005).

57. Chen, J. & Long, F. beta-catenin promotes bone formation and suppresses bone resorption in postnatal growing mice. *Journal of bone and mineral research : the official journal of the American Society for Bone and Mineral Research* **28**, 1160-1169 (2013).

58. Krishnan, V., Bryant, H.U. & MacDougald, O.A. Regulation of bone mass by Wnt signaling. *The Journal of clinical investigation* **116**, 1202-1209 (2006).

59. Ross, S.E., *et al.* Inhibition of adipogenesis by Wnt signaling. *Science* **289**, 950-953 (2000).

60. Bennett, C.N., *et al.* Regulation of Wnt signaling during adipogenesis. *The Journal of biological chemistry* **277**, 30998-31004 (2002).

61. Okamoto, M., *et al.* Noncanonical Wnt5a enhances Wnt/beta-catenin signaling during osteoblastogenesis. *Scientific reports* **4**, 4493 (2014).

62. Friedman, M.S., Oyserman, S.M. & Hankenson, K.D. Wnt11 promotes osteoblast maturation and mineralization through R-spondin 2. *The Journal of biological chemistry* **284**, 14117-14125 (2009).

63. Tu, X., *et al.* Noncanonical Wnt signaling through G protein-linked PKCdelta activation promotes bone formation. *Developmental cell* **12**, 113-127 (2007).

64. Chang, J., *et al.* Noncanonical Wnt-4 Signaling Enhances Bone Regeneration of Mesenchymal Stem Cells in Craniofacial Defects through Activation of p38 MAPK. *Journal of Biological Chemistry* **282**, 30938-30948 (2007).

65. Baron, R. & Kneissel, M. WNT signaling in bone homeostasis and disease: from human mutations to treatments. *Nature medicine* **19**, 179-192 (2013).

66. Yakar, S., Courtland, H.W. & Clemmons, D. IGF-1 and bone: New discoveries from mouse models. *Journal of bone and mineral research : the official journal of the American Society for Bone and Mineral Research* **25**, 2543-2552 (2010).

67. Lintern, K.B., Guidato, S., Rowe, A., Saldanha, J.W. & Itasaki, N. Characterization of wise protein and its molecular mechanism to interact with both Wnt and BMP signals. *The Journal of biological chemistry* **284**, 23159-23168 (2009).

68. Qin, L., Raggatt, L.J. & Partridge, N.C. Parathyroid hormone: a double-edged sword for bone metabolism. *Trends Endocrinol Metab* **15**, 60-65 (2004).

69. Powell, W.F., Jr., *et al.* Targeted ablation of the PTH/PTHrP receptor in osteocytes impairs bone structure and homeostatic calcemic responses. *The Journal of endocrinology* **209**, 21-32 (2011).

70. Wan, M., *et al.* Parathyroid hormone signaling through low-density lipoprotein-related protein 6. *Genes & development* **22**, 2968-2979 (2008).

71. Erson, A.E. & Petty, E.M. MicroRNAs in development and disease. *Clinical genetics* **74**, 296-306 (2008).

72. Huang, S., *et al.* Upregulation of miR-22 promotes osteogenic differentiation and inhibits adipogenic differentiation of human adipose tissue-derived mesenchymal stem cells by repressing HDAC6 protein expression. *Stem cells and development* **21**, 2531-2540 (2012).

73. Li, H., *et al.* miR-17-5p and miR-106a are involved in the balance between osteogenic and adipogenic differentiation of adipose-derived mesenchymal stem cells. *Stem cell research* **10**, 313-324 (2013).

74. Zhang, J.F., *et al.* MiR-637 maintains the balance between adipocytes and osteoblasts by directly targeting Osterix. *Molecular biology of the cell* **22**, 3955-3961 (2011).

75. Jenuwein, T. & Allis, C.D. Translating the histone code. *Science* **293**, 1074-1080 (2001).

76. Schuettengruber, B., Chourrout, D., Vervoort, M., Leblanc, B. & Cavalli, G. Genome regulation by polycomb and trithorax proteins. *Cell* **128**, 735-745 (2007).

77. Hassan, M.Q., *et al.* HOXA10 controls osteoblastogenesis by directly activating bone regulatory and phenotypic genes. *Molecular and cellular biology* **27**, 3337-3352 (2007).

78. Hassan, M.Q., *et al.* Molecular switches involving homeodomain proteins, HOXA10 and RUNX2 regulate osteoblastogenesis. *Cells, tissues, organs* **189**, 122-125 (2009).

79. Fan, Z., *et al.* BCOR regulates mesenchymal stem cell function by epigenetic mechanisms. *Nature cell biology* **11**, 1002-1009 (2009).

80. Hemming, S., *et al.* EZH2 and KDM6A act as an epigenetic switch to regulate mesenchymal stem cell lineage specification. *Stem cells* **32**, 802-815 (2014).

81. Lan, F., *et al.* A histone H3 lysine 27 demethylase regulates animal posterior development. *Nature* **449**, 689-694 (2007).

82. Klose, R.J., *et al.* The retinoblastoma binding protein RBP2 is an H3K4 demethylase. *Cell* **128**, 889-900 (2007).

83. Shi, Y. & Whetstine, J.R. Dynamic regulation of histone lysine methylation by demethylases. *Molecular cell* **25**, 1-14 (2007).

84. De Santa, F., *et al.* The histone H3 lysine-27 demethylase Jmjd3 links inflammation to inhibition of polycomb-mediated gene silencing. *Cell* **130**, 1083-1094 (2007).

85. Jepsen, K., *et al.* SMRT-mediated repression of an H3K27 demethylase in progression from neural stem cell to neuron. *Nature* **450**, 415-419 (2007).

86. Sen, G.L., Webster, D.E., Barragan, D.I., Chang, H.Y. & Khavari, P.A. Control of differentiation in a self-renewing mammalian tissue by the histone demethylase JMJD3. *Genes & development* **22**, 1865-1870 (2008).

87. Lee, S., Lee, J.W. & Lee, S.K. UTX, a histone H3-lysine 27 demethylase, acts as a critical switch to activate the cardiac developmental program. *Developmental cell* **22**, 25-37 (2012).

88. Seenundun, S., *et al.* UTX mediates demethylation of H3K27me3 at muscle-specific genes during myogenesis. *The EMBO journal* **29**, 1401-1411 (2010).

89. Sierra, J., *et al.* Regulation of the bone-specific osteocalcin gene by p300 requires Runx2/Cbfa1 and the vitamin D3 receptor but not p300 intrinsic histone acetyltransferase activity. *Molecular and cellular biology* **23**, 3339-3351 (2003).

90. Jensen, E.D., Gopalakrishnan, R. & Westendorf, J.J. Regulation of gene expression in osteoblasts. *BioFactors* **36**, 25-32 (2010).

91. Jeon, E.J., *et al.* Bone morphogenetic protein-2 stimulates Runx2 acetylation. *The Journal of biological chemistry* **281**, 16502-16511 (2006).

92. Shen, J., *et al.* Transcriptional induction of the osteocalcin gene during osteoblast differentiation involves acetylation of histones h3 and h4. *Molecular endocrinology* **17**, 743-756 (2003).

93. Villagra, A., *et al.* Reduced CpG methylation is associated with transcriptional activation of the bone-specific rat osteocalcin gene in osteoblasts. *Journal of cellular biochemistry* **85**, 112-122 (2002).

94. Dansranjavin, T., *et al.* The role of promoter CpG methylation in the epigenetic control of stem cell related genes during differentiation. *Cell cycle* **8**, 916-924 (2009).

95. Matsuo, K., *et al.* Fosl1 is a transcriptional target of c-Fos during osteoclast differentiation. *Nature genetics* **24**, 184-187 (2000).

96. Redlich, K. & Smolen, J.S. Inflammatory bone loss: pathogenesis and therapeutic intervention. *Nature reviews. Drug discovery* **11**, 234-250 (2012).

97. Takayanagi, H., *et al.* Induction and activation of the transcription factor NFATc1 (NFAT2) integrate RANKL signaling in terminal differentiation of osteoclasts. *Developmental cell* **3**, 889-901 (2002).

98. Teitelbaum, S.L. Osteoclasts: what do they do and how do they do it? *The American journal of pathology* **170**, 427-435 (2007).

99. Teitelbaum, S.L. RANKing c-Jun in osteoclast development. *The Journal of clinical investigation* **114**, 463-465 (2004).

100. Roodman, G.D. Regulation of osteoclast differentiation. *Annals of the New York Academy of Sciences* **1068**, 100-109 (2006).

101. Mizukami, J., *et al.* Receptor Activator of NF-κB Ligand (RANKL) Activates TAK1 Mitogen-Activated Protein Kinase Kinase Kinase through a Signaling Complex Containing RANK, TAB2, and TRAF6. *Molecular and cellular biology* **22**, 992-1000 (2002).

102. Lee, S.K. & Lorenzo, J.A. Parathyroid hormone stimulates TRANCE and inhibits osteoprotegerin messenger ribonucleic acid expression in murine bone marrow cultures: correlation with osteoclast-like cell formation. *Endocrinology* **140**, 3552-3561 (1999).

103. Horwood, N.J., Elliott, J., Martin, T.J. & Gillespie, M.T. Osteotropic agents regulate the expression of osteoclast differentiation factor and osteoprotegerin in osteoblastic stromal cells. *Endocrinology* **139**, 4743-4746 (1998).

104. Han, J.H., *et al.* Macrophage inflammatory protein-1alpha is an osteoclastogenic factor in myeloma that is independent of receptor activator of nuclear factor kappaB ligand. *Blood* **97**, 3349-3353 (2001).

105. Glass Ii, D.A., *et al.* Canonical Wnt Signaling in Differentiated Osteoblasts Controls Osteoclast Differentiation. *Developmental cell* **8**, 751-764 (2005).

106. Wei, W., *et al.* Biphasic and dosage-dependent regulation of osteoclastogenesis by beta-catenin. *Molecular and cellular biology* **31**, 4706-4719 (2011).

107. Maeda, K., *et al.* Wnt5a-Ror2 signaling between osteoblast-lineage cells and osteoclast precursors enhances osteoclastogenesis. *Nature medicine* **18**, 405-412 (2012).

108. Moverare-Skrtic, S., *et al.* Osteoblast-derived WNT16 represses osteoclastogenesis and prevents cortical bone fragility fractures. *Nature medicine* **20**, 1279-1288 (2014).

109. Kong, Y.Y., *et al.* Activated T cells regulate bone loss and joint destruction in adjuvant arthritis through osteoprotegerin ligand. *Nature* **402**, 304-309 (1999).

110. Roggia, C., *et al.* Up-regulation of TNF-producing T cells in the bone marrow: a key mechanism by which estrogen deficiency induces bone loss in vivo. *Proceedings of the National Academy of Sciences of the United States of America* **98**, 13960-13965 (2001).

111. Sugatani, T. & Hruska, K.A. MicroRNA-223 is a key factor in osteoclast differentiation. *Journal of cellular biochemistry* **101**, 996-999 (2007).

112. (!!! INVALID CITATION !!!).

113. Yasui, T., *et al.* Epigenetic regulation of osteoclast differentiation: possible involvement of Jmjd3 in the histone demethylation of Nfatc1. *Journal of bone and mineral research : the official journal of the American Society for Bone and Mineral Research* **26**, 2665-2671 (2011).

114. Mundy, G.R. Osteoporosis and Inflammation. *Nutrition reviews* **65**, S147-S151 (2007).

115. Ginaldi, L., Di Benedetto, M. & De Martinis, M. Osteoporosis, inflammation and ageing. *Immunity & Ageing* **2**, 14 (2005).

116. Redlich, K., *et al.* Repair of Local Bone Erosions and Reversal of Systemic Bone Loss Upon Therapy with Anti-Tumor Necrosis Factor in Combination with Osteoprotegerin or Parathyroid Hormone in Tumor Necrosis Factor-Mediated Arthritis. *The American journal of pathology* **164**, 543-555 (2004).

117. Lin, C.L., Moniz, C., Chambers, T.J. & Chow, J.W. Colitis causes bone loss in rats through suppression of bone formation. *Gastroenterology* **111**, 1263-1271 (1996).

118. Pihlstrom, B.L. Periodontal risk assessment, diagnosis and treatment planning. *Periodontology 2000* **25**, 37-58 (2001).

119. de Pablo, P., Chapple, I.L.C., Buckley, C.D. & Dietrich, T. Periodontitis in systemic rheumatic diseases. *Nat Rev Rheumatol* **5**, 218-224 (2009).

120. Arigbede, A.O., Babatope, B.O. & Bamidele, M.K. Periodontitis and systemic diseases: A literature review. *Journal of Indian Society of Periodontology* **16**, 487-491 (2012).

121. Kawai, T., *et al.* B and T Lymphocytes Are the Primary Sources of RANKL in the Bone Resorptive Lesion of Periodontal Disease. *The American journal of pathology* **169**, 987-998 (2006).

122. Teng, Y.-T.A., *et al.* Functional human T-cell immunity and osteoprotegerin ligand control alveolar bone destruction in periodontal infection. *The Journal of clinical investigation* **106**, R59-R67 (2000).

123. Haugeberg, G., Conaghan, P.G., Quinn, M. & Emery, P. Bone loss in patients with active early rheumatoid arthritis: infliximab and methotrexate compared with methotrexate

treatment alone. Explorative analysis from a 12-month randomised, double-blind, placebo-controlled study. *Annals of the Rheumatic Diseases* **68**, 1898-1901 (2009).

124. Jimi, E., *et al.* Selective inhibition of NF-[kappa]B blocks osteoclastogenesis and prevents inflammatory bone destruction in vivo. *Nature medicine* **10**, 617-624 (2004).

125. Ghosh, S. & Karin, M. Missing Pieces in the NF-ºB Puzzle. *Cell* **109**, S81-S96 (2002).

126. Wang, C.Y., Guttridge, D.C., Mayo, M.W. & Baldwin, A.S., Jr. NF-kappaB induces expression of the Bcl-2 homologue A1/Bfl-1 to preferentially suppress chemotherapy-induced apoptosis. *Molecular and cellular biology* **19**, 5923-5929 (1999).

127. Wang, C.Y., Mayo, M.W. & Baldwin, A.S., Jr. TNF- and cancer therapy-induced apoptosis: potentiation by inhibition of NF-kappaB. *Science* **274**, 784-787 (1996).

128. Franzoso, G., *et al.* Requirement for NF-κB in osteoclast and B-cell development. *Genes & development* **11**, 3482-3496 (1997).

129. Ruocco, M.G., *et al.* IκB kinase (IKK)β, but not IKKα, is a critical mediator of osteoclast survival and is required for inflammation-induced bone loss. *The Journal of experimental medicine* **201**, 1677-1687 (2005).

130. Chang, J., *et al.* Inhibition of osteoblastic bone formation by nuclear factor-kappaB. *Nature medicine* **15**, 682-689 (2009).

131. Gilbert, L., *et al.* Expression of the Osteoblast Differentiation Factor RUNX2 (Cbfa1/AML3/Pebp2αA) Is Inhibited by Tumor Necrosis Factor-α. *Journal of Biological Chemistry* **277**, 2695-2701 (2002).

132. Kaneki, H., *et al.* Tumor Necrosis Factor Promotes Runx2 Degradation through Up-regulation of Smurf1 and Smurf2 in Osteoblasts. *Journal of Biological Chemistry* **281**, 4326-4333 (2006).

133. Chang, J., *et al.* NF-kappaB inhibits osteogenic differentiation of mesenchymal stem cells by promoting beta-catenin degradation. *Proceedings of the National Academy of Sciences of the United States of America* **110**, 9469-9474 (2013).

134. Diarra, D., *et al.* Dickkopf-1 is a master regulator of joint remodeling. *Nature medicine* **13**, 156-163 (2007).

135. Li, X., *et al.* Sclerostin Binds to LRP5/6 and Antagonizes Canonical Wnt Signaling. *Journal of Biological Chemistry* **280**, 19883-19887 (2005).

136. Lam, J., *et al.* TNF-α induces osteoclastogenesis by direct stimulation of macrophages exposed to permissive levels of RANK ligand. *The Journal of clinical investigation* **106**, 1481-1488 (2000).

137. Kim, N., *et al.* Osteoclast differentiation independent of the TRANCE–RANK–TRAF6 axis. *The Journal of experimental medicine* **202**, 589-595 (2005).

138. Seeling, M., *et al.* Inflammatory monocytes and Fcγ receptor IV on osteoclasts are critical for bone destruction during inflammatory arthritis in mice. *Proceedings of the National Academy of Sciences* **110**, 10729-10734 (2013).

139. Zou, W., *et al.* Syk, c-Src, the alphavbeta3 integrin, and ITAM immunoreceptors, in concert, regulate osteoclastic bone resorption. *The Journal of cell biology* **176**, 877-888 (2007).

140. Cenci, S., *et al.* Estrogen deficiency induces bone loss by increasing T cell proliferation and lifespan through IFN-γ-induced class II transactivator. *Proceedings of the National Academy of Sciences* **100**, 10405-10410 (2003).

141. D'Amelio, P., *et al.* Estrogen deficiency increases osteoclastogenesis up-regulating T cells activity: A key mechanism in osteoporosis. *Bone* **43**, 92-100 (2008).

142. Kim, J.H., Kim, K., Youn, B.U., Jin, H.M. & Kim, N. MHC class II transactivator negatively regulates RANKL-mediated osteoclast differentiation by downregulating NFATc1 and OSCAR. *Cellular signalling* **22**, 1341-1349 (2010).

143. Mueller, R.B., *et al.* Regulation of myeloid cell function and major histocompatibility complex class II expression by tumor necrosis factor. *Arthritis & Rheumatism* **52**, 451-460 (2005).

144. Pacifici, R., *et al.* Effect of surgical menopause and estrogen replacement on cytokine release from human blood mononuclear cells. *Proceedings of the National Academy of Sciences* **88**, 5134-5138 (1991).

145. Zhao, R. Immune regulation of bone loss by Th17 cells in oestrogen-deficient osteoporosis. *European journal of clinical investigation* **43**, 1195-1202 (2013).

146. DeSelm, C.J., *et al.* IL-17 Mediates Estrogen-deficient Osteoporosis in an Act1-dependent Manner. *Journal of cellular biochemistry* **113**, 2895-2902 (2012).

147. Eghbali-Fatourechi, G., *et al.* Role of RANK ligand in mediating increased bone resorption in early postmenopausal women. *The Journal of clinical investigation* **111**, 1221 - 1230 (2003).

148. Takayanagi, H., *et al.* T-cell-mediated regulation of osteoclastogenesis by signalling cross-talk between RANKL and IFN-gamma. *Nature* **408**, 600 - 605 (2000).

149. Manolagas, S.C. & Parfitt, A.M. What old means to bone. *Trends in endocrinology and metabolism: TEM* **21**, 369-374 (2010).

150. Takayanagi, H. Osteoimmunology: shared mechanisms and crosstalk between the immune and bone systems. *Nat Rev Immunol* **7**, 292-304 (2007).

151. Jones, D., Glimcher, L.H. & Aliprantis, A.O. Osteoimmunology at the nexus of arthritis, osteoporosis, cancer, and infection. *The Journal of clinical investigation* **121**, 2534-2542 (2011).

152. Krebsbach, P.H., *et al.* Transgenic expression of COL1A1-chloramphenicol acetyltransferase fusion genes in bone: differential utilization of promoter elements in vivo and in cultured cells. *Molecular and cellular biology* **13**, 5168-5174 (1993).

153. Liu, F., *et al.* Expression and activity of osteoblast-targeted Cre recombinase transgenes in murine skeletal tissues. *The International journal of developmental biology* **48**, 645-653 (2004).

154. Weitzmann, M.N. & Pacifici, R. Estrogen deficiency and bone loss: an inflammatory tale. *The Journal of clinical investigation* **116**, 1186-1194 (2006).

155. Khosla, S., Westendorf, J.J. & Oursler, M.J. Building bone to reverse osteoporosis and repair fractures. *The Journal of clinical investigation* **118**, 421-428 (2008).

156. Jilka, R.L., *et al.* Dysapoptosis of osteoblasts and osteocytes increases cancellous bone formation but exaggerates bone porosity with age. *Journal of bone and mineral research : the official journal of the American Society for Bone and Mineral Research* (2013).

157. Hayward, M., *et al.* An extensive phenotypic characterization of the hTNFalpha transgenic mice. *BMC Physiology* **7**, 13 (2007).

158. Guo, R., *et al.* Ubiquitin ligase Smurf1 mediates tumor necrosis factor-induced systemic bone loss by promoting proteasomal degradation of bone morphogenetic signaling proteins. *The Journal of biological chemistry* **283**, 23084-23092 (2008).

159. Yao, W., *et al.* Overexpression of secreted frizzled-related protein 1 inhibits bone formation and attenuates parathyroid hormone bone anabolic effects. *Journal of bone and*

mineral research : the official journal of the American Society for Bone and Mineral Research **25**, 190-199 (2010).

160. Yao, Z., Xing, L. & Boyce, B.F. NF-kappaB p100 limits TNF-induced bone resorption in mice by a TRAF3-dependent mechanism. *The Journal of clinical investigation* **119**, 3024-3034 (2009).

161. Boyce, B.F., Yao, Z. & Xing, L. Functions of nuclear factor κB in bone. *Annals of the New York Academy of Sciences* **1192**, 367-375 (2010).

162. Pandey, A.C., *et al.* MicroRNA profiling reveals age-dependent differential expression of nuclear factor kappaB and mitogen-activated protein kinase in adipose and bone marrow-derived human mesenchymal stem cells. *Stem cell research & therapy* **2**, 49 (2011).

163. Garnero, P., Sornay-Rendu, E., Chapuy, M.C. & Delmas, P.D. Increased bone turnover in late postmenopausal women is a major determinant of osteoporosis. *Journal of bone and mineral research : the official journal of the American Society for Bone and Mineral Research* **11**, 337-349 (1996).

164. Glatt, V., Canalis, E., Stadmeyer, L. & Bouxsein, M.L. Age-Related Changes in Trabecular Architecture Differ in Female and Male C57BL/6J Mice. *Journal of Bone and Mineral Research* **22**, 1197-1207 (2007).

165. Bai, S., Zha, J., Zhao, H., Ross, F.P. & Teitelbaum, S.L. Tumor necrosis factor receptor-associated factor 6 is an intranuclear transcriptional coactivator in osteoclasts. *The Journal of biological chemistry* **283**, 30861-30867 (2008).

166. Lomaga, M., *et al.* TRAF6 deficiency results in osteopetrosis and defective interleukin-1, CD40, and LPS signaling. *Genes & development* **13**, 1015 - 1024 (1999).

167. Teitelbaum, S.L. & Ross, F.P. Genetic regulation of osteoclast development and function. *Nature reviews. Genetics* **4**, 638-649 (2003).

168. Asagiri, M., *et al.* Autoamplification of NFATc1 expression determines its essential role in bone homeostasis. *The Journal of experimental medicine* **202**, 1261-1269 (2005).

169. Jimi, E. & Ghosh, S. Role of nuclear factor-κB in the immune system and bone. *Immunological reviews* **208**, 80-87 (2005).

170. Kalaitzidis, D. & Gilmore, T.D. Transcription factor cross-talk: the estrogen receptor and NF-kappaB. *Trends Endocrinol Metab* **16**, 46-52 (2005).

171. Krum, S.A., Chang, J., Miranda-Carboni, G. & Wang, C.-Y. Novel functions for NF[kappa]B: inhibition of bone formation. *Nat Rev Rheumatol* **6**, 607-611 (2010).

172. Takada, I., *et al.* A histone lysine methyltransferase activated by non-canonical Wnt signalling suppresses PPAR-gamma transactivation. *Nature cell biology* **9**, 1273-1285 (2007).

173. Winkel, A., *et al.* Wnt-ligand-dependent interaction of TAK1 (TGF-beta-activated kinase-1) with the receptor tyrosine kinase Ror2 modulates canonical Wnt-signalling. *Cellular signalling* **20**, 2134-2144 (2008).

174. Schett, G., Zwerina, J. & David, J.P. The role of Wnt proteins in arthritis. *Nature clinical practice. Rheumatology* **4**, 473-480 (2008).

175. Lories, R.J., Corr, M. & Lane, N.E. To Wnt or not to Wnt: the bone and joint health dilemma. *Nat Rev Rheumatol* **9**, 328-339 (2013).

176. Sherlock, J.P., *et al.* IL-23 induces spondyloarthropathy by acting on ROR-gammat+ CD3+CD4-CD8- entheseal resident T cells. *Nature medicine* **18**, 1069-1076 (2012).

177. Ershler, W.B. & Keller, E.T. Age-associated increased interleukin-6 gene expression, late-life diseases, and frailty. *Annual review of medicine* **51**, 245-270 (2000).

178. Pfeilschifter, J., Koditz, R., Pfohl, M. & Schatz, H. Changes in proinflammatory cytokine activity after menopause. *Endocr Rev* **23**, 90 - 119 (2002).

179. Cao, J.J., *et al.* Aging increases stromal/osteoblastic cell-induced osteoclastogenesis and alters the osteoclast precursor pool in the mouse. *Journal of bone and mineral research : the official journal of the American Society for Bone and Mineral Research* **20**, 1659-1668 (2005).

180. Chien, K.R. & Karsenty, G. Longevity and lineages: toward the integrative biology of degenerative diseases in heart, muscle, and bone. *Cell* **120**, 533-544 (2005).

181. Katoh, M. WNT3-WNT14B and WNT3A-WNT14 gene clusters (Review). *International journal of molecular medicine* **9**, 579-584 (2002).

182. Heinonen, K.M., Vanegas, J.R., Lew, D., Krosl, J. & Perreault, C. Wnt4 Enhances Murine Hematopoietic Progenitor Cell Expansion Through a Planar Cell Polarity-Like Pathway. *PloS one* **6**, e19279 (2011).

183. Fodor, B.D., *et al.* Jmjd2b antagonizes H3K9 trimethylation at pericentric heterochromatin in mammalian cells. *Genes & development* **20**, 1557-1562 (2006).

184. Cloos, P.A.C., *et al.* The putative oncogene GASC1 demethylates tri- and dimethylated lysine 9 on histone H3. *Nature* **442**, 307-311 (2006).

185. Klose, R.J., Kallin, E.M. & Zhang, Y. JmjC-domain-containing proteins and histone demethylation. *Nature reviews. Genetics* **7**, 715-727 (2006).

186. Whetstine, J.R., *et al.* Reversal of Histone Lysine Trimethylation by the JMJD2 Family of Histone Demethylases. *Cell* **125**, 467-481 (2006).

187. Agger, K., *et al.* UTX and JMJD3 are histone H3K27 demethylases involved in HOX gene regulation and development. *Nature* **449**, 731-734 (2007).

188. Differentiation of human bone marrow osteogenic stromal cells in vitro: induction of the osteoblast phenotype by dexamethasone. *Endocrinology* **134**, 277-286 (1994).

189. Gronthos, S., Graves, S., Ohta, S. & Simmons, P. *The STRO-1+ fraction of adult human bone marrow contains the osteogenic precursors*, (1994).

190. Miller, S.A., Mohn, S.E. & Weinmann, A.S. Jmjd3 and UTX play a demethylase-independent role in chromatin remodeling to regulate T-box family member-dependent gene expression. *Molecular cell* **40**, 594-605 (2010).

191. Lan, F., *et al.* A histone H3 lysine 27 demethylase regulates animal posterior development. *Nature* **449**, 689-694 (2007).

192. Lee, M.-H., Kwon, T.-G., Park, H.-S., Wozney, J.M. & Ryoo, H.-M. BMP-2-induced Osterix expression is mediated by Dlx5 but is independent of Runx2. *Biochemical and biophysical research communications* **309**, 689-694 (2003).

193. Kawai, M. & Rosen, C.J. PPARgamma: a circadian transcription factor in adipogenesis and osteogenesis. *Nature reviews. Endocrinology* **6**, 629-636 (2010).

194. Rodríguez, J.P., Montecinos, L., Ríos, S., Reyes, P. & Martínez, J. Mesenchymal stem cells from osteoporotic patients produce a type I collagen-deficient extracellular matrix favoring adipogenic differentiation. *Journal of cellular biochemistry* **79**, 557-565 (2000).

195. Justesen, J., *et al.* Adipocyte tissue volume in bone marrow is increased with aging and in patients with osteoporosis. *Biogerontology* **2**, 165-171 (2001).

196. Sekiya, I., Larson, B.L., Vuoristo, J.T., Cui, J.-G. & Prockop, D.J. Adipogenic Differentiation of Human Adult Stem Cells From Bone Marrow Stroma (MSCs). *Journal of Bone and Mineral Research* **19**, 256-264 (2004).

197. Lian, J.B., *et al.* Networks and hubs for the transcriptional control of osteoblastogenesis. *Reviews in endocrine & metabolic disorders* **7**, 1-16 (2006).

198. Karsenty, G., Kronenberg, H.M. & Settembre, C. Genetic control of bone formation. *Annual review of cell and developmental biology* **25**, 629-648 (2009).

199. Caplan, A.I. Adult mesenchymal stem cells for tissue engineering versus regenerative medicine. *Journal of cellular physiology* **213**, 341-347 (2007).

200. Levi, B. & Longaker, M.T. Concise review: adipose-derived stromal cells for skeletal regenerative medicine. *Stem cells* **29**, 576-582 (2011).

201. Schroeder, T.M., Kahler, R.A., Li, X. & Westendorf, J.J. Histone deacetylase 3 interacts with runx2 to repress the osteocalcin promoter and regulate osteoblast differentiation. *The Journal of biological chemistry* **279**, 41998-42007 (2004).

202. Celil, A.B. & Campbell, P.G. BMP-2 and insulin-like growth factor-I mediate Osterix (Osx) expression in human mesenchymal stem cells via the MAPK and protein kinase D signaling pathways. *The Journal of biological chemistry* **280**, 31353-31359 (2005).

203. Barski, A., *et al.* High-resolution profiling of histone methylations in the human genome. *Cell* **129**, 823-837 (2007).

204. McEwen, K.R. & Ferguson-Smith, A.C. Distinguishing epigenetic marks of developmental and imprinting regulation. *Epigenetics & chromatin* **3**, 2 (2010).

205. Hassan, M.Q., *et al.* BMP2 Commitment to the Osteogenic Lineage Involves Activation of Runx2 by DLX3 and a Homeodomain Transcriptional Network. *Journal of Biological Chemistry* **281**, 40515-40526 (2006).

206. Kawane, T., *et al.* Dlx5 and mef2 regulate a novel runx2 enhancer for osteoblast-specific expression. *Journal of bone and mineral research : the official journal of the American Society for Bone and Mineral Research* **29**, 1960-1969 (2014).

207. Lee, H.L., Woo, K.M., Ryoo, H.M. & Baek, J.H. Distal-less homeobox 5 inhibits adipogenic differentiation through the down-regulation of peroxisome proliferator-activated receptor gamma expression. *Journal of cellular physiology* **228**, 87-98 (2013).